UNIVERSITI TEKNOLOGI MARA

NUMERICAL SIMULATION AND OPTIMIZATION OF HIGH-EFFICIENCY GAAS/P-SI AND ALGAAS/P-SI BASED SOLAR CELLS

FAZLIN BINTI MOHAMAD RAHIMI

MSc

February 2026

UNIVERSITI TEKNOLOGI MARA

NUMERICAL SIMULATION AND OPTIMIZATION OF HIGH-EFFICIENCY GAAS/P-SI AND ALGAAS/P-SI BASED SOLAR CELLS

FAZLIN BINTI MOHAMAD RAHIMI

Thesis submitted in fulfilment
of the requirements for the degree of
Master of Science
(Applied Physics)

Faculty of Applied Sciences

February 2026

CONFIRMATION BY PANEL OF EXAMINERS

I certify that a Panel of Examiners has met on 3 December 2025 to conduct the final examination of Fazlin Binti Mohamad Rahimi on her Masters of Science thesis entitled "Numerical Simulation and Optimization of High-Efficiency GaAs/P-Si and AlGaAs/P-Si Based Solar Cells" in accordance with Universiti Teknologi MARA Act 1976 (Akta 173). The Panel of Examiner recommends that the student be awarded the relevant degree. The Panel of Examiners was as follows:

Rosnah Zakaria, PhD
Assosiate Professor
Faculty of Applied Sciences
Universiti Teknologi MARA
(Chairman)

Noor Asnida Asli, PhD
Associate Professor
Faculty of Applied Science
Universiti Teknologi MARA
(Internal Examiner)

Yasmin Abdul Wahab,PhD
Senior Lecturer
Nanotechnology and Catalysis Research Center
University of Malaya
(External Examiner)

PROFESSOR DR HJH ZURAEDA IBRAHIM
Dean
Institute of Postgraduate Studies
Universiti Teknoogi MARA
Date: 28 February 2026

AUTHOR'S DECLARATION

I declare that the work in this thesis was carried out in accordance with the regulations of Universiti Teknologi MARA. It is original and is the results of my own work, unless otherwise indicated or acknowledged as referenced work. This thesis has not been submitted to any other academic institution or non-academic institution for any degree or qualification.

I, hereby, acknowledge that I have been supplied with the Academic Rules and Regulations for Post Graduate, Universiti Teknologi MARA, regulating the conduct of my study and research.

Name of Student	Fazlin Binti Mohamad Rahimi
Student ID. No.	2024573665
Programme	Master of Science (Applied Physics) - AS760
Faculty	Applied Sciences
Thesis Title	Numerical Simulation and Optimization Of High-Efficiency GaAs/P-Si And AlGaAs/P-Si Based Solar Cells
Signature of Student	
Date	February 2026

ABSTRACT

Malaysia has a significant biomass, solar and hydro potential under investigation as in request for clean and sustainable energy keep on growing which has led to much research on solar cell technologies. Solar panels, in particular those made from Gallium Arsenide (GaAs) and Aluminium Gallium Arsenide (AlGaAs) materials have demonstrated the conceivable to be more energy effective than traditional silicon based solar cells. The goal of the study is to find a solar cell structure with the highest possible efficacy: a GaAs/p-Si and AlGaAs/p-Si solar cells are simulated using PC1D software. Performance of solar cell was improved by optimizing key parameters including device thickness, doping concentration and Anti-Reflection Coating (ARC) design. Simulations showed that GaAs/p-Si solar cells reached a maximum efficiency of 24.02% when the n-region thickness was reduced to 0.1 um, and efficiency improved to 24.01% with an optimum silicon thickness of 150 um. The doping concentration strongly influenced performance, with an optimal level of 1 x 10^{17} $cirr^{3}$ in both n- and p-regions giving a maximum efficiency of 25.22%). For single-layer ARC (SLARC, ZnO), the best efficiency was 23.62%. at 600 nm, while with double-layer ARC (DLARC, ZnO/TiCh) the efficiency slightly decreased to 23.36%, and without ARC it dropped to 16.43%). Similarly, AlGaAs/p-Si solar cells achieved 23.04%) efficiency with a thin 0.1 um n-region and 23.05%) at an optimum thickness of 120 um. The best n-region doping was again lxlO^{17} $cirr^{3}$ giving 23.97%> efficiency, while p-region doping between lxio^{i2}-lxio^{13} cnr^{3} gave 20.86%. For SLARC, the peak efficiency was 21.23% at 600 nm, and with DLARC it rose to 20.98% at 400-500 nm, compared to 14.56% without ARC. The outcome indicated that the efficacy of a GaAs based solar cell could be significantly enhanced by carefully engineering thickness, doping, and ARCs by future renewable energy generation solutions.

ACKNOWLEDGEMENT

First and foremost, I would like to thank Almighty Allah for the opportunity to begin and complete this rigorous and lengthy process of achieving my master degree. Special thanks to my supervisor, Dr. Mohd Zaki bin Mohd Yusoff and co-supervisor, Dr Nurkhaizan Bt Zulkepli and Dr Megat Mohd Izhar Bin Sapeli for their assistance and guidance throughout the master degree programme.

I thank my colleagues and friends for their help, encouragement and feedback which have greatly contributed to the completion of this work. I would also to acknowledge all those people who directly or indirectly help me to enriched the quality of my work.

Finally, I'd like to thank my parents for their vision and their effort to educate and support me throughout my entire master's journey. To both of you, I dedicate this victory piece. Alhamdulillah.

TABLE OF CONTENTS

LIST OF TABLES

LIST OF FIGURES

LIST OF ABBREVATIONS

Abbreviations

ARC	Anti-Reflective Coating
a-Si	Amorphous Silicon
Cm^{-3}	Cubic centimetre
DLARC	Double Layers Anti-Reflective Coating
EFG	Edge-Defined Filmed Growth
eV	Electron Volt
£R	The relative permittivity
FF	Fill Factor
GaAs	Gallium Arsenide
I-V	Current Voltage
k	Boltzmann's Constant
K	Kelvin
kW	kilowatt
PC1D	Personal Computer One Dimension
PMP	Power Maximum Point
PV	Photovoltaic
Si	Silicon
T	Temperature
TiC-2	Titanium Dioxide
ZnO	Zinc Oxide
Tl	The efficiency of the solar cell
£F	Fermi Energy
/cs	Short Circuit Current
Pin	Power Input
r_{max}	Maximum Power
Koc	Open Circuit Voltage
m^2	Meter Square
m	Cubic meter

CHAPTER 1
INTRODUCTION

1.1 Research Background

The population of the earth has been exposed to challenging ecological issues and a severe energy disaster since the start of the twenty-first century. Clean energy sources come in various forms, including solar, hydro, wind, biomass, thermal, and waves. Malaysia's potential for biomass, solar, and hydro is considerable. Solar cells are a capable and potentially important expertise and are the upcoming of doable energy for human evolution (Ranabhat et al., 2016). Solar panels, also referred to as photovoltaic cells are semiconductor gadgets that transform sunlight into energy. They are essential, for producing energy.

Numerous types of silicon solar cells are employed extensively at various levels. Because of their affordable prices, these cells are frequently used and readily available on the market. They can operate without requiring a lot of maintenance and have a lifespan of more than 25 years. Over 30% reflectivity in bare silicon can result in significant optical losses. In order to achieve better performance, silicon solar cells must be equipped with certain thickness, doping concentration and an anti-reflective coating (ARC) that has been carefully planned and developed. By regulating the thickness of this layer, researchers can control the light absorption and carrier generation within the solar cell (Bhusal, 2024). For solar cells, doping concentration is a key factor in shaping the efficiency and functionality of the device (Humaidan et al., 2022). Optimizing the doping concentration in the base layer (p-type GaAs) is crucial for maximizing the alteration efficacy of the solar cell (Bhusal, 2024). The development for ARCs and the search for suitable materials for these coatings are very crucial (Shanmugam et al., 2020).

Next, the importance that simulation has rather than experimental work is the cost-effective, faster, safer, and the main importance is flexibility. For example, the simulated model can be changed easily compared to the experimental work. In the solar cell industry and community, GaAs and AlGaAs materials can bring more effectiveness in improving solar cell such as GaAs has higher conversion efficacy rather than the

traditional silicon resources and they can be combined with each other to create multi-junction solar cells.

1.2 Motivation for This Work

Personal Computer One Dimension (PC1D) modelling and simulator software are used in analysis to improve the performance of AlGaAs/GaAs solar cells. Much effort has been expended to understand and improve solar cell designs based on the GaAs material system due to its promise as a material for photovoltaic applications including direct band gap and high efficiency potential. But their performance is constrained by large surface recombination velocities which cause carrier loss and by optical reflection at front surface that diminishes the light absorption. The current research endeavours to systematically simulate the device by modifying the thickness and doping concentrations of several layers (window, emitter, base, and back surface field). To overcome these issues, the PC1D simulation focuses on optimizing the thickness and doping levels of the emitter and absorber layers, while also analysing the effects of surface recombination velocity and anti-reflection coatings (ARCs), with the lead of developing high-performance solar cells that are both economical and efficient.

In particular, the AlGaAs/GaAs/Si materials are based on stack order from large to small band-gap energy and are selected for the appropriate band gap alignment, lattice match, fluency and the possibility to achieve higher conversion efficiency than that of the known Multi-Junction Solar Cells (MJSCs) using the InGaP/GaAs/Ge cell. PC1D simulation aids in optimizing the design before fabrication to minimize the cost and time expenditure. Adopting an analytical model, this study aimed at addressing the issues which were not taken into account in the previous research, e.g., the dispersion and non-normal incidence, obtaining a more in-depth knowledge of optical behaviour of ARCs on both planar substrate and textured substrates. Designing ARCs for improved top cell performance is important in that lower reflectance may directly increase the amount of solar power absorbed by solar cells, allowing for overall or individual cell thickness, costs, and efficiencies to be reduced.

Another motivation arises from the economic challenges associated with III-V solar cells. Their fabrication cost remains a barrier for large-scale application, making

it crucial to investigate strategies that reduce material usage and improve overall cost-effectiveness. Research that supports more efficient device design, therefore, has direct implications for making these technologies commercially competitive.

Furthermore, the integration of GaAs/AlGaAs structures into next-generation applications such as concentrator photovoltaics (CPVs), tandem perovskite-silicon devices, and flexible solar cells underlines the relevance of such investigations. Beyond efficiency, the capacity to engineer devices that remain stable and scalable is vital for real-world adoption.

In this light, the present work addresses an important research gap by contributing to the broader pursuit of optimizing advanced solar cell architectures that balance performance, durability, and affordability—paving the way for the next generation of photovoltaic technologies.

1.3 Problem Statement

Solar panels suffer from inefficiency and lack of power. Given these constraints, dozens of studies have focused on improving solar panel efficiency by studying various factors (e.g., surface area, thicknesses doping concentration) and conditions such as temperature type. Nonetheless, a majority of studies has depended on conventional resources including silicon that limits the potential for efficiency upgrades (Kc et al., 2020). Despite advances made in the past years, silicon-based SCs encountered various challenges that prevent them from fully utilization of solar spectrum and degrade efficiencies over time (Sathya & Supriya, 2017). Nonetheless, this can be overcomed by developing the layers of the solar cell with the right materials so that it can harness the solar spectrum accordingly (Martin A. Green et al., 2015). Moreover, the main problem in the device structure is the material compability. By combining different materials in the heterostructures can cause lattice mismatch that led to low efficiency the solar cells. Thus, simulation of GaAs/p-Si and AlGaAs/p-Si -based solar cell can be tested to find the highest efficiency.

However, a lot of existing research doesn't look at how these materials actually work in practice. For example, exposure to sunlight increase temperature during day as well as part of the material is shaded and its not perfectly efficient all over as compared to when they are uniformly illuminated under standard laboratory test conditions. By choosing the proper material mix and optimizing multi-layer structures, we anticipate that this study will be an innovative approach to increase efficiency beyond both theoretical limits of interfacial disorder in a homogeneous system all through practical understanding. This research work will close these gaps producing novel material combinations, forming strengthening structures and implementing energy efficiency optimization strategies to fill the gap between theoretical limits of efficiencies and real-world performance.

1.4 Research Objective

The main objectives of this project are:

- To create thorough and realistic models for optimizing the thickness, anti-reflection coating (ARC) design, and doping concentration for solar cells using PC ID simulation.
- To achieve the highest possible efficiency for GaAs/p-Si and AlGaAs/p-Si-based solar cells through the simulation and modelling process, targeting a minimum power conversion efficiency (PCE) of 20% under standard AM1.5G illumination conditions.
- To analyze the IV-characteristics, open circuit voltage, and fill factor of GaAs/p-Si and AlGaAs/p-Si solar cells using a developed model that considers the contributions of the thickness, anti-reflection coating (ARC), and doping concentration parameters.

1.5 Research Question

i. How the GaAs/p-Si and AlGaAs/p-Si -based solar cell can achieve the highest efficiency through the simulation and modelling process?

ii. How to build thorough and realistic models for optimizing the thickness, anti-reflection coating (ARC) design, and doping concentration for solar cells using PC ID simulation?

iii. How can the IV- characteristics, open circuit voltage, and fill factor of GaAs/p-Si and AlGaAs/p-Si solar cells be analysed using a developed model that considers the contributions of thickness, anti-reflection coating (ARC), and doping concentration parameters?

1.6 Significance of study

The resolution of this research is to find Si/GaAs solar cells with an actual high efficacy. This purpose can be obtained by preparing some study on certain parameters such as material properties, device structure, optical properties, and electrical properties. These parameters were chosen since they significantly influence on the solar cell efficiency and the optimization study is focused on finding an optimal value of thickness, anti-reflection coating design and doping concentration one can expect to achieve peak performance. Moreover, this research was accomplished by using the PC1D software instead of hardware. The simulated open-circuit voltage is about 0.05-0.10 V lower than the values found in the literature for similar reference cells, because PC ID limits its ability to correctly simulate heterojunction band offsets and interface recombination effects which can cause an under-estimation of Voc. Nonetheless, the simulation serves as a useful benchmark for optimizing multi-junction solar cells (Sathya & Supriya, 2017) . PC ID simulation were used to optimize the device parameters including thickness, doping, energy band gap etc., and thus reducing the development cost and efforts.

Furthermore, this research can provide valuable contributions to academic studies focused on improvising solar cell production. By using solar cell technology, there are a lot of environmental problems that can be solved. For example, the greenhouse effects can be reduced because solar cell technology is ecological related to other technologies that can worsen the contamination on the earth. Hence, this research is suggested to improve the quality of the earth's environment.

In conclusion, the study presents useful reference tools and results for designing and fabricating a more cost-efficient high-performance solar cells, which are of great importance for the development of sustainable energy technologies to meet global challenges of energy and environmental issues. This optimization is significant as it overcomes the recombination and material quality related restrictions, which usually diminish the efficiency of GaAs-based solar cells. Results of this work will benefit both the development for the design and fabrication of the higher efficiency solar cells and contribute to the progress of renewable energy technologies with high efficiency and quality, important to meet global energy demands in a sustainable way.

1.7 Limitation

It's a limitation of the study that there are so few published articles and journals to be called "information sources" in this sense. Especially true in the case of zinc oxide and AlGaAs/p-Si, solar cell simulation with PC ID software, since there is not much work an active simulation in this regard, particularly for PC ID software and since zinc oxide-based solar cell is the newest material used as solar cells instruction and is still under development and time of growing. Therefore, a fair evaluation of the results may be difficult without external evaluation benchmarks. Hence, the simulation results are verified through comparison with experimentally reported data, performance values from industrial and white papers to make sure that the predicted trends and performance metrics do fall within practical and commercially feasible regimes. On the other hand, efficiency as high as 20% was reported for sputtering-based GaAs/Si heterojunction devices in early experiments, which indicates that there may be practical difficulty of realizing ideal conditions from simulation results directly(Gulyaev et al., 2016). This validation method increases the robustness and reliability of the modelling calculations.

There are currently few research studies on GaAs/p-Si and AlGaAs/p-Si solar cells, in part because it can be costly to develop new materials, technologies, or manufacturing processes for solar cells. This restricts the number of research (and funding) opportunities which can be made available, even in an increasingly competitive financial world. There are also major issues in material science, in manufacturing and in electrical engineering regarding solar cell technology. The complex nature of these issues requires multidisciplinary research and cooperation, which can be very costly and time-consuming.

In addition, much of the work in solar technology in general has focused on incremental improvements to existing technologies such as durability and cost as opposed to something as appealing as making some kind of new material, but that's kind of what it takes to make solar viable to a much larger audience. Solar cells are still the subject of intense scientific and commercial activity, in spite of possibly problematic issues or misunderstandings, which may be holding back development. With the present research one will lift various existing limitations and allow the solar

energy more accessible and cheaper as an alternative for the world-wide electricity supply.

A further limitation is the absent of the experimental verification. Since we use numerical simulations only in the present work, the predictions are not directly comparable with the fabricated samples. In reality, practical material imperfections, fabrication tolerances and non-ideal growth conditions frequently result in efficiency of less value than those estimated from the simulations. It is also unclear, without equivalent experimental work, how well the modeled devices would actually perform. The discrepancy between simulation and manufacturing still represents a significant problem in future works must be addressed.

A downside of environmental stability, which cannot be included in PC1D simulations, is that it imposes a limitation. In real-world use, solar cells are exposed to temperature, humidity, UV light, and mechanical stresses, all of which can degrade materials. For example, ZnO layers may undergo chemical instability in the presence of moisture or under acid exposure, a representation that is missing from the current work. Therefore, the long-term reliability of the proposed device structures is not guaranteed.

1.8 Thesis Outline

The outline for this thesis starts with Chapter 1, which introduce the background of the research, issue concerning the research topic and the significance of study regarding the solar cell, specifically the application of different thickness, doping concentration and materials of single layer ARC and double-layers ARC on GaAs/p-Si and AlGaAs/p-Si solar cell.

Then, followed by the literature review on Chapter 2 which explains the fundamental and knowledge of the solar cell such as the basic operation of solar cells, the concept of thickness, doping concentration and ARC as well as the types of materials used as ARC on the solar cells that will be implemented for this research. The optical properties of the solar cells, which consists of reflectance, absorption, thickness and others also explained in this chapter.

Next, Chapter 3 basically explains about the methodology used for this study, which is the PC1D simulation software which helps to generate different outcomes depending on the parameters applied for the simulation of thickness, doping

concentration and ARC on GaAs/p-Si and AlGaAs/p-Si solar cells. This chapter also discussed regarding the parameters used as well as the flow chart of the simulation of thickness, doping concentration and ARC on both GaAs/p-Si and AlGaAs/p-Si solar cells.

The results of the simulation which mostly contained the data of short circuit current (Isc), open circuit voltage (Voc), maximum power output (Pmax), efficiency and the fill factor as well as the results for I-V curve was analysed and explain in Chapter 4 and Chapter 5 separately. Lastly, Chapter 6 will conclude the overall research regarding this study of different thickness, doping concentration and ARC on both GaAs/p-Si and AlGaAs/p-Si solar cells.

CHAPTER 2
LITERATURE REVIEW

2.1 Introduction of Solar Cell

Alexandre-Edmond Becquerel discovers the photovoltaic (PV) effect for the first time in 1839. Russell Ohl went on to create the first silicon-based modern solar cell in 1946. In the past, photovoltaic solar cells, which were composed of thin silicon wafers, converted light energy from sunlight into electrical power (Sharma et al., 2017). As seen in Figure 2.1. (Sharma et al., 2017), the new and inventive photovoltaic technology is now based on the idea that electron-holes generated in each cell made up of two distinct layers known as p-type and n-type semiconductor materials

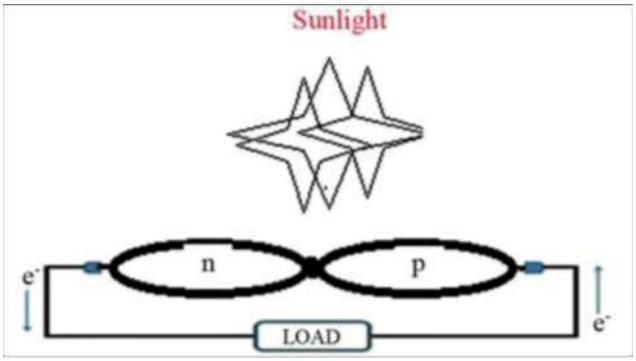

Figure 2.1 P-n Junction Solar Cell

A solar panel is fabricated of countless of these solar cells, and a photovoltaic range consists of a few of these panels (Jordehi, 2016). The three core of PV cell technologies such as monocrystalline silicon, polycrystalline silicon, and thin film can rule the global energy need (Chenni et al., 2007).Due to their excessive rate, advanced efficacy PV technologies like gallium arsenide and multi-junction cells are not well-liked but ideal for use in space purposes and resolute photovoltaic systems (Chenni et al., 2007). An assortment of latest PV cell technologies is also being established, including Perovskite cells, organic solar cells, dye-sensitized solar cells, and quantum dots (Kaygusuz, 2001).

One of the untainted structures of silicon, monocrystalline Silicon, was used to form the early solar cells that were advertised wholesale as shown in Figure 2.2 (Lum, 2021). They are beyond high-priced than their polycrystalline or thin film counterparts despite their high efficiency but labour-intensive and slow manufacturing process. Next, polycrystalline silicon PV cells, which accounted for over 70% of the earth's PV fabrication in 2015, lead the market (Jordehi, 2016).They can be constructed by purely establishing a Silicon ingot into the shape of a cube, sawing it, and then compressing it in a manner akin to how monocrystalline cells are packaged. Drafting a thin ribbon of polycrystalline silicon from a mass of molten silicon is an additional methodology recognized as edge-defined film-fed growth (EFG).

Figure 2.2 Polycrystalline Silicon PV cells and Monocrystalline Silicon PV cells. (Lum, 2021)

Thin film cells also can make a cell even if crystalline PV cells conquer the market because thin film cells are far more adaptable and durable. Amorphous Silicon (a-Si), a type of thin film PV cell, is fabricated by dropping thin layers of silicon on a glass substrate as shown in Figure 2.3. As a result, fewer than 1% of the Silicon involved for a crystalline cell is used, constructing a very thin, flexible cell. Amorphous Silicon cells are much less pricy to fabricate because of this reduction in raw material necessities and a less energy-intensive fabricating method (Peake, 2018). Even so, because the silicon atoms are much less systematized than in their crystalline forms, they discard behind "dangling bonds" that tie with other components to supply them

electrically inactive, critically dropping their efficacy. These cells also undergo a 20% decrease in efficacy during the first few months of use before alleviating, so their power ratings are based on their turnout deprivation rather than their factual operation (Peake, 2018).

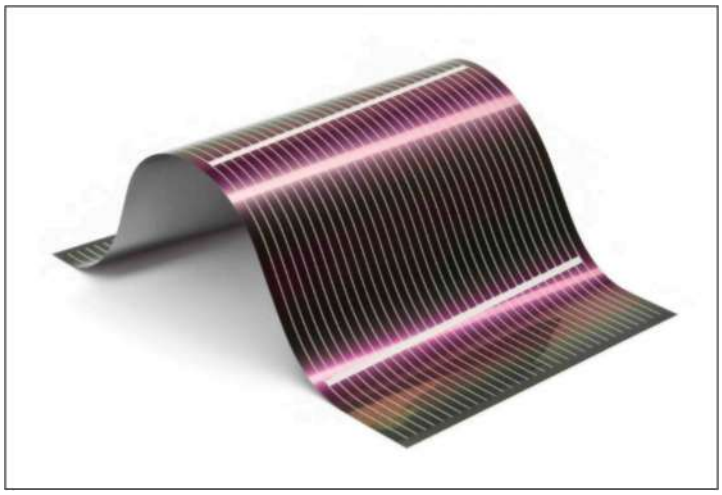

Figure 2.3 Thin Film Cells.
Source: (LaMonica, 2024)

2.2 Basic Working Principle of Solar cell

A solar cell is the necessary unit of a solar energy origination system in which sunlight is directly transformed to electrical energy. The solar cell is a p-n junction device. n-type designates negatively charged electrons given by donor impurity atoms and p-type indicates positively charged holes made by acceptor impurity atoms, refers to Figure 2.4 of a PV composition (Al-Ezzi & Ansari, 2022).

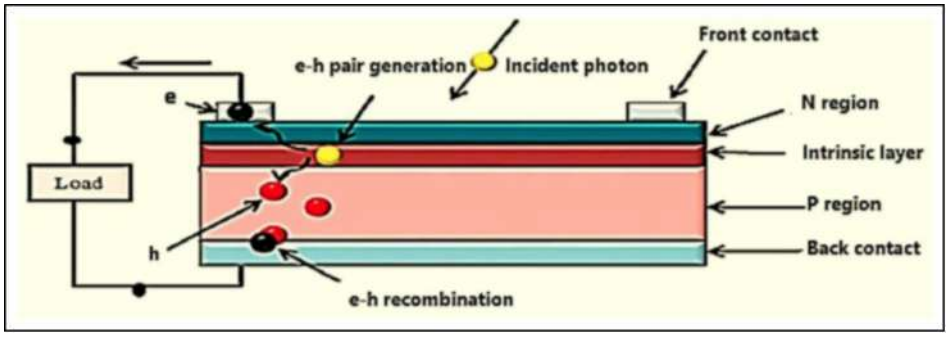

Figure 2.4 A p-n junction PV cell
Source: (Al-Ezzi & Ansari, 2022).

The operating principle of solar cells is based on the photovoltaic effect. The PV effect can be separated into three essential developments. Firstly, the charge carriers which is electron-hole pairs was generated as photons were absorbs in a p-n junction electronic semiconductor. The immersion of a photon with energy (E = hu) greater than the gap energy 'E_g' of the doped semiconductor material infers that its energy is used to excite an electron from the valence band 'ED' to the conduction band 'Ec' leaving avoid which are hole at the valance level. Excessive kinetic energy is supplied to the electron or hole by the excess photon energy (hu-huo). 'hi)o' is the least energy or work role of the semiconductor required to construct an electron-hole pair. The work function here embodies the energy gap. Heat is released in the semiconductor because excess energy is dissipated (Al-Ezzi & Ansari, 2022)

In the external circuit, the holes can wander away from the junction through the p-region while electrons can flow out past the n-region and exit through the circuit before they assemble with the holes as a subsequent from the departure of the light-generated charge carriers. Lastly, the detached electrons can be use up to run an electric circuit. Electrons will recombine with the holes after they passed through the circuit (Al-Ezzi & Ansari, 2022).

The design of n-type must be delicate than the p-type so that the electrons can cross the circuit in a short phase of time and produce current before they recombine with the holes through defects. Besides, reflection at the surface and diffusion of the light to the semiconductor material can be reduced by applying an anti-reflective coating over the n-layer (Al-Ezzi & Ansari, 2022).

The model of the solar cell is intentional to produce a very effective model. A solar cell's maximum power *(Pmax),* open circuit voltage (V_{oc}), and short circuit current *(Ics)* are all measures of how well it performs. The fill factor and efficiency are computed in the study using a certain equation. The equation gives the fill factor's expression (2.1). For the and standard isolation can be calculated using expressions (2.3), (2.4), and (2.5). The efficacy of the solar cell can then be evaluated using the fill factor (2.2) (Salman, 2017).

$$FF = \frac{\text{p}}{IscVoc} \tag{2.1}$$

Where FF represents the fill factor of the solar cell, PMax is the maximum power output (W), Voc indicated the open circuit voltage (V) and Isc is the short circuit current (A). The fill factor indicates the quality of a solar cell. A more powerful fill factor demonstrates a solar cell with more efficient performance. While open-circuit voltage and short-circuit current are significant, the fill factor illustrates how effectively the cell performs between both of these factors. It has an immediate impact on the overall efficiency of the solar cell.

$$i] = - \wedge - \wedge \text{——} x\ 100\% \quad (2.2)$$
$$"in$$

$$Pmax = percentage\ q\ x\ P_{in} \quad (2.3)$$

$$P_{in} = Standard\ insolation\ x\ Area\ of\ Panel \quad (2.4)$$

$$Standard\ Insolation = \text{——} \quad (2.5)$$

2.2.1 Theoretical Efficiency Limit

The single-junction solar cell is limited in its theoretical efficiency by the Shockley-Queisser (SQ) limit, which defines about 33% as the upper limit under standard sunlight conditions (AMI. 5 spectrum)(Giebink et al., 2011). This is because not all solar energy can be efficiently transformed into electric energy. One of the primary sources for this is thermalization loss, in which high-energy photons with energies much larger than the semiconductor bandgap excite the electrons into higher energy states of the conduction band(Javadi, 2020). The additional energy, however, cannot be utilized, and will dissipate as heat in the material.

Another efficiency sink is transmission losses by which sub bandgap photons do not have enough energy to excite the photoelectrode electrons and simply pass through the material, without absorbing. In Si, for instance, infrared photons with wavelengths longer than about 1100 nm are a major contribution to this loss process(Giebink et al., 2011). In addition, recombination losses are also crucial, because the electron hole pairs created by photon absorption can recombine before they reach

the terminals. This recombination can occur via radiative or non-radiative channels and decrease the carrier collection efficiency of the solar cell.

Because of these loss mechanisms all single-junction solar cells cannot exceed the SQ limit. This natural limit inspires the intense study of multijunction solar cells (MJSCs) as the GaAs/AlGaAs/Si MJSCs. When different bandgaps are stacked against one another, it is possible to both absorb and use a larger portion of the solar spectrum in a multi-junction device, thereby surpassing the limit to efficiency of a single-junction device, and reaching the pathway toward the ultra-high efficiency photovoltaic technologies(A. Luque & Hegedus, 2011).

2.2.2 Loss Mechanisms in Solar Cells

Beyond the theoretical Shockley-Queisser limits, practical solar cells also suffer from additional losses that lower their practical performance in real operation(Hirst & Ekins-Daukes, 2011). One significant of these categories is the optical losses, which result from surface reflection and incomplete absorption of incoming sunlight in the absorber layer. Unmitigated, up to 30% of incident solar radiation can be lost via surface reflection(Hirst & Ekins-Daukes, 2011). To mitigate this, methods such as antireflection coatings (ARCs) and surface texturing are often utilized, so that additional photons are coupled into the device.

Another significant category is recombination losses, where excited carriers do not contribute to the photocurrent. These pathways can be classified into three broad mechanisms. Radiative recombination is when an electron recombines with a hole, emitting a photon, and is the typical loss mechanism in direct bandgap semiconductors such as GaAs (Mackenzie et al., 2016). In the case of SRH recombination, trap states within the bandgap scatter carriers and influence the recombination process by modifying the carrier chemistry, whereas fairly insignificant recombination is allowed in the direct process. In the case of Auger recombination, on the other hand, the recombination energy is directly transferred to some other electron or hole which immediately releases this energy as heat (S. Wang et al., 2022). Auger recombination is especially significant to highly-doped materials hence an optimization of the doping levels is necessary.

Last, the resistive losses also lower the conversion efficiency of the solar cell. These are typically described as series resistance (Rs) and shunt resistance (Rsh). High-series resistance owing to the resistive elements in the semiconductor layers, metallic contacts, or interconnections results in sulfuration of FF and maximum power output (Lei et al., 2022). On the other hand, a low shunt resistance can provide undesired leakage across the junctions as well as it may increase inefficiency of the cell. In order to describe these effects, a simplified equivalent circuit model is employed, in which the solar cell is modelled by a photocurrent source in parallel with a diode, and addition with the series and shunt resistance Rs and Rsh. This model yields a description of the ideal and practical behavior of a solar cell(Lei et al., 2022).

2.3 Gallium Arsenide, GaAs

GaAs is known as a semiconductor, with an energy bandgap of 1.42 eV as in Table 1 making it a popular choice for solar cells. Figure 2.5 shows the crystal structure of the GaAs. GaAs-based solar cells have been broadly used over Si-based semiconductors for the respecting reasons which are direct bandgap, higher carrier mobility than silicon, ability to withstand a higher temperature gradient than silicon, and higher absorption coefficient compared to silicon (A. Luque & Marti, 2011). Additionally, GaAs semiconductors have bandgap values that align well with the optimal absorption range for various technology. These features, combined with their attributes have resulted in GaAs being widely utilized in various fields such as optoelectronics, microwave devices, and power electronics. In summary, GaAs semiconductors provide a foundation, for creating high-performance devices in technological sectors (Devendra et al., 2020).

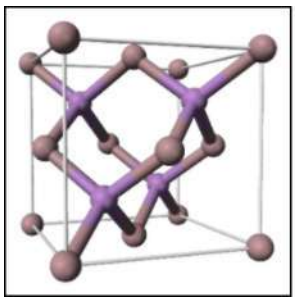

Figure 2.5 Crystal Structure of GaAs
(Blakemore, 1982)

GaAs has a variety of features which make it well-suited for semiconductor applications as the properties shown in the Table 1. It has an utmost refractive index of 5.0 at photon energy = 3.1 eV, indicating how slow light propagates through the medium compared to free space vacuum (Akinlami & Ashamu, 2013).

Table 2.1
Physical and semiconductor properties of GaAs (Inspec et al., 1996)

Properties	GaAs
Formula weight	144.63
Crystal structure	zinc blende
Lattice constant	5.6532
Melting point (°C)	1238
Density (g/cm^3)	5.32
Thermal conductivity (W/cm.K)	0.46
Band gap (eV) at 300 K	1.424
Intrinsic carrier conc. (cm^{-3})	1.79×10^6
Intrinsic resistivity (ohm.cm)	10^8
Breakdown field (V/cm)	4×10^5
Minority carrier lifetime (s)	10^{-8}
Mobility ($cm^2/V.\ s$)	8500

Furthermore, with a high thermal conductivity grade, GaAs can transfer heat extremely well which is essential in order to avoid overheating in electronic equipment (Plante & LaPierre, 2008). The zincblende crystal structure of GaAs is attributed to many of its exclusive electronic and optical properties, such as the enhancement in performance of various applications.

With respect to optical properties, GaAs absorbs infrared light very well but is transparent for visible light, ideal for devices like lasers and photodetectors. Despite its chemical stability, GaAs can be susceptible to moisture, so must be handled carefully to prevent degradation (Plante & LaPierre 2008). The actual part of the optical conductivity shows a peak value of $14.2 \times 10^{15} s^{-1}$ at 4.8 eV, whereas the invented part reveals its maximum value at $\sim 6.8 \times 10^{15} s^{-1}$ observed around 5.0 eV suggesting light conducting behaviour (Akinlami & Ashamu, 2013).

Moreover, doping GaAs with impurities like silicon to create n-type conductivity or zinc to yield p-type conductivity makes it possible for engineers to modify its electrical properties and manufacture features like p-n junctions that form the foundation of many semiconductor devices. That is why GaAs has become an important material for electronics and optoelectronics (Martin et al., 1991).

2.4 Aluminium Gallium Arsenide, AlGaAs

In the multi-junction solar cell structure, bandgap of aluminium gallium arsenide (AlGaAs) as 1.81 eV is inserted intentionally to see a descending order of band gaps (AlGaAs/GaAs/Si), for increased absorption of the spectrum and extracting more current from the incoming photons. Figure 2.6 shows the crystal structure of the AlGaAs. In addition, the usage of double anti-reflective coating (DLARC) helps to diminish surface reflections and suppress the recombination at the back AlGaAs layer. The important role played by the AlGaAs layer is demonstrated in improving solar cell efficiency and performance. The all-important AlGaAs material in the solar cell design acts as a high band gap window layer. This causes the solar to help in the efficacy of the cell (Humaidan et al., 2022).

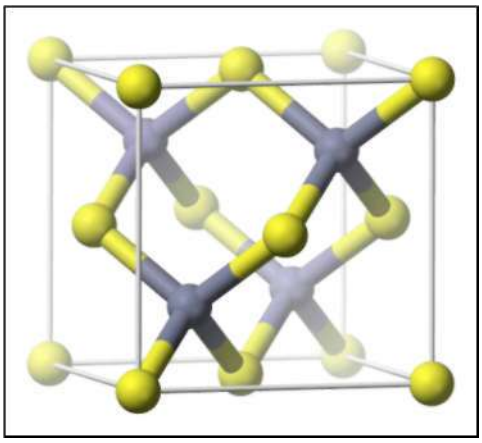

Figure 2.6 Crystal structure of AlGaAs
(Shenai-Khatkhate et al., 2004)

The lattice mismatch of AlGaAs and GaAs is 0.2% almost negligible at room temperature. This provides a chance for the epitaxial growth of high-quality AlGaAs films on GaAs substrates, thereby keeping interface defect densities low during the deposition of heterostructures (Nair & Dhoble, 2021). This high electron mobility in AlGaAs ensures very efficient transport of charges within solar cells. This direct band gap is what allows for efficient sunlight absorption and conversion to electricity. In addition, AlGaAs has surface passivation properties that suppress recombination losses of charge carriers. It is also compatible with high-quality epitaxial growth and can be used to develop the performance and efficacy of solar cells (Righini & Enrichi, 2019).

Qiao et al. (2013) carried out an analysis of the thermal properties of AlGaAs/GaAs laser diode bars using a transient thermal system. For efficiency, this requires that the transient temperature rise be computed and the thermal crosstalk between emitters is understood (Qiao et al., 2013). The AlGaAs chip dimensions are invariant to temperature and its effective thermal diffusivity (0.18 cm^2/s) is measured reproducible for all operation shortcuts conducted over the measurement process lifetime, indicating stable thermal properties of heat conduction in the material chip (Qiao et al., 2013).The AlGaAs interlayer facilitates better electrical characteristics and light detection performance to be employed as a photo-device (Gullu et al., 2024).

2.5 Silicon

Silicon is easily accessible and has suitable properties that can be used to make solar cell. They can be divided into two types: intrinsic and extrinsic. Extrinsic silicon is a semiconductor composed of dopant. An intrinsic silicon is an innate semiconductor with no contaminants added to enhance conductivity. Figure 2.7 shows the crystal structure of the silicone. A semiconductor is a type of substance, such as silicon or germanium that can be used to create electrical and protecting devices. The semiconductor substances provide very little confrontation to the current of the electric carrier.

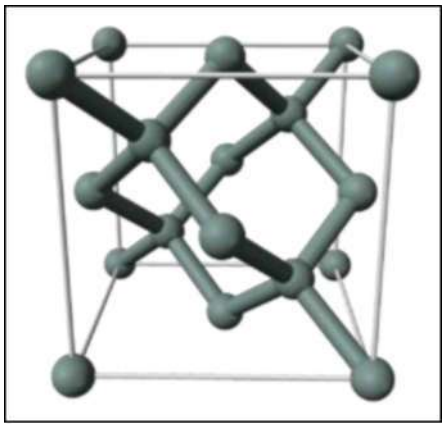

Figure 2.7 crystal structure of silicone
(Arblaster, 2018)

Furthermore, the semiconductor could turn as an insulator, totally blocking the flow of electric current. Silicon semiconductors are more commonly consumed than

Germanium semiconductors. Silicon is easily accessible and has an infinite element and some electric insulators that can be used to make solar cells.

2.5.1 Electrical Properties of Silicon

A member of the fourth group of the periodic table, Silicon shares diamond's crystal structure. In a tetrahedral shape, each silicon atom establishes covalent bonds with four of its close neighbours. The melting point is 1420 ℃, and the specific gravity is around 2.4. There is approximately a 13 dielectric constant. If there are impurities present, the conductivity will change at room temperature. A resistivity of roughly 10 *o,cm* is thought to be the ideal value for pure silicon (Dolecek et al., 1954).

The PN-junction prevents the merger of the electron and hole. To give the electron carriers a path to combine with the hole, the external circuit must be connected simultaneously. If the Silicon solar cell has been exposed to sunlight, carriers will always produce. The two mobility carriers that make up Silicon material are holes in the valence band and electrons in the conduction band. The energy band gap divides the valence band from the band of conductors. 1.12 eV is the energy band for Silicon material (Klimm, 2014). The electron continuously transitions between the valence band and conduction band in these regions. An electron-hole pair fades away because of recombination when an electron moves from the conduction band to the valence band.

The energy of the recombination will manifest as a light photon. In contrast, a valence electron will transfer to the conduction band and produce an electron-hole pair when it absorbs energy equivalent to the band gap. Reliant on the energy input throughout the development, in research from Tayyib et al claims that the electron-hole pair can be formed in a variety of origination types, including photo generation, thermal generation, and ionization impact (Tayyib et al., 2013).

2.6 Multi-Junction Solar Cells (MJSCs)

Gallium Arsenide (GaAs) and Aluminum Gallium Arsenide (AlGaAs) have recently arisen as excellent materials for photovoltaics owing to their great potential in converting solar to electrical energy. These materials exhibit a higher absorption coefficient than standard silicon and can therefore still efficiently convert sunlight even when used in very thin layers(Bahrami et al., 2013a). In addition, this property of not only omits the waste materials with the implement of the device, but also lowers the used material, and the costs there of as compared to the prior art, so that the resulting device can be thinner and more economical.

GaAs/AlGaAs has a significant advantage, in particular, since the technology is compatible with silicon (Si)(Goryashin & Sidorov, 2013). This hybrid strategy paves the way to multi-junction solar cells that utilize the best aspects of each material. By layering cells that are in materials that matterials respond to different frequencies of sunlight, these systems can far exceed the capacity of conventional silicon-only solar cells. These types of hybrid systems are currently being investigated in different fields of application, from terrestrial power to space harsh environments(Laurent, 2016).

Efficiency serves as the cornerstone of solar cell performance, and GaAs/AlGaAs-based multi-junction cells have demonstrated remarkable results, achieving efficiencies exceeding 40% under concentrated sunlight(Z. Wang et al., 2022). This performance places them among the highest-performing solar technologies available. In contrast, traditional silicon photovoltaic cells typically achieve a maximum efficiency of around 22%, highlighting the substantial gap that GaAs/AlGaAs devices effectively bridge.

The key contributor to this performance is bandgap engineering. By carefully adjusting the composition of GaAs and AlGaAs layers, researchers can optimize their bandgaps to capture a wider range of the solar spectrum. This design reduces energy losses due to heat and non-ideal solar conditions, thereby enhancing overall efficiency(Sandhu & Thakur, 2017). Moreover, multi-junction cells display greater resilience to variations in temperature and solar spectrum compared to silicon cells, making them more reliable for deployment in a wide range of environmental conditions.

Based on these material merits, this paper addresses GaAs/p-Si and AlGaAs/p-Si solar cell structures, and searches for the remarkable enhancements of the cells'

performances using systematic simulations and optimizations. By integrating the excellent absorption and bandgap engineering properties of GaAs/AlGaAs devices with the mass-production capability and mechanical robustness of silicon, new optimized device designs are sought that offer an efficient balance between performance and complexity. Moreover, Anti-Reflection Coatings (ARC) are taken into account in order to minimize the optical losses at the front surface and enhance.the light coupling into the device. Utilizing PC ID simulation, the layer thicknesses, doping concentrations and ARC scheme have been investigated in order to facilitate study aim of optimizing efficiency and offering further guidelines for high-efficiency heterojunction solar cells.

2.7 Parameter

In solar cell analysis and design, many different physical and electrical parameters play an important role in determining device efficiency. Key among these are the wafer thickness, which affects the amount of light absorption; thicker wafers tend to absorb more photons, possibly increasing the short-circuit current (JSC), but may also introduce more recombination centers and increase material costs

2.7.1 Thickness

Sub-cell thickness in multifunction solar cells is important for balancing optical absorption and electrical behaviour. Usually, the thickness is selected such that majority of the incident photons would have been absorbed on a specific energy range or an equivalent range to the sub-cell's band gap. But if the layer is too thick, photogenerated carriers have to travel longer before being collected at the contacts leading to higher chances for recombination and hence reduction in efficiency (Sathya & Supriya, 2017).

There is also a way to maximise light absorption while minimising carrier recombination as solar cells designer simply need the absorber to be as thick as possible but certainly no more than several microns. This increases the likelihood of the generated electrons and holes participating in the generation of electric current, as

opposed to recombining prior to collection. Thinner layers are also useful in the preservation of material quality and the strength of the cell especially for multijunction cells comprising layers of different materials arranged in series (Sathya & Supriya, 2017). Figure 2.8 is a diagram of the GaAs/p-Si solar cell. In this work, the base layer of the solar cell was made of p-Si while the emitter layer was made of n-GaAs.

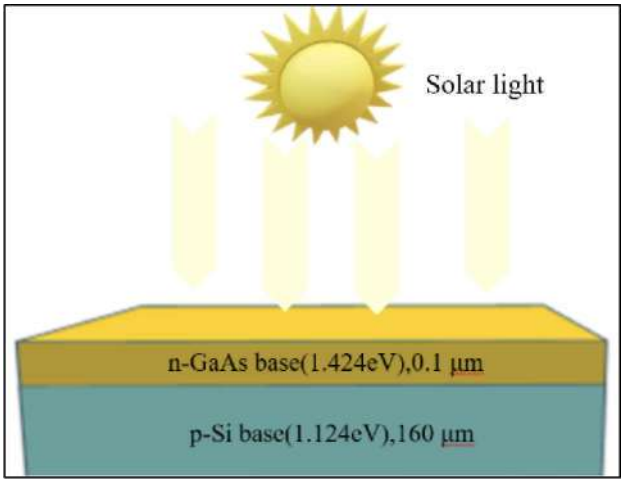

Figure 2.8 A diagram of GaAs/p-Si based solar cell.

The window layer, typically composed of N-type GaAs, enacts a vital part in reducing recombination rates and improving efficiency. By regulating the thickness of this layer, researchers can control the light absorption and carrier generation within the solar cell (Bhusal, 2024). The emitter layer, usually made of N-type GaAs as in the Figure 2.7, is responsible for facilitating the extraction of photo-generated carriers. These affect the efficiency of carrier collection and electron-hole pair separation within the solar cell (Bhusal, 2024). The base layer, typically P-type Si, assists as the region where electron-hole pairs are created and separated (Bhusal, 2024). The Back Surface Field (BSF) Layer, composed of P-type Si, helps reduce surface recombination velocity and develop the inclusive efficacy of the solar cell devices. Table 2.1 shows some works that involves the thickness but using a different material.

Table 2.2
Previous work involves the thickness using PC ID simulation

Materials	Thickness (urn)		References
	N-region	P-region	
GaN/p-Si	0.1	150	(Khairuddin et al., 2023)
GaAs/p-GaAs	0.1	30	(Singh et al., 2022a)

In conclusion, each sub-cell thickness is effectively adjusted to balance between the efficient light absorption and low electrical loss, while maintaining their physical integrity, resulting in the improved photovoltaic performance of the multijunction solar cells.

2.7.2 Doping Concentration

Doping concentration involves deliberately presenting contaminations into a semiconductor substance to adjust its electrical characteristics. For solar cells, doping concentration is a key factor in shaping the efficiency and functionality of the device (Humaidan et al., 2022). The doping density in the base layer (p-type GaAs) is one of the most important parameters that should be closely adjusted for achieving excellent modification effectiveness in a solar cell (Bhusal, 2024). Solar cell efficiency was driven by doping concentration of window layer and absorber layer. In 2020, Devendra et al. wrote PC ID software for 4-layer AlGaAs/GaAs solar cells. The n-AlGaAs served as the window layer, n-GaAs was the emitter layer, p-GaAs was the base layer, and p-AlGaAs was the back surface field (BFS) layer. The research based on investigating the influence of variation in the base layer doping concentration and thickness was conducted.

Optimizing doping levels for each layer in multi-junction solar cells is essential for each of the layer's performance. For example, the window layer (n-AlGaAs) is normally of a low resistivity with high doping in order to reduce the resistivity and allowing the carriers to be rapidly transported. A heavier doping for this region assists in the suppression of the surface recombination so that more of the incident photons can be absorbed in the absorber (Sozzi et al., 2014). Moderate doping of the n-GaAs emitter layer is essential to trade-off conductivity and recombination at the junction. In practice,

the bottom layer (p-GaAs or p-Si) is usually weakly doped to extend carrier lifetime, as well as acting as the dominant absorption region where the majority of the e-h pairs are generated(Kamdem et al., 2019). Back surface field (BSF) is generally the highly doped layer at the rear surface to reflect minority carriers back to the absorber region, so recombination in the rear surface can be reduced while current collectability is enhanced. This layer-by-layer doping strategy emphasizes the necessity of controlling the doping concentration in each sub-layer of the device (Shah et al., 2021).

Carrier lifetime and the impact of recombination losses can be affected by the level of doping in the solar cells. In case of very high doping, it may even increase Auger recombination, the phenomenon of energy going from one type of carrier to another instead of participating in the generation of current (Schygulla et al., 2023). This drastically decreases the minority carrier lifetime causing a decrease in the short circuit current density (Jsc) and overall efficiency. On the other hand, if the doping concentration is too small, the conductivity of the semiconductor decreases, thus leading to the resistance loss and the inefficiency of carrier transportation(Shah et al., 2022). The necessity of well-controlled doping level in GaAs- and AlGaAs-based solar cells is hence clear to obtain high carrier mobility and adequate carrier lifetime for photogenerated carriers to transit the junction to avoid recombination.

This fine balance is usually kept by doping levels chosen in between $lxlO^{15}$ $cirr^{3}$ and $lxlO^{16}$ $cirr^{3}$ in the different layers, as in the present simulations. The careful tuning of these thicknesses also has a direct impact on the carrier densities, the internal electric field of the device, and ultimately on the PV performance of the AlGaAs/GaAs solar cell. Table 2.2 shows some works that involves the doping concentration but using a different material.

Table 2.3
Previous work involves the doping concentration using PC ID simulation

Materials	Doping Concentration (cm''^{3})		References
	N-region	P-region	
GaN/p-Si	$lxio^{18}$	$lxlO^{17}$	(Khairuddin et al., 2023)
GaAs/p-GaAs	$lxlO^{17}$	$lxio^{16}$	(Singh et al., 2022a)

2.7.3 Anti-Reflection Coatings (ARCs)

ARCs are essential for reducing reflection through manipulating light phase changes and leveraging the relationship between reflectivity and refractive index. The application of ARCs is aimed at reducing optical losses in solar cells, ultimately enhancing their conversion efficiency significantly(Hashmi, Rashid, et al., 2018a).

Anti-reflective coatings (ARCs) improve solar cell performance by diminishing reflection losses and enhancing light absorption. These thin films are intended to reduction the quantity of light reflected from the solar cell's surface, granting lighter to pass into the cell and be converted into power. ARCs are widely utilised in semiconductor technology to address concerns with light reflection. Researchers hope that by attaching ARCs to solar cells, they would improve their overall performance and energy conversion efficiency.

A selection of ARC materials is crucial to the performance of ARCs. Dielectric and transparent conductive oxides used are, for example, silicon dioxide (SiCh), silicon nitride (SisN4), titanium dioxide (TiCh), zinc oxide (ZnO), aluminum oxide (AI2O3) and magnesium fluoride (MgF2). Each of these materials has different benefits in refractive index, optical transmittance, chemical stability and cost. For example, SisN4 is routinely employed in commercial silicon solar cell technology, not only due to its optical behavior, but also due to its ability to passivate the surface (Fedawy et al., 2018). Conversely, ZnO and indium tin oxide (ITO) serve as both ARCs and transparent conductive electrodes, providing multi-function for the advanced device configurations(Balent et al., 2022).

ARCs operate under the principle of light interference, for which engineered thin films are deposited to suppress reflection at the air-semiconductor interface. Part of the light incident on the solar cell surface is reflected back because of refractive index difference between air and the absorber material (Hashmi, Rashid, et al., 2018a). ARC is designed to have the reflected light waves from the upper and lower surfaces of the coating and thereby the resulted destructive interference between them. This leads to maximal photon transmission into the absorber layer and ultimately to the production of a maximum amount of charge carriers (Shanmugam et al., 2020). The level of effectiveness is highly dependent on both the refractive index and the coating physical thickness which can be tailored to the desired wavelengths of the solar spectrum.

The selection of ARC material heavily influences the performance of solar cell. The best material must have an intermediate refractive index between the one of air (1.0) and the absorber material, which, for semiconductors as silicon or GaAs, ranges between 3 and 4 (Martin et al., 1991). Furthermore, the coating should have wide optical transparency to the vast majority of the solar spectrum, particularly the visible and near-infrared range where most solar energy is. Environmental and chemical resistance is also crucial, because the coatings work for an extended period of time outdoors where they are subjected to water vapor, dust and UV light (Channa et al., 2022). Therefore, for industrial applications, it is desirable to prefer materials with a high durability, strong adhesion, and degradation resistance.

Fabrication techniques applied to ARCs also greatly affect their work performance and market practicability. For deposition of thin and uniform films, techniques such as chemical vapour deposition (CVD), atomic layer deposition (ALD), sputtering and sol-gel processes are commonly used. Of particular interest, ALD is capable of depositing highly conformal nano-scale dense semiconductor thin films with excellent uniformity, which is essential for high-efficiency solar cells (Saari et al., 2022). However, for large scale commercial applications low cost and high throughput technology is generally sought which makes a compromise deleterious to precision, price, and longevity (Sun et al., 2021).

While being beneficial, ARC also has its challenges and drawbacks. One coating cannot completely suppress the reflection over the full solar spectrum (from 300 to 1200 nm for most of the cells). Furthermore, it is possible that, through time, the performances of such coatings deteriorate due to the surface contamination, UV-induced degradation or damage from thermal cycling. There is also a trade-off between optimizing optical performance and providing mechanical stability over the long term, since harder coatings tend to crack when subjected to stress (X. Wang et al., 2021).

In addition to classical designs, new generations of ARC designs (advanced ARC) are being developed to enhance performance beyond these limitations. Inspired by natural moth-eye surfaces, nanostructured coatings utilize gradually varying refractive indices through nano-patterns to minimize reflection over broad spectral ranges and a range of angles of incidence (Plante & LaPierre, 2008). Graded-index ARCs (GARC) having continuously changed refractive index in their thickness direction have also attracted attention for the broadband anti-reflection application. One

promising approach for simultaneous optical performance and mechanical flexibility are hybrid inorganic-organic designs (Sathya & Supriya, 2017).

More generally, the issue of ARCs is not simply a question of making things look good, it's also a question of the bottom line. By introduction of more light into the cells, ARCs increase the power yield of a solar cell without adding much cost, ultimately reducing the levelized cost of energy (LCOE). ARCs also serve as protective barriers to reduce surface degradation and contamination; thus, achieving a long module lifetime. Trends toward superiority and low cost of the solar power industry require that the development of broadband and durable ARCs at a low cost becomes an active research area.

2.7.3.1 Single layer coating (SLARC)

A variety of ARCs, including single layer ARCs (SLARCs), double or bilayer ARCs, and even triple layer ARCs, are used in research to assess their efficiency in improving efficiency of solar cells (Parajuli et al., 2023) . Silicon dioxide (SiO2), magnesium fluoride (MgF2), titanium dioxide (TiO2), zinc oxide (ZnO), and other materials are routinely used for ARCs, each with their own set of qualities that can affect solar cell efficiency. Typical SLARC materials include SiO2, MgF2, TiO2, ZnO, and a variety of other elements suitable for this research. Materials used for bilayer ARC consist of MgF2/SiO2, Al2O3/TiO2, and MgF2/ZnS, while MgF2/Al2O3/ZnS and GaInP/GaAs/Ge are examples of triple ARC materials (Jamaluddin et al., 2024a).

For instance, glass and transparent plastic with anti-reflective coating that has a refractive index of about 1.5 require a film material with a refractive index of 1.22 with a quarter wavelength thickness. Materials with a refractive index lower than 1.22 are insufficient, and typically such low refractive index is achieved by stacking multiple layers. Figure 2.9 shows the illustration of the diffusion of light in single layer thin film. It is not possible to achieve zero reflectance with a single layer. The figure 2.10 shows A diagram of GaAs/p-Si based solar cell. SLARC is typically developed to slightly reduce the reflection to about 2.5% at normal incidence for a wide spectral range, from 450 to 1100 nm (Shanmugam et al., 2020).

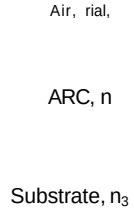

Figure 2.9 The illustration of the diffusion of light in single layer thin film.

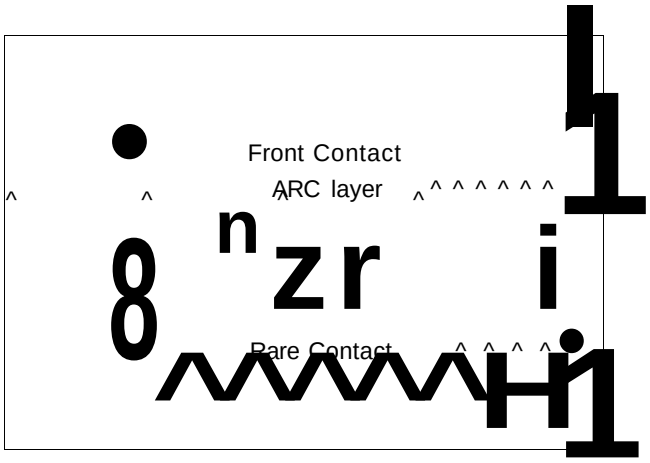

Figure 2.10 A diagram of GaAs/p-Si based solar cell with 1 layer of ARC.

The anti-reflection coating (ARC) had the greatest improvement in efficiency in this simulation. To develop the ARC layer, the following equations (Luque & Hegedus, 2011) were used to compute its thickness and refractive index. Refractive index of ARC,

$$T|ARC = V (T|air * r|Si(Ao)) \quad (2.6)$$

Thickness of ARC,

$$d= Ao/4*T|ARC \quad \textbf{(2.7)}$$

where T|ARC is the refractive index of ARC and r|$_a$ir is the refractive index of an ARC for a certain wavelength (Ao) (Hashmi, Rashid, et al., 2018b). Further examination of Eq. (6) reveals that the refractive index of ARC is affected by mutually the refractive index of air and the wavelength-dependent refractive index of the particular anti-reflection coating (Hashmi, Rashid, et al., 2018b).

Simplicity is one of the most important advantages of a SLARC. Because a single thin film is needed, the manufacturing process is less complicated and more cost effective than that of double- or triple-layer coatings. SLARC is therefore particularly attractive when budget constraints are an issue or where large-area deposition is necessary, for example, for commercial photovoltaic modules(Bahrami et al., 2013b). The deposition is quicker, and therefore easy for manufacturers to ramp it up.

However, despite these advantages, SLARC structures have a serious drawback: they are only useful at a single wavelength and near normal incidence (Parajuli et al., 2023). For increasing values of the angle of incidence (or as the wavelength of the incident light moves away from the design point), the reduction in the reflectance is not effective. For instance, a SLARC designed in the green region of the solar spectrum (550-600 nm) will not work as effective in the near-infrared or ultraviolet, where the reflection losses can still be large (Sharma et al., 2017). This is the fundamental reason why bi-layer and multi-layer coatings are widely adopted in current high-efficiency solar cells.

The deposition technique as well has an influence on the behaviour of SLARC. Techniques like PVD, CVD, sol-gel processing, and ALD have been widely used. ALD is one of these processes, and it is known for its extreme thickness control, so it is suitable for research, whereas sol-gel processes are a cost-effective approach for large area coating of glass substrates(F. Liu et al., 2025). The type of deposition chosen for the coating also affects its optical performance, as well as its adhesion, surface quality, and environmental durability.

Excepting for solar cells, SLARCs have been extensively used in other optical devices. For example, if it's eyeglasses, camera lenses, optical sensors and display screens, all tend to employ single-layer coatings to minimize the glare and even to enhance light transmittance. In such practical systems, the limited operation band is not a is not a severe problem because such devices usually work at a specific wavelength at fixed wavelength or under certain illumination source. In photovoltaics, the solar

spectrum is broad and the multilayer approaches are more appropriate to achieve a maximum efficiency(Goryashin & Sidorov, 2013).

In addition, there have been some studies on the research of SLARC structures to avoid the narrowband problem. Inspired from the natural "moth-eye effect," nanostructured coatings were fabricated to offer gradual transition of refractive index from air to substrate (Sulciute et al., 2021). These graded-index films may considerably widen the antireflection effect, leading to better performance in the visible as well as the near-infrared regions. These are even more difficult to manufacture, but are potentially promising for the future of solar.

2.7.3.2 Double Layers Anti-Reflective Coating (DLARC)

Apart from the single ARC model, there are numerous different coating models. Among them are the double-layer ARC model. The efficiency of a solar cell is also influenced by the angle at which the surface and the solar panel itself are inclined, aside from the coating. Sharma et al. 2019 researched Double Layer ARC (DLARC) of Si3N4 at a number of angles, where the angle of incidence was related to the angle of reflection. The adaptation efficacy reduced by 1.7% with the rise of the angle from 0° to 60° (Sharma et al., 2017). Maiga et al. 2012 experimented the DLARC and angle and initiate them beneficial to the single-layer ones (Beye et al., 2013).

DLARC comprises of two layers of the same or different thickness on the substrate to produce antireflection characteristic. Use of DLARC or bilayer anti-reflection coatings are used to minimize the effect of reflection to greater degrees; additionally, the many layers often adhere to any rough substrate, which helps to minimize reflection (Dhungel et al., 2006). DLARC was designed to minimize reflection from solar cells that is, to estimate the efficiency of the incident rays and the efficiency is much greater than single layer anti-reflection coating (Battaglia et al., 2016).

To achieve zero reflectance with double layer AR coatings of equal film thickness, one condition must be met: m/m = V(no/n_s), where nl and m correspond to the refractive index of two layers, ns_s is the substrate refractive index, and n_0 is the refractive index of air, which is unity. DLAR coating could reduce the effective reflectance significantly, which were close to zero at the design wavelengths but

increased with increasing wavelengths. Thus, a V-shaped reflectance curve was seen in the range of the tested wavelength.

The optimization of a double-layer antireflection coating relies heavily on the selection of materials to be used in each layer. In practice, the researchers usually pick combinations of a high-refractive-index material and a low-refractive-index material to obtain a specific interference effect (Dhungel et al., 2006). Examples include magnesium fluoride (MgF2) or silicon dioxide (SiCh) as low-index materials and titanium dioxide (TiCh), aluminium oxide (AI2O3) or zinc oxide (ZnO) as high-index layers in each case (Dhungel et al., 2006). The different refractive indices are far from perfect for reflection over a range of wavelengths as opposed to a single-layer coating. Additionally, ZnO and Ti02 are commonly used in photovoltaic applications due to their transparency, chemical stability and low cost of deposition(Ali et al., 2014).

Another key feature of DLARC is the method of construction. Exact control of the thickness is necessary to achieve the effective destructive interference of a reflected light. Various deposition processes are used, including techniques such as PVD (physical vapor deposition), CVD (chemical vapor deposition), sputtering, and ALD (atomic layer deposition). Of these GI material transfer, ALD is a particularly promising method for solar cells because it provides atomic-level control over layer thickness, has good conformality on rough surfaces, and is able to cover a very large area (F. Liu et al., 2025). These fabrication methods also affect the coating's durability and environmental stability, which are key aspects for long-term outdoor usage.

Not only does DLARC enhance optical absorption, but also it has more merits in reliability. The bilayer construction can provide an improved resistance to a surface degradation from ultraviolet radiation and temperature cycling and also to moisture and dust contamination (Sharma et al., 2017). This is especially important for photovoltaic modules used in the outdoors where they must maintain spectral performance over the course of many decades to remain commercially competitive. Furthermore, multilayer coatings are frequently more durable, and are bound more effectively to rough or textured silicon substrates relative to single-layer coatings (Saari et al., 2022).

The application of the DLARCs is not restricted to solar cells. They are broadly employed in optical and photonic devices, including camera lenses, photodetectors, light emitting diodes (LEDs) and more particularly, laser optics, as backward reflections can drastically affect system performance even when reflection losses are quite small (Ji et al., 2022). Both narrow and wide spectra reflective performances enable them to

be essential to high performance optical systems. This so-called "V-coating" property of DLARCs is especially useful for applications in laser optics, where the coatings can be designed to have low reflectance values at a specific wavelength (Mercy & Wilson, 2024).

Although these benefits, DLARCs are also faced with a number of challenges. Highest performance might not be achieved at very high angles of incidences or outside the bandwidth for which their design is optimized. Moreover, the additional processing involved in the multi-layer of the coatings usually results in a higher cost than the single-layer schemes (Dhungel et al., 2006). However, material pairs, deposition pathways, and design strategies are being further developed to reduce cost while maintaining performance. Therefore, DLARCs are still a hopeful candidate for next generation photovoltaic and optoelectronic devices.

2.7.4 Properties of ARC

Because ARC materials vary in thickness and refractive index, different ARC materials produce varying results for the solar cells. Optimizing the efficiency, cost-effectiveness, and performance of solar cells under a range of conditions requires the use of various materials for ARC. It helps identify the best materials for specific uses, expedites the production process, and promotes innovation in solar technology. By researching different types of materials, researchers may be able to go beyond what is now possible in solar energy and contribute to the development of more efficient and cost-effective renewable energy solutions.

In the absence of being reflective, the optical and structural features of the ARC materials are the principal parameters which characterize them. An ideal ARC is supposed to have high optical transparency over the solar spectrum, particularly in the range of 300-1200 nm with respect to the case of silicon-based cells, so that the incident photons can easily transmit into the absorber layer(Shanmugam et al., 2020). Materials with a wide bandgap, like ZnO or Ti02, are preferred being non-absorbing and have low reflectance. Another important optical parameter is the refractive index contrast. In order to realize destructive interference for reflected waves, most ARCs are fabricated by the quarter-wavelength structure, and the thickness of the material is precisely adjusted to the target wavelength(Parajuli et al., 2023). This guarantees broadband AR

performance, which is quite useful for practical applications in different lighting environments.

Nanostructured, multifunctional coatings are new achievements based on the ARC studies. For example, roughened ZnO layers serve to reduce reflection and the texturing can also scatter incoming light, thus enhancing the optical path length through the absorber and increasing photon absorption. In a like manner, porous ARCs or gradient-index ARCs have been studied primarily as the broadband-omnidirectional anti-reflection coatings (ARCs) which are superior to the conventional single layer coatings(Hu et al., 2018). As well as in optics, the research on multifunctional ARCs has now extended its applications to surface passivation, hydrophobicity and thermal regulation for overall better performing and longlasting solar devices.

In brief, the functionality of the ARC materials is not limited to the mere anti-reflective features. The optical transparency, refractive index tunability, mechanical robustness, environmental durability, low-cost, and potential for multi-functionality render them a fundamental platform for solar cell adaptation. With the continuing development of research, creative nanostructured and hybrid coatings will be expected to allow to further extend the barriers of the solar energy conversion efficiency obtaining long-term stable and practical scalable(Yang et al., 2021).

Finding materials for the ARC's manufacturing as well as doing research and development on anti-reflective coatings are crucial. In this study, 2 different materials which are ZnO and TiO2 were applied as ARC for the simulation of silicon and zinc oxide solar cell.

2.7.4.1 Titanium Dioxide (TiO2)

The white and opaque organic mineral the titanium dioxide (TiO2) can exist in several crystalline structural forms of which anatase and rutile are the most significant (Patra, 2023). Titanium oxides occur in ores, ore powders, sands, and soils as a product of the spontaneous combination of titanium with oxygen. Titanium is coordinated by 6 oxide oxygen atoms in all its three major dioxides and exhibits octahedral geometry. The oxides later link the three Ti centres. Brookite has orthorhombic crystal structure, and rutile and anatase have tetragonal structures. The crystal structure of TiO2 is given in Figure 2.11.

Figure 2.11 Crystal structure of anatase. Together with rutile and brookite, one of the three major polymorphs of TiCh.
(Alderman etal., 2014)

Titanium has a band gap of 3.2 eV, a relative permittivity (£R) of 85, and an extremely high melting point of almost 1843 °C. After a single coating, all of the films show a transmittance of over 80% in the visible spectrum, meaning they are opaque in the UV spectrum but highly transparent in the visible. Ti02 thin films' exceptional transparency is one factor contributing to their popularity in solar cell applications (Karoui et al., 2015). Ti02 has a refractive index of 2.6142, a dielectric strength of 4 $kVmm^{-1}$, and a thermal conductivity of 11.7 WmK^{-1}. Due to its excellent physicochemical properties and because it can absorb light at many different frequencies, titanium is a promising material for this kind of applications (Battaglia et al., 2016). Ti02 could be used to enhance light absorption and solar cell efficiency through the enhancement of light scattering and trapping.

Ti02 was specifically selected as the optical material of the ARC because it has a much higher refractive index than other optical material films. Combined with a low refractive index difference from the interface of the ARC and the III-V semiconductor solar cells, it is another excellent candidate for the fabrication of the simulated refractive index ARC. Ti02 is an indispensable precursor in typical and promising solar cell techniques as Ti02 possesses good transparency and is nontoxic, chemically stable and mechanically stable as well (Yeo et al., 2015).

The deposition type during fabrication is an important factor in the optical quality of titanium dioxide thin films. Various techniques are known, including sol-gel method, sputtering, atomic layer deposition (ALD), chemical vapor deposition (CVD)

(Ozmentes. & Hassanien, 2025). The sol-gel method, which is low cost and easily prepared and can achieve films with large area and high optical transparency, is widely used. Yet, sol-gel films can be porous as well, the porous structure of which can affect the film's refractive index and stability (Priyalakshmi Devi et al., 2022). On the other hand, dense and adherent T1O2 films can be obtained with (RF)-sputtering and CVD, in which case a long-time outdoor use of solar cells may be foreseen (Saari et al., 2022). ALD is of high relevance for current day photovoltaics because of the atomic thickness control and uniformity it offers for even complex device structures. Such technique is crucial in design of the ARC, as the thickness has to be equal to a quarter of the wavelength of the incident to minimize reflection (Saari et al., 2022). Therefore, the deposition method selected directly determines the performance of Ti02 antireflection coatings.

Ti02 is not only used as an antireflection material, it has also become a multifunctional material in the devices of solar cells. In the dye-sensitized and perovskite solar cells case, Ti02 acts as an electron transport layer (ETL) (Hou et al., 2021). In this function, it can quickly extract photogenerated electrons from the absorber layer to the collector and then blocking holes, reducing recombination process. This joint performance reveals that Ti02 serves not only as an antireflection interface to improve light harvesting but also as a component to facilitate effective charge transport in the device(Yan et al., 2025). Its flexibility is evidenced by the fact that Ti02 is still one of the most widely investigated materials in the context of photovoltaics.

In spite of its superior characteristics, the use of Ti02 in the solar cells has some limitations. Its large band-gap of about 3.2 eV leads to absorption of only the ultraviolet (UV) part of the solar spectrum (about 5%) (Rengifo-Herrera et al., 2022). As a result, it makes Ti02 unable to assist directly in visible or near infrared light harvesting but only optical light enhancement but not photon conversion(Ebanezar John et al., 2024). Moreover, defects like oxygen vacancies can form recombination centres and decrease the carrier lifetime in the adjacent layer (Khlyustova et al., 2021). A second difficulty is related to its high refractive index which can give rise to unwanted interference fringes at specific wavelengths, unless carefully designed. These limitations underscore the significance of further studying the optimization of the performance of Ti02 used in solar energy devices.

In order to solve these problems, a number of enhancement methods for Ti02 films have been introduced by many research groups. One possibility is to dope

chemically the material with elements like nitrogen, carbon or transition metals which lower the band gap and push the absorption edge into the visible region(Khlyustova et al., 2021). Another approach is to nanostructure HO2 in the form of nanotubes, nanorods, or textured surfaces. These nanostructures enhance light scattering and trapping, resulting in even less reflectance than the flat thin film case. Furthermore, when TiO 2 is mixed with lower refractive index materials as bilateral or multilayer ARCs, its AR scope is expanded and the devices-based can efficiently absorb light in the ultraviolet-visible to near-infrared range (Rengifo-Herrera et al., 2022). These advances demonstrate that it is possible to control the material beyond its natural state to suit the needs of future photovoltaics.

A further advantage of TiCh when applied for ARC is the self-cleaning and the durability feature (Lukong et al., 2022). TiC>2 is a common photocatalyst which can decompose organic pollutants under ultraviolet (UV) illumination. When coated on the surface of solar cells, TiCh films can kill bacteria and break down organic materials, thereby reducing dust and dirt while still allowing rainwater to remove these residues(Y. Liu et al., 2024). Along with the excellent self-cleaning function, the high mechanical strength and the chemical stability of the material can long-term keep the optical performance of TiC>2 coatings in outdoor applications(Lukong et al., 2022). This impressive reliability is the reason why TiC>2 is considered a sustainable and low-cost material for use in solar cell production.

Lastly, Ti02 is pointed as material for advanced and tandem solar cells, since the device architecture is more sophisticated than the typical silicon cell. For example, in GaAs/Si, and Pe/Si tandem cells, Ti02 can play the role of ARC as well as a selective contact or buffer layer linking up optical and electronic benefits. This way, researchers could realize concomitant enhancements in light management, charge transport, and stability by incorporating Ti02 into these very efficient device architectures. This double character makes Ti02 not only an attractive next-generation material, but that it will continue to play an important role in the development of photovoltaic technologies.

2.7.4.2 ***Zinc*** *Oxide (ZnO)*

The full name of ZnO is zinc oxide and it is a mineral. It is a white powder that is water repellent. ZnO, and indeed the Earth's crust, contains a ZnO mineral called zincite. However, the bulk of the known industrial uses of ZnO is in the form of synthetic ZnO (Materials, 2011). ZnO material is one of the classes semi products of group IIV-I compound semiconductors, also, has been extensively studied for solar energy applications in the synthesized form as a semiconductor in the field of electronic due to its good electron mobility, stability, high conductivity and strong electron affinity. The crystal structure diagram for ZnO is given in Figure 2.12.

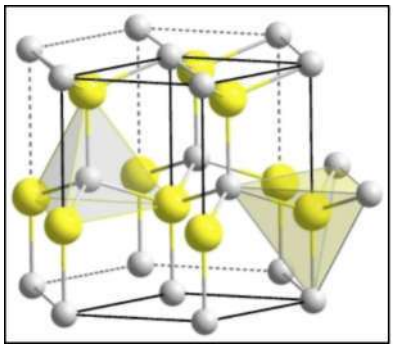

Figure 2.12 crystal structure of ZnO
(Borysiewicz, 2019).

It is to be noted here, that zinc oxide is soluble in dilute acids and in dilute bases, but is absolutely insoluble in water. It has a band gap of 3.37 eV, ultraviolet (UV) emission and also has a high melting point of 1975 °C, at which it decomposes (Zinc Oxide, 2014) (Shimizu, 2013). For example, the dielectric constants of solid ZnO ceramics are from 8.2 to 10.9, and those of ZnO films are from 7.5 to 10 (Alexander et al., 1996). ZnO thin films exhibit relatively high optical absorption coefficient (up to 5 x 104 cm^{-1}) and high transmittance (up to 80%).

The high absorption coefficient of this material might enable it to absorb more photons (Mursal et al., 2018). Room temperature ZnO was found to have n = 2.0034 and G = 7.261 x 10^{-7} S/cm. Introductions of ZnO is a promising dielectric ARC material, as it is highly transparent and allows textured coatings to be formed using anisotropic growth (Lee et al., 2008).

The choice of deposition method in obtaining ZnO thin films is one of the key factors that determine the optical and electrical features of these films. There are several strategies which have been used to prepare ZnO coatings for solar cells, which have their unique advantages. Among them, sol-gel process is favoured with low cost and simplicity, which is applicable to the preparation of large area coating with good uniformity (Khorsand Zak et al., 2024). In contrast, sputtering permits fine tuning of the film thickness and refractive index, which is important when designing an optical anti-reflective layer with an adjusted thickness at a certain wavelength of sunlight(Al-Ariki et al., 2021). Spray pyrolysis and Chemical Vapor Deposition (CVD) are also common, particularly for larger scale production whereas ALD can deliver ultrathin, highly conformal coatings with unmatched uniformity even on complex shapes(F. Liu et al., 2025). The selection of deposition technique is critical to modulate the surface morphology, grain size, and optical transmittance of ZnO, and consequently, the performance of solar cells(Sun et al., 2021).

Apart from traditional thin-film structures, new attention is being turned to nanostructured ZnO such as nanomaterials, nanorods, nanowires and nanotubes. The one-dimensional nanostructures possess higher optical scattering that results in more photons being absorbed by the active layer of the solar cell (Yang et al., 2021). Because of its high surface-to-volume ratio, it is appealing for dye-sensitized and perovskite solar cells, in which it not only can act as anti-reflection layer but also as an electron transport layer(Benkhira et al., 2024). Since the growth of ZnO nanostructures can be controlled in a precise way, it is potentially to form textured ARC surfaces that are effective in reducing reflection over a wider range of wavelengths than can be achieved with the flat ZnO films.

One more notable property of ZnO is that it can work as UV barrier layer. ZnO has a wide bandgap and can effectively block UV, as well as being transparent in the visible range(X. Wang et al., 2021). This feature not only increases the utilization of the visible light but also prolongs the lifespan of the lower absorber due to the UV, which can potentially cause degradation(Irede et al., 2024). In perovskite or organic solar cells, the implementation of ZnO as a protective ARC may largely broaden device lifetime, indicating that ZnO directly endows both efficiency increase and stability improvement.

ZnO, on the other hand, has some disadvantages that need to be solved for its practical usage. Among intrinsic defects, oxygen vacancies and zinc interstitials commonly create mid-gap levels leading to recombination centers that reduce the carrier

lifetime(Vetrivel et al., 2024). Furthermore, ZnO films are hygroscopic, which may result in change of their structural and electrical features in time. A further issue concerns doping as well: doping can improve conductivity, but doping too much can decrease transparency and increase free-carrier absorption, both of which are detrimental to ARC effects (Makableh et al., 2014). These troubles bring the necessity to improve the structural and chemical properties of ZnO in photovoltaic applications into focus.

Several risk realization enhancement mechanisms have been studied to address these limitations. Doping ZnO with aluminum (Al), gallium (Ga), or indium (In) is very effective in increasing the electrical conductivity while retaining high transparency. These doped materials, including Al-doped ZnO (AZO), Ga-doped ZnO (GZO) and In-doped ZnO (IZO), have increasingly been studied as promising alternatives to the conventional transparent conducting oxides. Another possibility would be to mix ZnO with other materials to create multi-layered ARCs; stacks such as ZnO/SiO 2 or ZnO/MgF 2 could extend the anti-reflection range into the solar spectrum (Bahrami et al., 2013b). The texturing of the surface of ZnO/Al also scatters light and reduces reflected losses by bringing incident light at normal incidence onto a sloped graded effective refractive index of ZnO by having such a grooved-like profile (Ray et al., n.d.).

Finally, the economic and environmental benefits of ZnO make it especially fit for industrial application. Compared with ITO and other TCOs that contain rare and expensive components, ZnO is low-cost, abundant in earth, and non-toxic(Channa et al., 2022). Besides, eco-friendly methods of synthesis, such as hydrothermal synthesis and low-temperature chemical method, have been developed to reduce the consumption of energy and the environmental harm. These benefits make ZnO a kind of high-performance and practical ARC material, and also an ideal material for sustained growth of the photovoltaic industry(X. Wang et al., 2021).

2.8 Personal Computer One Dimension (PC1D)

It is critical for any simulation program to keep up with new developments in experimental work, theoretical models, and computer working environments. PC1D is the most widely used simulation program in the photovoltaic community. PC1D has been cited at least twenty times in peer-reviewed journals in the last year (Garfield,

2007). As a result, it is critical that the program's rapid development be maintained. A journal article has already discussed the new free-carrier absorption model and its importance for spectral analysis of cells (Clugston & Basore, 1997). The research also shows that increasing the light-trapping of near bandgap wavelengths is much less advantageous than originally anticipated, which was not covered in that paper. In Figure 2.13 shown the typical device displayed by the PC1D.

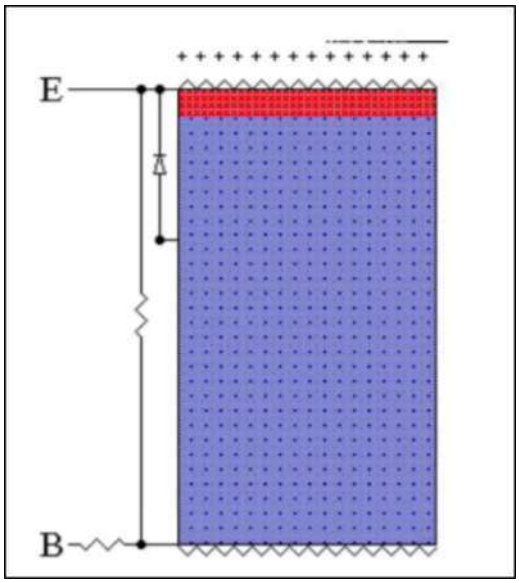

Figure 2.13 The typical device displayed by PC1D
Source: *(Clugston & Basore, 1997)*

PC1D is frequently used to evaluate experimental data to establish the structure of a device. Several critical device parameters can be identified, for example, by matching a calculated IQE curve to an experimental one. Performing such a match in previous PC1D editions was time-consuming. Version 5 enables rapid comparison by displaying experimental data and simulation results on the same graph within PC1D.

The simplicity and efficiency as compared to the complex software of device simulators is one of the motivations of why PC1D is highly used in the photovoltaic field. Rather than complicated software dominated by physics, requiring advanced coding skills such as MatLab, PC1D is built with an easy-to-use Graphical User Interface to quickly prototype different cell designs with little programming. It produces fast computation solutions, and hence suitable for parametric studies involving a large number of simulations(Roshi et al., 2022). Furthermore, PC1D has been widely validated with experimental measurements, making reliable performance predictions.

The software also takes into account other loss mechanisms such as series resistance, recombination losses, and optical reflection, affording users a thorough perception of the limitations of solar cell efficiency(Roshi et al., 2022). Such strengths have made PC ID particularly appropriate for researchers, who want to address the effect from material properties and structrual parameters on device performance efficiently but not in a long period.

Figure 2.14 shows an example of how the PC1D model must utilize a larger value for the rear optical reflectance to match the experimental data at near bandgap wavelengths, and a lower front-surface recombination velocity to match the experimental data at the blue end of the spectrum (Clugston & Basore, 1997).

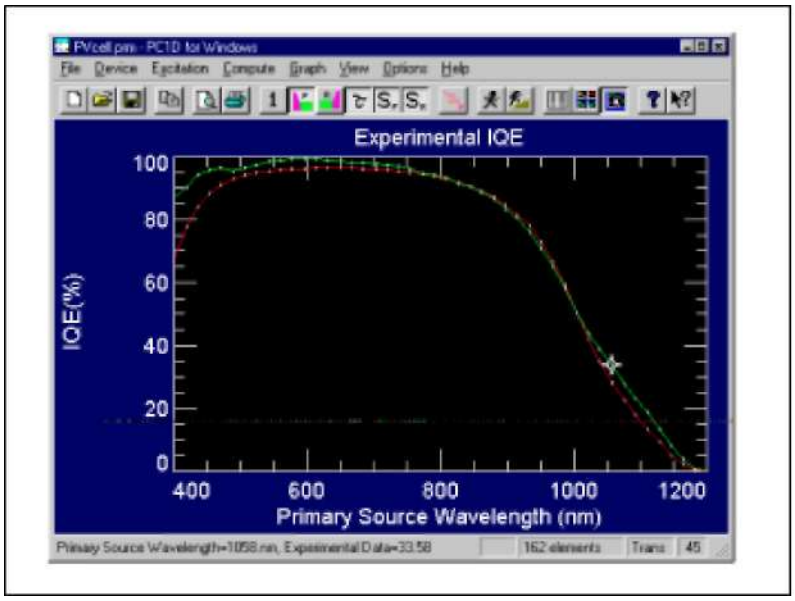

Figure 2.14 Experimental data displayed in PC1D
Source: *(Clugston & Basore, 1997)*

In summary, each simulator has its own advantages and disadvantages when compared with PC ID. For instance, another popular software for that purpose is Solar Cell Capacitance Simulator - 1 Dimension (SCAPS-1D), especially better suited to complex device structures such as in Cadmium Telluride (CdTe), Copper Indium Gallium Selenide (CIGS), or perovskite solar cells. Sentaurus TCAD and Silvaco ATLAS are more complete semiconductor device simulators that can take into account two-dimensional and three-dimensional effects; however, they require proficient

programming capabilities, huge computing resources, and longer simulation time (Saidarsan et al., 2025). Multiphysics simulation with COMSOL Multiphysics, which enables coupled optical-electrical-thermal analysis is an example of a Multiphysics simulation tool, although it is computationally demanding and generally too complicated for typical PV design (Andras et al., 2024). Automat FOR Simulation of Heterojunction Solar Cells (AFORS-HET), the freely available simulation tool for heterojunction devices, offers a more convenient approach to investigate heterojunction structures (Aswad et al., 2021). In this context, PC1D is recognized as a fast, efficient, and user-friendly simulator of crystalline silicon and III-V solar cells (in particular if fast parameter optimization is the objective).

CHAPTER 3
METHODOLOGY

3.1 PC1D Software

The PC1D software will be described in detail in this section. The most important window of the software will be depicted in Figure 3.1 below, and each component of the software will be denoted by a number. It is labelled with numbers ranging from "1" to "5". The '1' will represent the 'device,' and it will contain general information about the device we will simulate. For '2,' the 'region' will introduce critical component parameters such as thickness, gap, and doping in this section. The maximum region area that can be added will be five. Following that, '3' will explain the concept of 'excitation.' The excitation modes will be specified as 'one-sun.exc' and 'scan-qe.exc.' Then '4' will be the 'result'; this will be the location of the result obtained after the software is run. The final '5' will be the 'device schematic,' which will be a representation of the device that will be created. It will change instantly when the region's parameters are changed (Belarbi et al., 2014). For instance, if the doping level changes, the color of the region will change.

The software will include an excitation mode file, which will be used. Both files, 'one-sun.exc' and 'scan-qe.exc,' will be distinct. The 'one-sun.exc' will return the short circuit current, open circuit voltage, and maximum power output values. For 'scan-qe.exc,' the output will be limited to the values of the short circuit current and the maximum power output. As a result, most of the simulation runs will use the 'one-sun.exc' file. Additionally, the temperature unit will be able to be changed from Kelvin to Celsius.

PC1D was selected in this work for its rapid calculation, user-friendliness and reliability in photovoltaic simulations. It enables rapid parametric optimization of important design parameters like layer thicknesses, doping concentration and anti-reflection coating properties, which renders it capable for analyzing GaAs/p-Si and AlGaAs/p-Si structures as solar cell. In comparison to more detailed simulation tools, PC1D offers an accurate performance evaluation with much less computational cost and therefore is a good fit in the frame of this work.

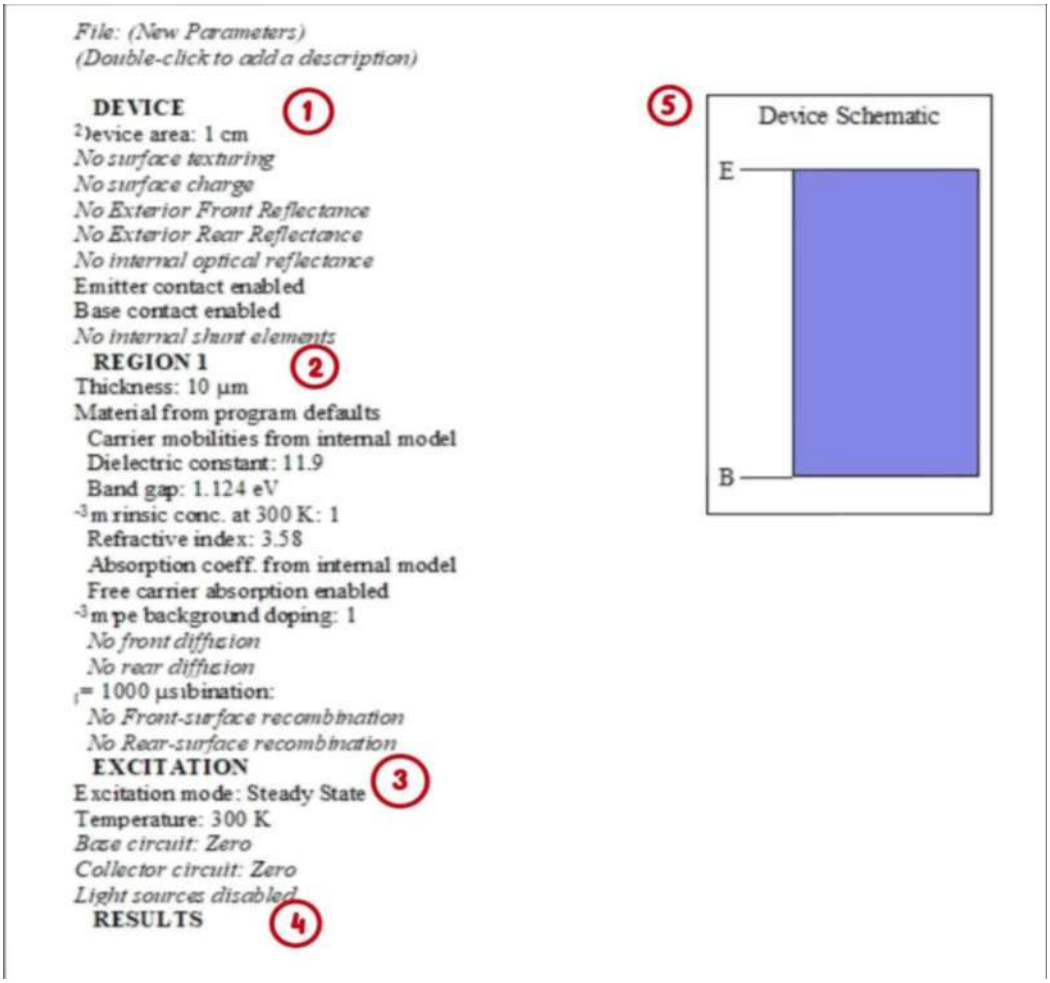

Figure 3.1 PC1D basic Window.

3.2 Simulation Using PC1D Software

This section describes the simulation carried out by the PC1D program. Tables 3.1 below provide an overview of the initial set of parameters that were used in the simulation before moving to a new set. In this study, the main parameter was GaAs/Si solar cells, which led to the identification of the most effective simulation of solar cells. This research altered ARCs, thickness, and doping concentration.

Table 3.1
The value of the device parameter for PC ID for thickness and doping concentration.

Parameter	Value	
Device area	$10\ cm^2$	
Region	n-GaAs layer	p-Silayer
Thickness	0.1 urn	160um
Band gap	1.424 eV	1.124 eV
Intrinsic cone. (300K)	$2.59x10^6cm^{-3}$	$1x10^{10}cm^{-3}$
Background doping	$1x10^{16}cm^{-3}$	$1x10^{16}cm^{-3}$
Bulk recombination lifetime	**0.4 us**	1000 us
Recombination velocity (front surface)	70000 us	-
Recombination velocity (back surface)	-	-
Excitation mode	One-sun (transient; 16 timesteps)	
Spectrum	AM1.5G	
Intensity	$0.1W/cm^2$	
Temperature	25°C	

The files used in this simulation for excitation mode are "one-sun.exc". This is because the investigation must acquire the short circuit current (I_{sc}), open circuit voltage (Voc), and maximum power output values (Pmax). Belarbi et al. (2014) reported that "one-sun.exc" restored the values of I_{sc}, V_{oc}, and Pmax. In Table 3.2, for ARCs, the bandgap of the GaAs and Si which is 1.424 eV and 1.124 eV respectively, have been used in this simulation. The Si substrate thickness is 150 urn and for the GaAs substrate is 0.1 urn. For the doping concentration, n-region and p-region has been set 1×10^{16} cm^{-3} for n- regions and 1×10^{17} cm^{-3} for p- region. All this data was obtained from the result of the thickness and doping concentration simulation.

Table 3.2

The simulated structure of the GaAs/p-Si based solar cell for ARC simulation.

Parameter	Value
Device	
Device area	10 cm^2
Surface texturing	None
Surface charge	None
Exterior front reflectance	10%
Exterior rear reflectance	None
Internal optical reflectance	None
Emitter contact	
Base contact	
Region 1	
Thickness	0.1 urn
Material	GaAs
Band gap	1.424 eV
Intrinsic concentration	$2.59x10^6cm"^3$
Refractive index	Fixed
Absorption coefficient	Enabled
Free carrier absorption	Enabled
N-type background doping	$1x10^{16}cm"^3$
Bulk recommendation	**0.4 us**
Recombination velocity (front surface)	70000 ^s
Region 2	
Thickness	150 urn
Material	Silicon
Band gap	1.124 eV
Intrinsic concentration	$1x10^{10}cm-^3$
Refractive index	Fixed
Absorption coefficient	Enabled
Free carrier absorption	Enabled
P-type background doping	$1x10^{17}cm"^3$
Bulk recommendation	1,000 us
Recombination velocity (front surface)	None
Excitation	
Excitation mode	Transient, 16 timesteps
Temperature	25 °C
Base circuit	-0.8 to 0.8 V
Collector circuit	0
Primary light source	Enabled
Constant intensity	0.1 Wcm-2
Spectrum	Am 1.5 g
Secondary light source	Disabled

One of the sections in PC1D with the DEVICE label is depicted in Figure 3.2, where the user can apply specific double-layer ARC materials under "exterior front reflectance." Users will enter the ARCs' thickness and reflective index data, with the middle layer representing the first layer and the inner layer being the second. An effective reflectance will be calculated for these structures across the entire spectrum of incident sunlight wavelengths, rather of focusing on the reflecting properties of a single wavelength (Moradi & Rajabi, 2013). In this study, ZnO-based materials will be used as ARC materials. Materials of double layers of ARC, ZnO/TiO2, will then be applied to silicon solar cells for analysis using PC1D software to determine which ARC materials are best suited for the solar cells going forward.

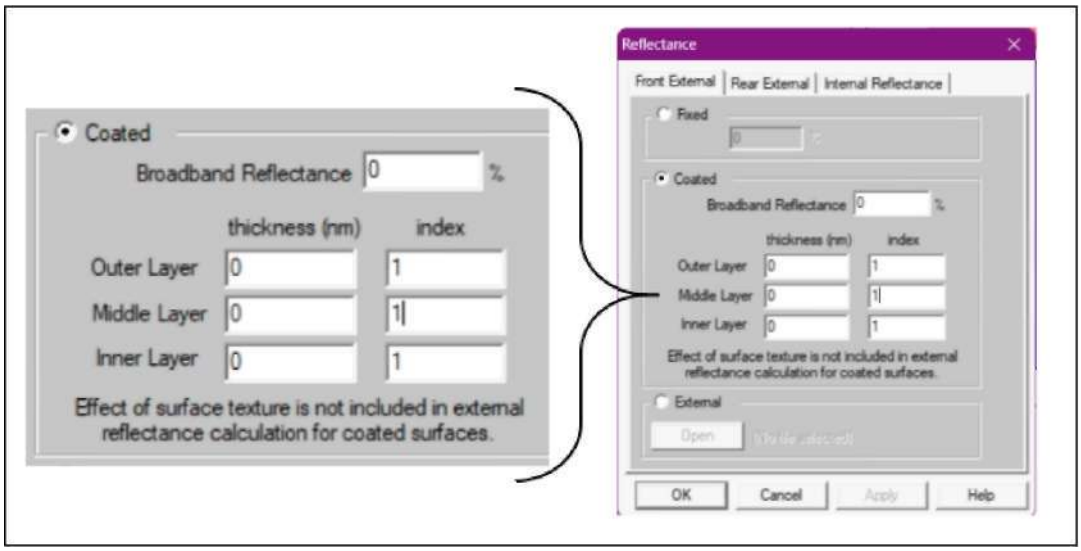

Figure 3.2 The section of the PC1D simulation to input the layers of ARC

3.3 Flowchart of Research

The simulation's flowchart describes the procedure for simulating PC ID for thickness, doping concentration and ARC. The elaboration of the simulation over time is depicted in Figure 3.3 and Figure 3.4. The method for Figure 3.3 was broken down into three discrete steps. The simulation was first initialized by launching the PC ID software and selecting the one-sun excitation mode, which represents standard solar illumination conditions. Subsequently, the material specifications for silicon and GaAs were selected, and all relevant physical parameters were entered into the software based on the values listed in the corresponding data tables. Following this, key device parameters including layer thickness and doping concentration for both n-type and p-type regions were defined to model the solar cell structure accurately. Once all parameters were specified, the simulation was executed to evaluate the electrical performance of the device, allowing the determination of critical output parameters such as short-circuit current (Isc), open-circuit voltage (Voc), and maximum power output (Pmax). Additional outputs, including efficiency and current-voltage (IV) characteristics, were generated and exported for further analysis. The simulation process was then repeated by systematically varying the thickness and doping concentration to identify the optimized parameter values that yield the highest power conversion efficiency.

For Figure 3.4, the parameter data that get the highest efficiency in the Figure 3.3 used to gained the result for the ARC's PC ID simulation. The simulation was initialized by entering all essential parameters, including the selection of materials such as GaAs and silicon and their corresponding properties, such as thickness and doping concentration. Three ARC conditions were then tested: no ARC as a baseline, single-layer ARC (e.g., SiCh) to reduce surface reflection, and double-layer ARC (e.g., SiCh and MgF2) to further enhance light absorption. For each condition, the simulation was executed to obtain key performance parameters, including short-circuit current (Isc), open-circuit voltage (Voc), and maximum power output (Pmax). The resulting data, particularly the I-V curves, were analysed to determine which ARC configuration yielded the highest efficiency, and the optimal ARC setup was selected to complete the simulation process.

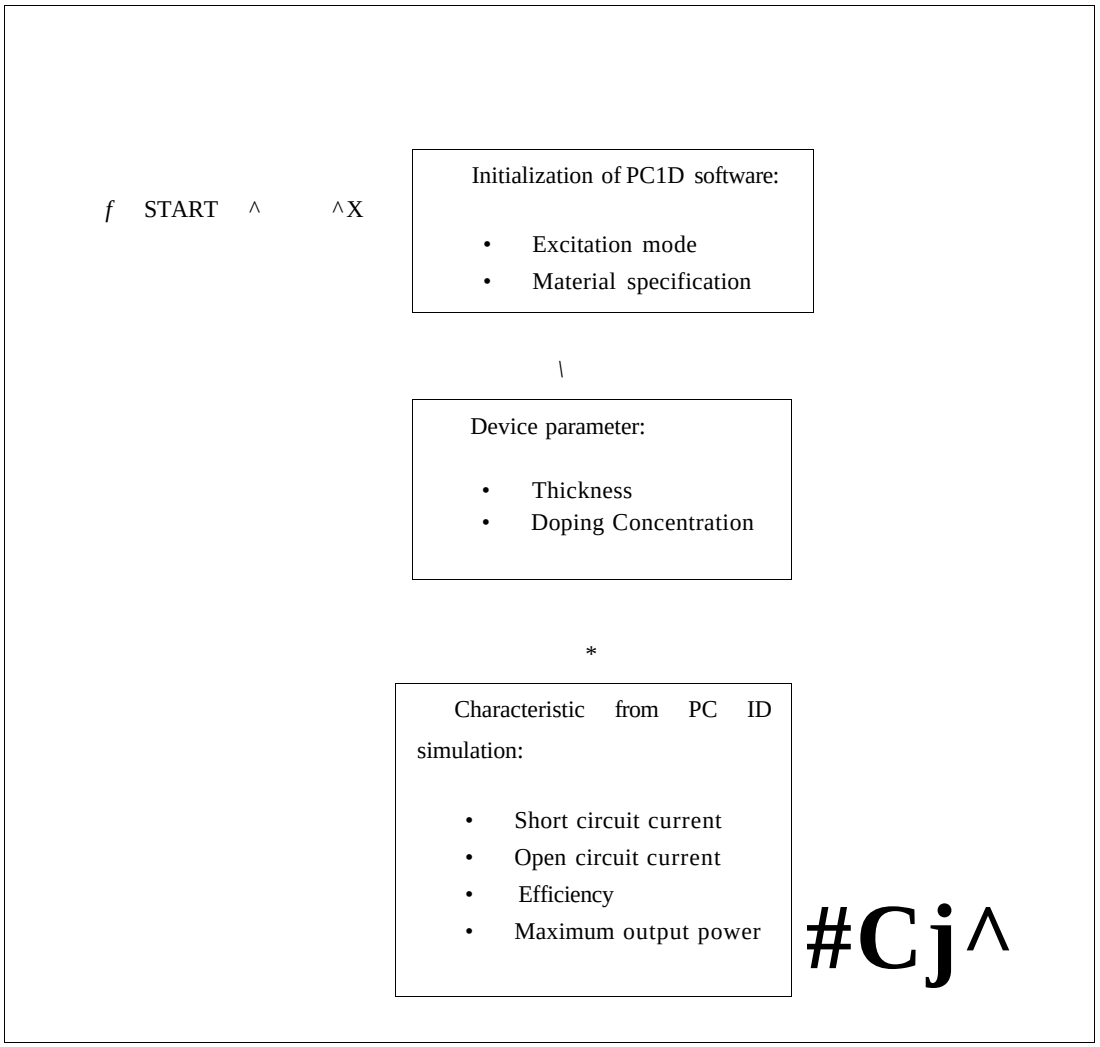

Figure 3.3 Flowchart of the PC ID simulation for parameter of thickness and doping concentration.

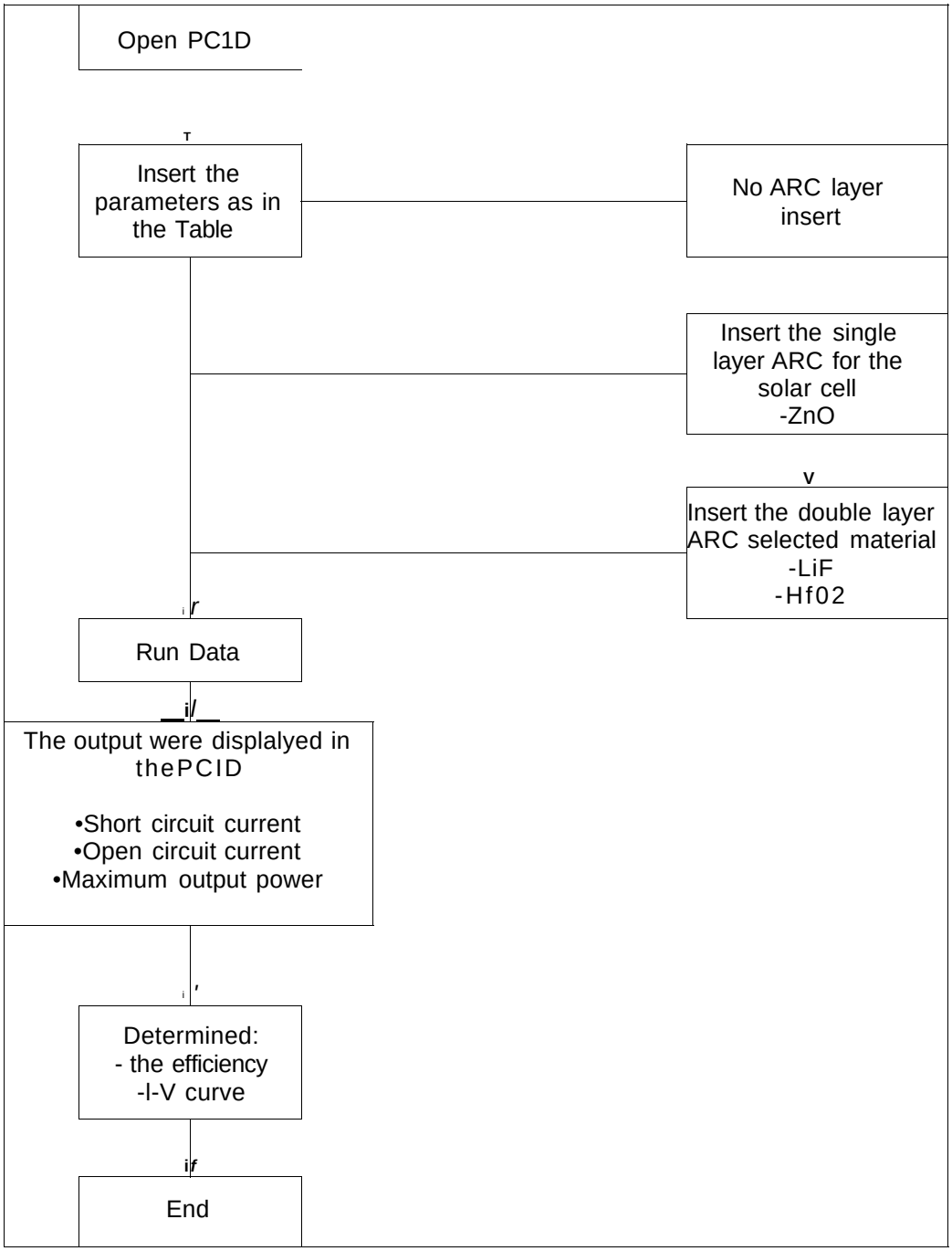

Figure 3.4 Flowchart for simulation for ARC layer of solar cell.

CHAPTER 4
RESULT AND DISCUSSION FOR GAAS/P-SI

In this part, the result of a simulation of a solar cell based on GaAs/p-Si using PC1D software will be discussed. The efficiency of the p-Si/n-GaAs solar cell capable be obtained by adjusting the thickness and doping concentration parameters. From the PC1D software, the results of Isc,Voc and Pmax can demonstrate the outcomes of the p-Si/n-GaAs solar cell panels by finding the efficiency and the IV- characteristic. To obtain the most efficient solar cell model, the parameters were changed and the findings from the simulation were evaluated. Hence, using the results, one may create a solar cell model with high efficiency based on the values chosen for each parameter. Figure 4.1 shows the IV characteristic graph of the thickness of n-GaAs region which is the GaAs layer. The altering of thickness starts from 0.1 µm until 2 µm. From this graph it proven that the thickness of the n-GaAs section will affect the efficiency of the solar cell. The centre of the curve matches the thinnest layer of GaAs (0.1 µm).

4.1 Thickness and Doping Concentration

Table 4.1 shows the decreases of the efficiency with the increasing thickness of GaAs from 24.02% at 0.1 µm to 14.02% at 2 µm. This can be proven that the thickness influenced the solar cell efficiency. Once the result value received from locked at the short circuit current (Isc) was increasing in the range of the open circuit voltage (Voc), thus the efficiency of the solar cell also grows, which is directly linked to the accelerating rate of power absorbed. (Khairuddin et al., 2023). Increasing layer thickness resulted in conversely decreasing outcomes and eventually decreasing efficiency (Khairuddin et al., 2023).

Table 4.1

Different thicknesses of GaAs/p-Si solar cells in the n-region.

N-region thickness (µm)	Isc (A)	Voc(V)	Pmax (W)	Fill factor	Efficiency (%)
0.1	0.3886	0.7416	0.2402	0.8335	24.02
0.5	0.3643	0.7387	0.2145	0.7971	21.45
1	0.3101	0.7343	0.1815	0.7971	18.15
1.5	0.2686	0.7305	0.1578	0.8042	15.78
2	0.2382	0.7272	0.1402	0.8094	14.02

The short-circuit current of a solar cell is determined by its area, incident light spectrum, photon count, and material parameters (Winkler et al., 2014). Short circuit current falls significantly when carriers recombine. Open circuit voltage is the maximum voltage generated through a photovoltaic cell once there is no current flowing through it (Singh et al., 2022a). Hence, as shown in Figure 4.1, the most efficient of GaAs/p-Si was at 0.1 µm at 24.02% efficiency with Voc = 0.7416 V, Isc= 0.3886 A, Pmax= 0.2402 W and FF = 0.83345.

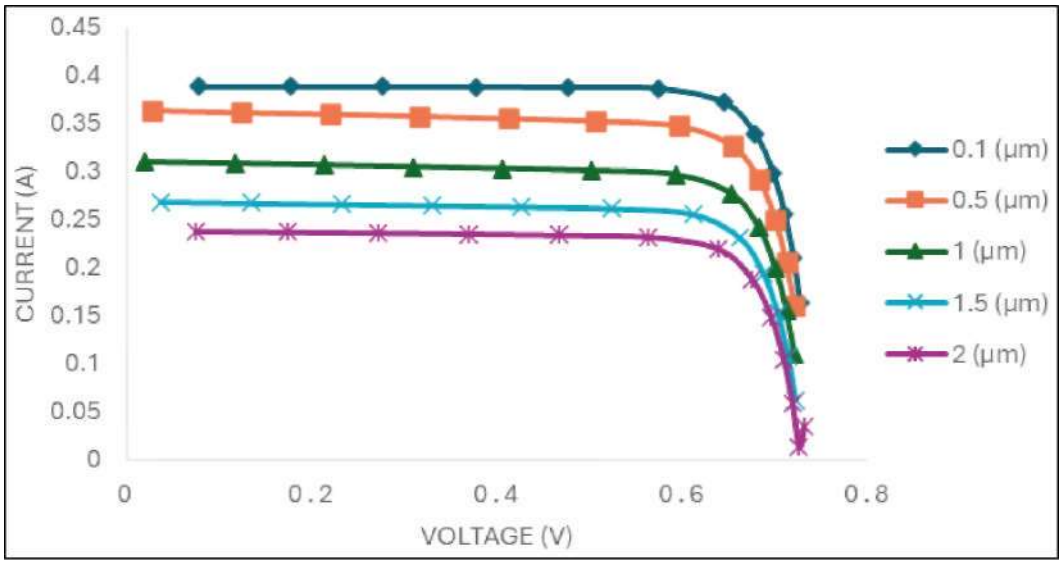

Figure 4.1 Variation of ISC and VOC with thickness of n-region.

The effect of silicon thickness upon the GaAs/p-Si solar cell structure has been explained. Figure 4.2 depicts how thicknesses at the substrate made from silicon have an effect the effectiveness for the GaAs/p-Si photovoltaic device.

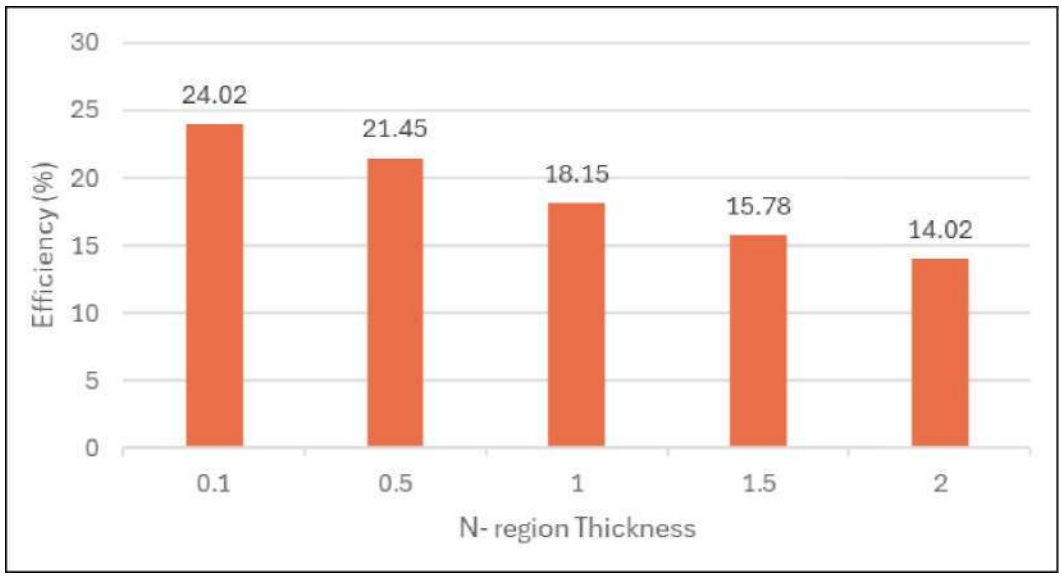

Figure 4.2 Efficiency with n- region thickness.

The findings indicate the amount of thickness of the silicon matter in GaAs/p-Si solar energy cells could affect the effectiveness of them. Figure 4.3 shows that a Si substrate thickness of 150 µm results in the best current reading, while a thickness of 30 µm yields the lowest current value. The outcome of increased layer thickness in the p-region were gradually rises in efficiency (W.-J. Wang et al., 2022). A restriction in this variable has been identified using PC1D.

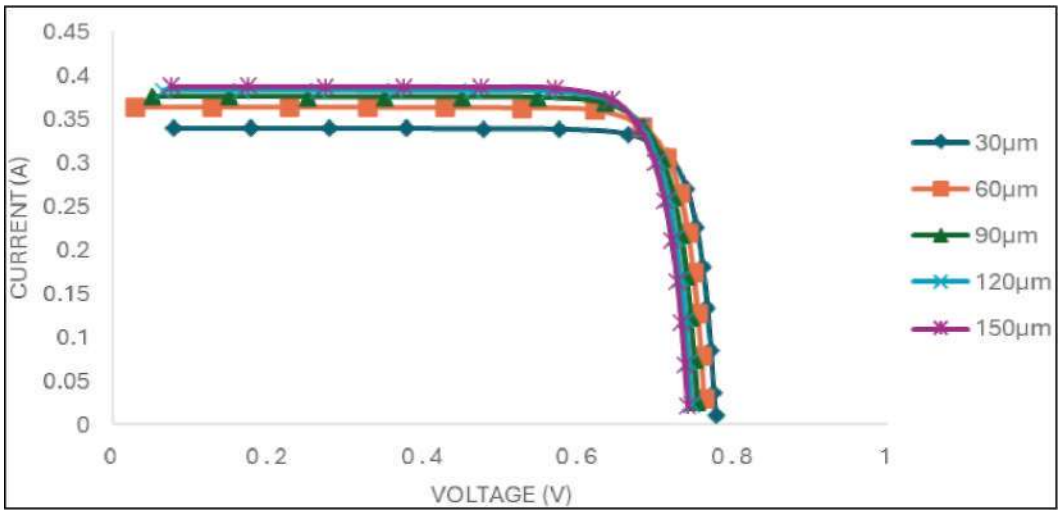

Figure 4.3 ISC and VOC differ with the thickness of the p-region.

As the p-region thicknesses got closer 300um, energy turned it down. In the Table 4.2, it shown that increasing the thickness of the p- region from 30 um to 150 um, also increasing the I_{sc} due to the rise in the number of the charge carriers (Singh et al., 2022a). Thus, recombination of charge carriers also increased and affects the value of V_{oc} by decreasing from 0.7767 V to 0.7432 V. Hence, as shown in Figure 4.4, the most efficient of GaAs/p-Si was at 150 um at 24.01 % efficiency with V_{oc} = 0.7432 V, I_{sc}= 0.3873 A, P_{max}= 0.2401 W and FF = 0.8341.

Table 4.2

Different thicknesses of GaAs/p-Si solar cells in the p-region.

P-region thickness(um)	Isc (A)	Voc(V)	Pmax(W)	Fill factor	Efficiency
30	0.3392	0.7767	0.2238	0.8495	22.38
60	0.3636	0.7635	0.2332	0.8400	23.32
90	0.3752	0.7549	0.2373	0.8378	23.73
120	0.3823	0.7485	0.2393	0.8363	23.93
150	0.3873	0.7432	0.2401	0.8341	24.01

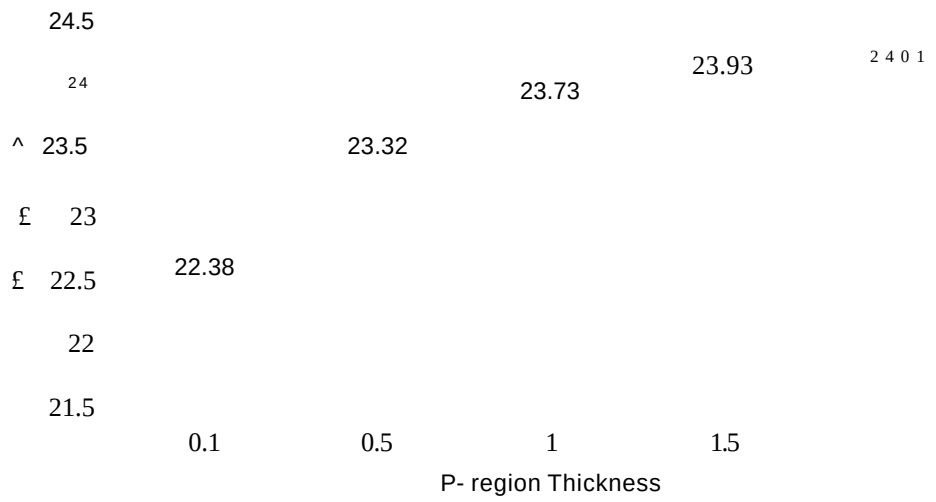

Figure 4.4 Efficiency with p- region thickness.

Figure 4.5 shows that the effect of variety doping concentration on GaAs/p-Si solar cells. To find the optimal efficiency for a solar cell, doping concentration plays an important role in efficiency estimates (Khairuddin et al., 2023). Figure 4.5 show the outcome of the affect doping concentration at GaAs substrate from $1x10^{15}$ cm^{-3} to $1x10^{19}$ cm^{-3} respectively.

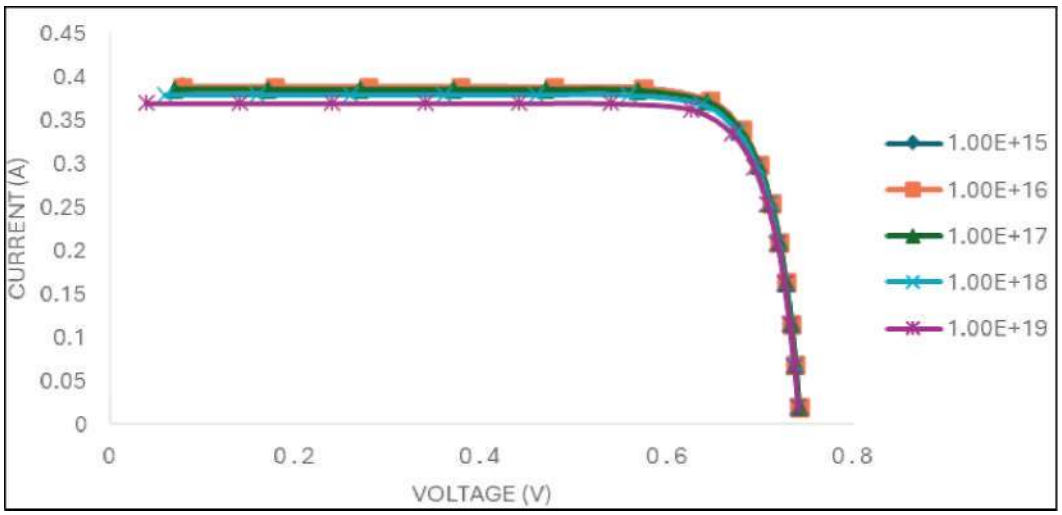

Figure 4.5 Variation of Isc and Voc with doping concentration of n-region.

The result of the different doping concentration from $1x10^{15}$ cm^{-3} to $1x10^{16}$ cm^{-3} shows the same efficiency which are 24.02%. This occurs because, in this moderate doping range, the increase in carrier concentration does not significantly affect recombination rates or the built-in electric field, so the overall efficiency is unaffected (Chuah et al., 2026). As shown in the Table 4.3 and Figure 4.6, as the doping concetrarion increasing the efficiency of the solar cell decreasing.

Table 4.3
Result on different doping concentration at n-region GaAs/p-Si solar cell

N-region doping cone. (cm)	Isc (A)	Voc(V)	Pmax(W)	Fill factor	Efficiency (%)
$1x10^{15}$	0.3887	0.7414	0.2402	0.83350	24.02
$1x10^{16}$	0.3886	0.7416	0.2402	0.83349	24.02
$1x10^{17}$	0.3848	0.7414	0.2383	0.83529	23.83
$1x10^{18}$	0.3792	0.7411	0.2352	0.83694	23.52
$1x10^{19}$	0.3694	0.7404	0.2287	0.83619	22.87
$1x10^{20}$	0.2859	0.7333	0.1746	0.83281	17.46

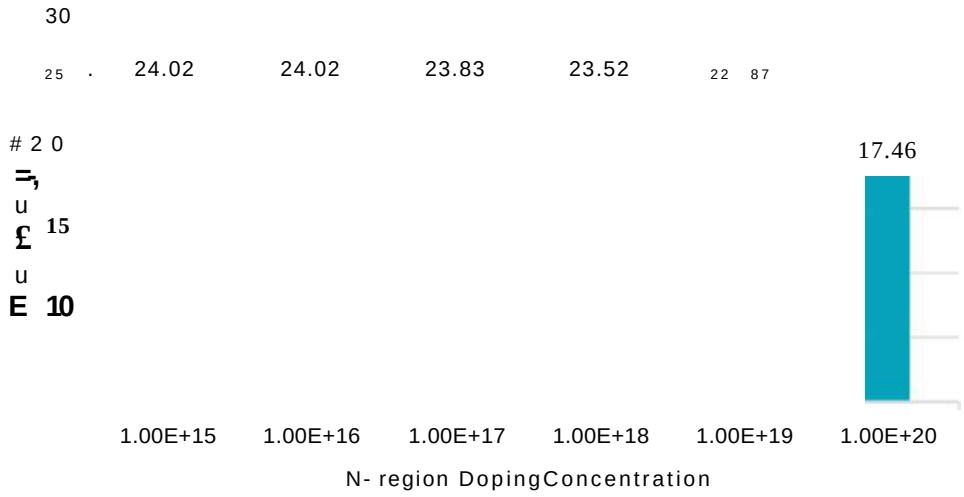

Figure 4.6 Efficiency with n- region doping concentration.

High levels of doping concentration can impact the transport characteristics of carriers within the solar cell. Elevated doping levels introduce additional defects and impurities into the material, resulting in heightened carrier scattering and diminished carrier mobility (Belghachi et al., 2010). Therefore, the most optimal doping concetration that can give the best efficiency is between $1x10^{15}$ cm^{-3} and $1x10^{16}$ cm^{-3} .

In this study, the varying doping concentrations over the p-region of GaAs/p-Si solar cell outcome has been shown in Figure 4.7.

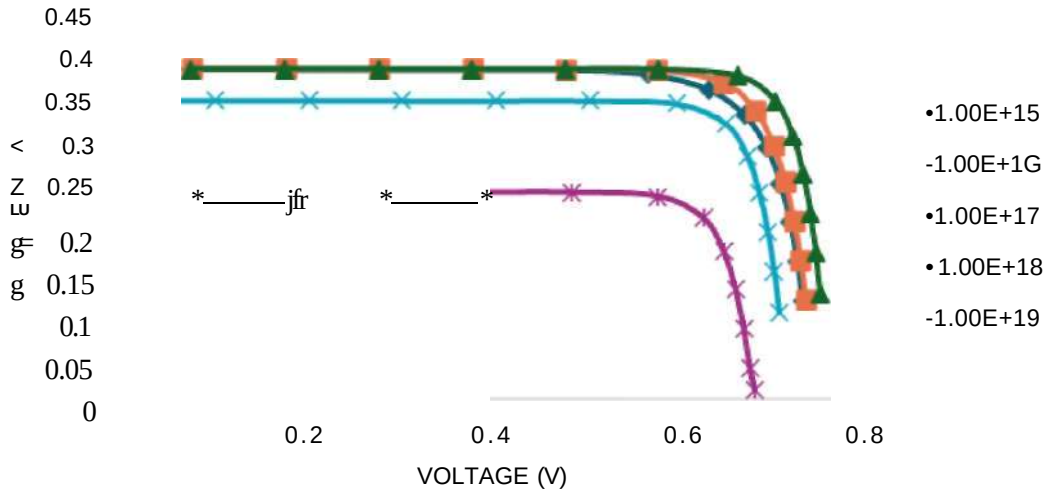

Figure 4.7 Variation of I_{sc} and V_{oc} with doping concentration of p-region.

The different doping concentration that has been use in this study are from $lxlO^{15}$ cm^{-3} and $lxlO^{20}$ cm^{-3}. The GaAs/p-Si solar cell achieves its greatest effectiveness of 25.22% with a doping concentration of $1\ xlO^{17}$ cm^{-3} .The lowest efficiency that obtanied from the Figure 4.8 is $lxlO^{20}$ cm^{-3}. Table 4.4 indicates the effect of multiple doping concentrations in the p-region on solar panel performance.

Table 4.4
Result on different doping concentration at p-region GaAs/p-Si solar cell.

P-region doping cone, (cm^{3})	Isc (A)	Voc(V)	Pmax(W)	Fill factor	Efficiency (%)
$lxlO^{15}$	0.3876	0.7386	0.2289	0.7996	22.89
$lxlO^{16}$	0.3886	0.7416	0.2402	0.8335	24.02
$lxlO^{17}$	0.388	0.7554	0.2522	0.8605	25.22
$lxlO^{18}$	0.3509	0.7127	0.2107	0.8425	21.07
$lxlO^{19}$	0.2424	0.6772	0.1377	0.8389	13.77
$lxlO^{20}$	0.1544	0.6373	0.0815	0.8283	8.15

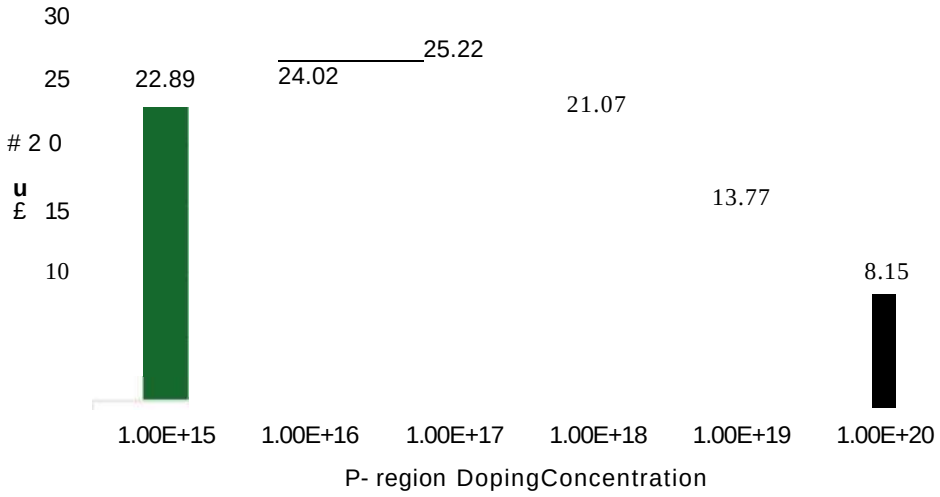

Figure 4.8 Efficiency with p- region doping concentration.

Excessive doping concentration affects solar power cells' conversion rate by decreasing light transmission, absorption, and greater recombination rates (Singh et al., 2022a). Elevated doping concentrations can worsen surface recombination effects, where charge carriers are lost at the semiconductor material's surface. Higher doping levels can elevate surface recombination velocities, thereby impeding the collection of generated carriers and diminishing the efficiency of the solar cell (Belghachi et al., 2010). As a result, the most optimal doping concentration that can give the best efficiency is $1x10^{17}$ cm^{-3} as shown in Figure 4.8.

4.2 **ARC**

Next, in this section the result of the simulation of PC ID is shown. The data output of open circuit voltage (Voc), maximum power output (Pmax), short circuit current (Isc), and efficiency (r|) it was shown in the Table 4.5. Here single layer ARC (SLARC) of ZnO and double layer ARC (DLARC) of ZnO/ Ti02 is used. In this section, the result of the simulation of PC ID is shown. The data output of open circuit voltage (V_{oc}), maximum power output (Pmax), short circuit current (I_{sc}), and efficiency (r|) of no ARC was shown.

Table 4.5
Result data output of no ARC.

	ISC (A)	VOC (V)	Pmax (W)	**Efficiency** (%)
NO **ARC**	0.2575	0.7476	0.1643	16.43

In the Table 4.5 shows the results of stimulating solar cell without an anti-reflective layer using PC ID software. The results for V_{oc}, Pmax and I_{sc} were 0.7476V, 0.1643W and 0.2527A respectively. The efficiency which is 16.43% also as the lowest efficiency. A solar cell with no anti-reflective coating (ARC) often has a lower efficiency than one with an ARC (Zhang et al., 2021). This is as without an ARC, a considerable part of incident light is reflected back, resulting in fewer light absorption and, as a result, lower efficiency when converting light into energy (Jamaluddin et al., 2024a).

In the Table 4.6, result data of single layer ARC (SLARC) ZnO shown. The result of the simulation shows SLARC of ZnO has the highest efficiency which is 23.42%). The wavelength *(X)* that get the highest efficiency is at 600 nm and the result for Voc and I_{sc} were 0.7553V and 0.3618A respectively. Next, the second highest efficiency which is 23.27% at the wavelength of 700 nm and the V_{oc} and I sc were 0.7551V and 0.3593A respectively.

Table 4.6
Result data output of SLARC ZnO.

X, (nm)	**Refractive index**	**Thickness** (^{nm})	Isc **(A)**	Voc **(V)**	**Efficiency** (%)
250	2.388	26.173	0.2795	0.7495	17.93
300	2.404	31.198	0.2908	0.7504	18.73
400	2.114	47.304	0.3132	0.752	20.12
500	1.968	63.516	0.3515	0.7546	22.79
600	1.913	78.411	0.3618	0.7553	23.42
700	1.883	92.937	0.3593	0.7551	23.27
800	1.864	107.296	0.3488	0.7545	22.63
900	1.851	121.556	0.335	0.7536	21.69

In Table 4.7, data output of double layer ARC (DLARC) $ZnO/Ti0_2$ that was used shown. The highest efficiency is at 500 nm wavelength which is 23.04%) and followed by at the 400 nm wavelength which is 23.00%) efficiency. The result for V_{oc} and Isc at 500 nm were 0.7549V and 0.3555A respectively.

Table 4.7
Result data output of DLARC.

	ZnO		**TiOi**				
X, (nm)	**Refractive index**	**Thickness (nm)**	**Refractive index**	**Thickness (nm)**	Isc (A)	**Voc (V)**	**Efficiency (%)**
250	2.388	26.173	2.46	25.407	0.3374	0.7537	21.85
300	2.404	31.198	3.326	22.55	0.3151	0.7522	20.24
400	2.114	47.304	2.68	37.213	0.3548	0.7548	23.00
500	1.968	63.516	2.48	50.403	0.3555	0.7549	23.04
600	1.913	78.411	2.404	62.396	0.3506	0.7546	22.74
700	1.883	92.937	2.364	74.027	0.3447	0.7542	22.36
800	1.864	107.296	2.341	85.434	0.3379	0.7537	21.89
900	1.851	121.556	2.325	96.774	0.3336	0.7535	21.59

Figure 4.9 indicates the I-V characteristic curve for the SLARC result with different wavelength using PC ID simulation. The curve at wavelength 250nm has the lowest relationship with the current and voltage. The curve at wavelength 600nm has the highest which is 23.42%) and followed by a wavelength 700nm which is slightly different 23.27%. The wavelength of incident light is also critical with respect to the interaction of light with the ARC and the solar cell. The ARC manifests in controlling the incident light for specific wavelengths through proper design of the refractive index and thickness of the ARC material, which acts to enhance the efficiency of the solar cell (Jamaluddin et al., 2024a).

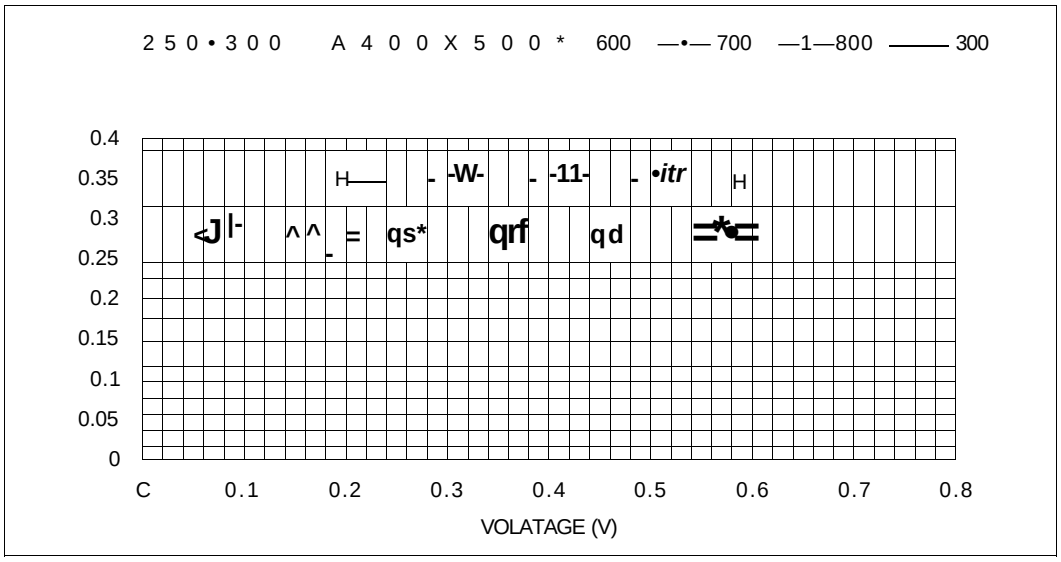

Figure 4.9 I-V characteristic curve for SLARC.

The study of Parajuli et al. (2023) found that after adding the A R C layer, the ISC jumped to 2.39 A, compared to 1.73 A without the A R C. The improvement in ISC indicates greater absorption of light and electron development in the solar cell, which leads to increased efficiency (Hashmi, Akand, et al., 2018; Parajuli et al., 2023). The improved configuration of the anti-reflective coating completed by multi-objective optimization is essential for increasing photon energy absorption, enhancing short-circuit current (ISC), and optimizing power generation (Zhang et al., 2021). As a result, this increase significantly improves the efficiency of photoelectric conversion.

Figure 4.10 shows the characteristic curve of D L A R C of ZnO/TiO2. Wavelength at 500nm has the highest point in the I-V curve and the lowest point in the I-V curve is at wavelength 300nm. The gap between these wavelengths highest point is just slightly different and unnoticeable. The wavelength plays a role in the interaction of the light with the A R C and the solar cell. The refractive index of the selected A R C material, alongside its thickness, may be adjusted to maximize the light management at specific wavelength regions, resulting in an overall improvement in solar cell performance (Jamaluddin et al., 2024b).

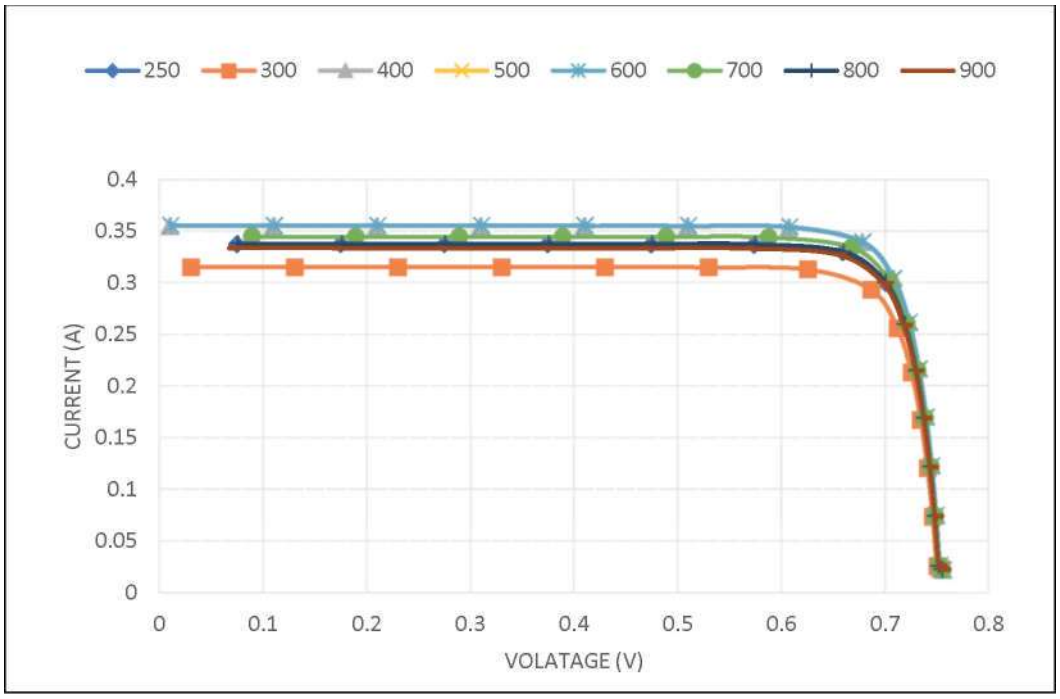

Figure 4.10 I-V characteristic curve for DLARC

Figure 4.11 shows the I-V characteristic curve among no ARC, SLARC and DLARC simulated in PC1D. The highest point is SLARC of ZnO and followed by the DLARC of ZnO/TiO2. Lastly, the lowest point is the no ARC curve. The gap between SLARC and DLARC is very little. SLARC is typically less layered, which can simplify fabrication and improve light interaction with the active layer of the solar cell. That can mean fewer interfaces at which light could be lost through reflection or scattering (Hashmi, Akand, et al., 2018).

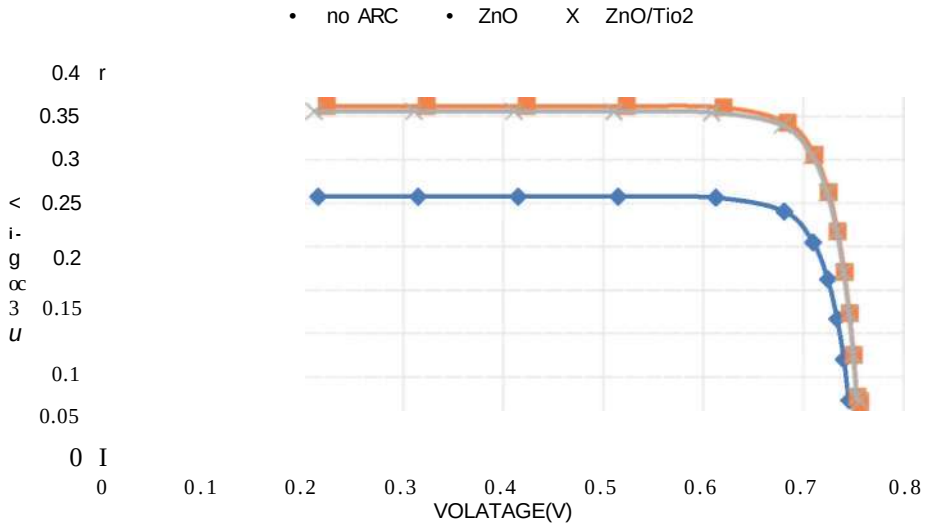

Figure 4.11 I-V characteristic curve for no ARC, SLARC and DLARC.

The result is that SLARC greatly minimizes light reflection away from the solar cell and maximizes light penetration into the cell for electricity generation by simply tailoring the refractive index of this coating to match that of silicon. In a single-layer ARC, light interacts with a more single interface, reducing the likelihood of destructive force that could arise in multi-layer structures. Such anti-reflective layers can thus increase light transmission into the solar cell and reduce reflectance (Hashmi, Akand, et al., 2018). DLARCs can expand reflectance suppression across a wider spectral range, but at the cost of increased angular dependence.

While DLARCs can reach lower reflectance minimums, they can also have more variability of reflectance under varying angles of incidence that can hurt efficiency during real-world application (Bahrami et al., 2013b). Some DLARCs (e.g., *MO3/T1O2)* may in some circumstances have less optimal performance than few selected SLARCs because of angle-averaged incidence onto textured substrates. Thus, although DLARCs are inclined to moderately boost solar cell efficiency, DLARC benefits are highly dependent on the material, on the surface texturization and on the incidence angle, and successful optimization is required for the added complexity(Al-Turk, 2011).

CHAPTER 5
RESULT AND DISCUSSION FOR ALGAAS/P-SI

5.1 Thickness and doping

This section discusses the outcome of a simulation of an AlGaAs/p-Si solar cell using PC 1D software. By varying the thickness and doping concentration parameters, the p-Si/n-AlGaAs solar cell's efficiency can be increased. By determining the efficiency and the IV-characteristic, the PC 1D software's Isc, Voc, and Pmax findings can illustrate the performance of the p-Si/n-AlGaAs solar cell panels. The parameters were altered and the simulation's outcomes compared in order to determine the most effective solar cell model. Therefore, based on the values selected for each parameter, one may use the results to design a solar cell model with high efficiency.

The IV characteristic graph of the AlGaAs layer's thickness in the n-region is displayed in Figure 5.1. Starting at 0.1 µm and continuing until 2 µm, the thickness changes. This graph demonstrates how the n-GaAs region's thickness will impact the solar cell's efficiency. The curve's center corresponds to the thinnest AlGaAs layer (0.1 µm).

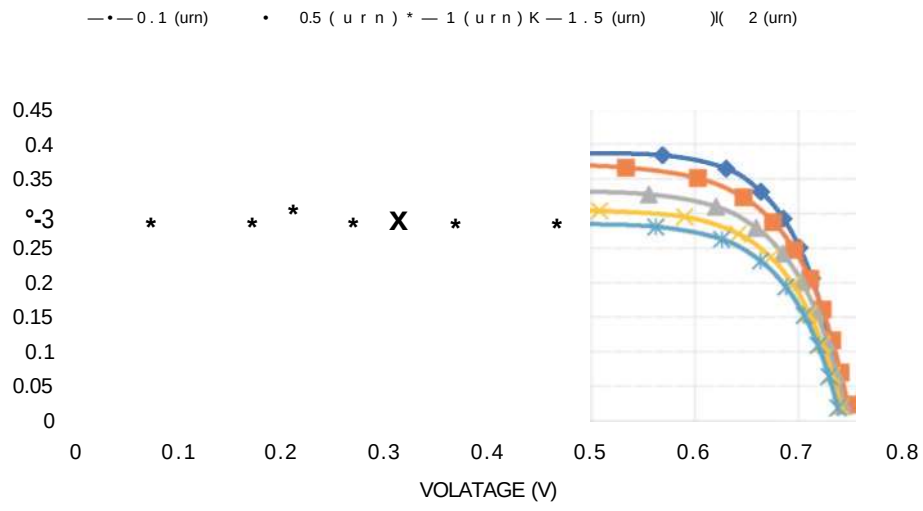

Figure 5.1 Variation of Isc and Voc with thickness of n-region.

Table 5.1 illustrates how the efficiency drops as the AlGaAs thickness increases, going from 23.04% at 0.1 µm to 16.49% at 2 µm. It is demonstrable that the thickness affected the efficiency of the solar cell. The efficiency of the solar cell, which is directly related to the accelerating rate of power absorption, increases as soon as the result value obtained from locked at the short circuit current (Isc) was rising within the range of the open circuit voltage (Voc). In 2023, Khairuddin et al. Conversely, declining results and ultimately decreasing efficiency were the results of increasing layer thickness (Mohamed et al., 2021). A solar cell's area, incident light spectrum, photon count, and material characteristics all affect it short-circuit current (Winkler et al., 2014). A solar cell's area, incident light spectrum, photon count, and material characteristics all affect it short-circuit current (Winkler et al., 2014). When carriers recombine, short circuit current decreases dramatically.

Table 5.1
Different thicknesses of AlGaAs/p-Si solar cells in the n-region.

N-region thickness (µm)	Isc (A)	Voc(V)	Pmax (W)	Fill factor	Efficiency (%)
0.1	0.3875	0.7645	0.2304	0.7778	23.04
0.5	0.377	0.7512	0.2132	0.7496	21.32
1	0.3376	0.7477	0.1926	0.7630	19.62
1.5	0.3085	0.7444	0.1767	0.7699	17.67
2	0.2881	0.7417	0.1649	0.7703	16.49

The highest voltage produced by a solar cell when no current is passing through it is known as the open circuit voltage (Singh et al., 2022a). Thus, the most efficient AlGaAs/p-Si was at 0.1 µm at 23.04% efficiency with Voc = 0.7645 V, Isc = 0.3875 A, Pmax = 0.2304 W, and FF = 0.83345, as illustrated in Figure 5.2.

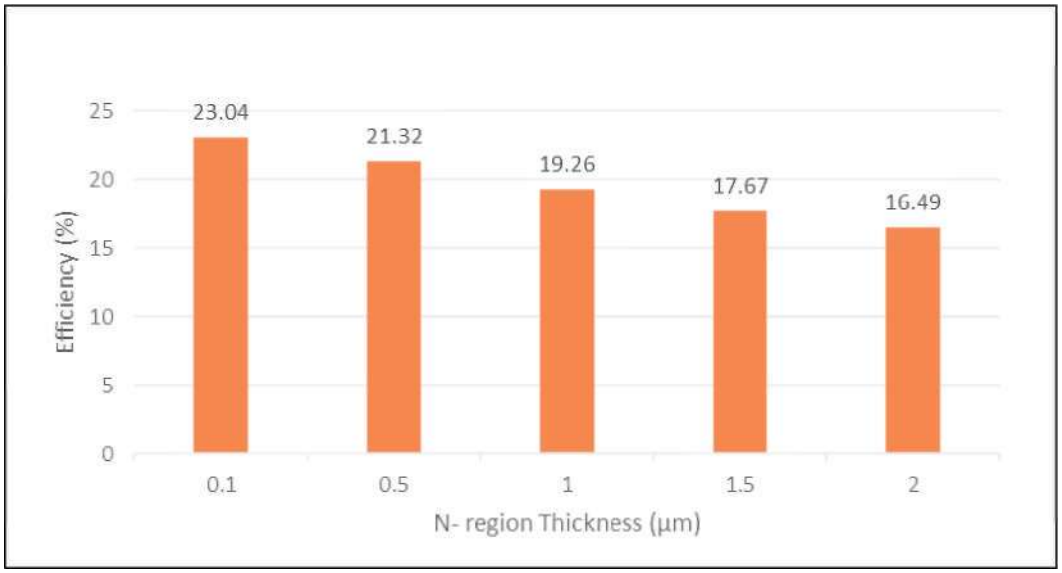

Figure 5.2 Efficiency with n- region thickness.

It has been explained how the thickness of silicon affects the structure of AlGaAs/p-Si solar cells. The impact of thicknesses on the silicon substrate on the AlGaAs/p-Si photovoltaic device's efficiency is shown in Figure 5.3.

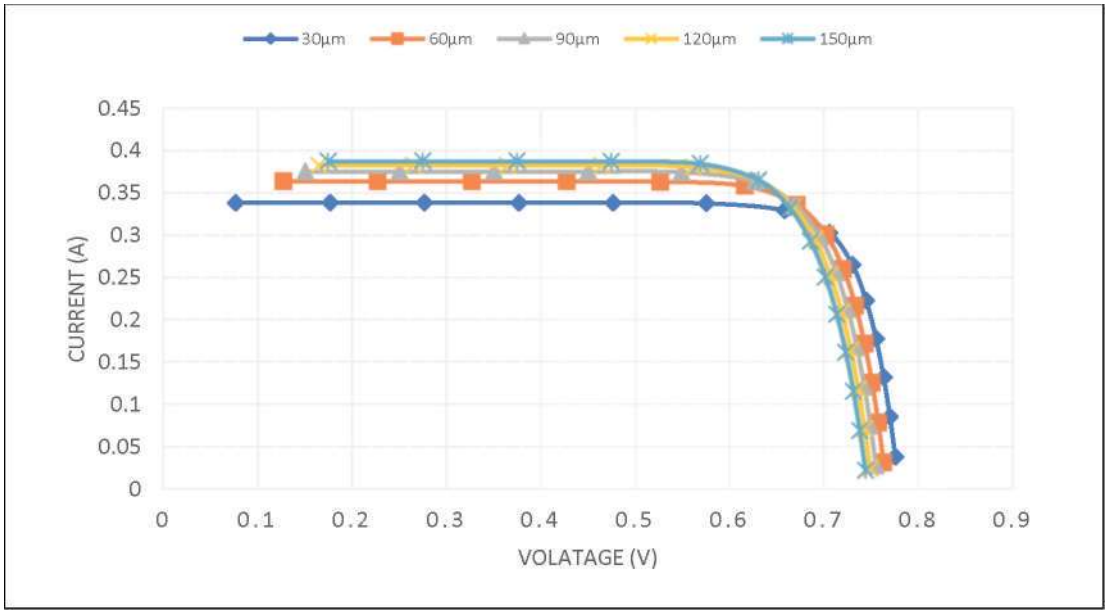

Figure 5.3 Isc and Voc differ with the thickness of the p-region.

The results suggest that the efficiency of AlGaAs/p-Si solar energy cells may be impacted by the thickness of the silicon substance. According to Figure 5.3, the best current reading is obtained with an AlGaAs substrate thickness of 150 µm, and the

lowest current value is obtained with a thickness of 30 um. Efficiency gradually increased as a result of thicker layers in the p-region (W.-J. Wang et al., 2022). Using PC ID, a restriction in this variable has been found. Energy turned it down as the p-region thicknesses approached 300um. As the thickness of the p-region increases from 30 um to 150 um, Table 5.2 demonstrates that the increase in the number of charge carriers likewise causes an increase in the I_{sc} (Singh et al., 2022b).

Table 5.2
Different thicknesses of AlGaAs/p-Si solar cells in the P-region.

P-region thickness(um)	Isc (A)	Voc(V)	Pmax(W)	Fill factor	Efficiency
30	0.3384	0.7796	0.2185	0.8282	21.85
60	0.3637	0.7666	0.2261	0.8116	22.61
90	0.3754	0.7581	0.2298	0.8075	22.98
120	0.3825	0.7517	0.2305	0.8017	23.05
150	0.3875	0.7465	0.2304	0.7965	23.04

As a result, charge carrier recombination also increased, causing the value of Voc to drop from 0.7796 V to 0.7465 V. The most efficient AlGaAs/p-Si was thus at 120 um at 23.05% efficiency with V_{oc} = 0.7465 V, I_{sc} = 0.3875 A, P_{max} = 0.2304 W, and FF = 0.83414, as illustrated in Figure 5.4.

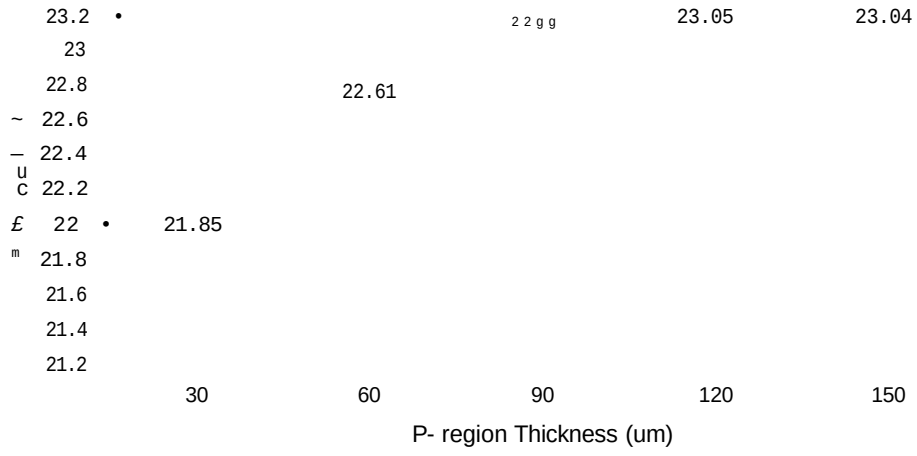

Figure 5.4 Efficiency with p- region thickness.

The impact of different doping concentrations on AlGaAs/p-Si solar cells is depicted in Figure 5.5. Doping concentration is a crucial factor in efficiency calculations for determining a solar cell's ideal efficiency (Khairuddin et al., 2023). The effect of doping concentration at the AlGaAs substrate is shown in Figure 5.5 as a change from $1x10^{14}$ cm^{-3} to $1x10^{19}$ cm^{-3}, respectively.

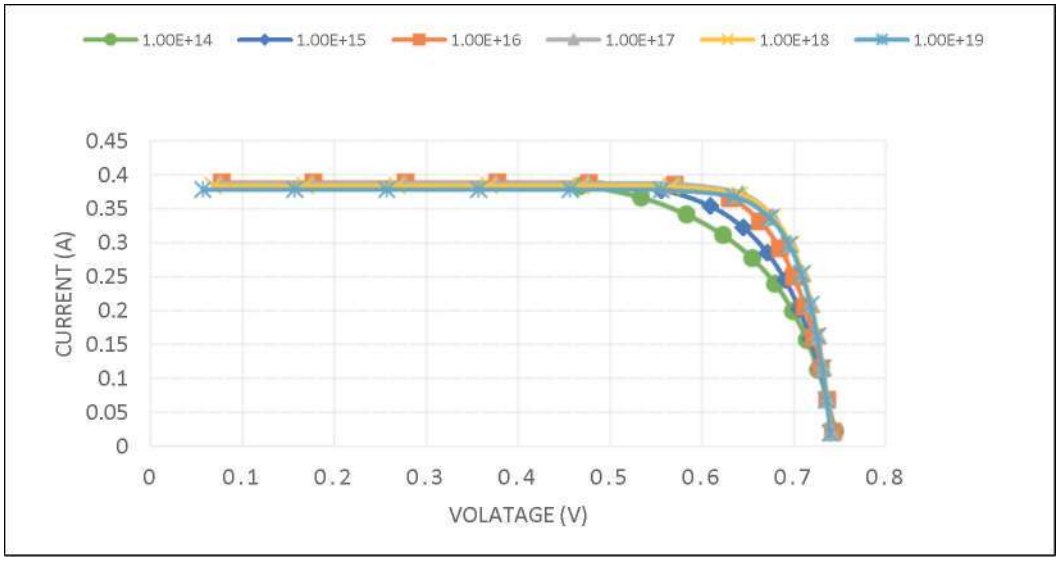

Figure 5.5 Variation of Isc and Voc with doping concentration of n-region.

The efficiency is at its best, 23.97%, when the doping concentration is different from $1x10^{17}$ cm^{-3}. Table 5.3 and Figure 5.6 demonstrate that the efficiency of the solar cell decreases as the doping concentration rises.

Table 5.3
Result on different doping concentration at n-region AlGaAs/p-Si solar cell

N-region doping conc. (cm^{-3})	Isc (A)	Voc(V)	Pmax (W)	Fill factor	Efficiency (%)
$1x10^{14}$	0.3889	0.7483	0.1992	0.6845	19.92
$1x10^{15}$	0.3889	0.7467	0.2158	0.7431	21.58
$1x10^{16}$	0.3888	0.7449	0.2303	0.7952	23.03
$1x10^{17}$	0.388	0.7421	0.2397	0.8308	23.97
$1x10^{18}$	0.3841	0.7414	0.2382	0.8364	23.82
$1x10^{19}$	0.3784	0.7409	0.2347	0.8371	23.47

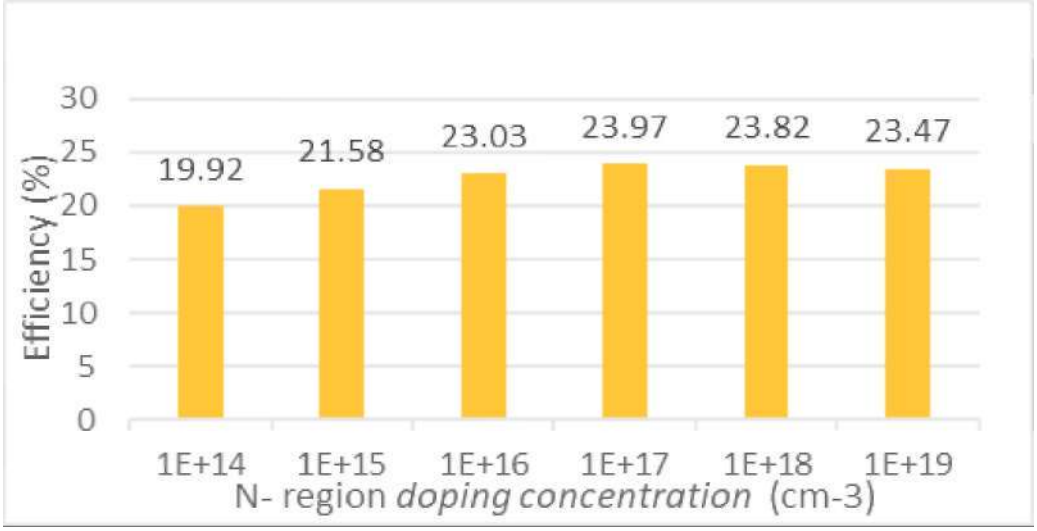

Figure 5.6 Efficiency with n- region doping concentration.

Carriers' transport properties inside the solar cell may be impacted by high doping concentrations. Higher doping concentrations cause the material to contain more flaws and impurities, which increases carrier dispersion and reduces carrier mobility (Belghachi et al., 2010). Consequently, $1x10^{17}$ cm $-^{3}$ is the most ideal doping concentration that can provide the highest efficiency.

Figure 5.7 in this work illustrates the different doping concentrations over the p-region of the AlGaAs/p-Si solar cell result. The various doping concentrations used in this investigation range from $1x10^{12}$ cm $-^{3}$ to $1x10^{17}$ cm $-^{3}$.

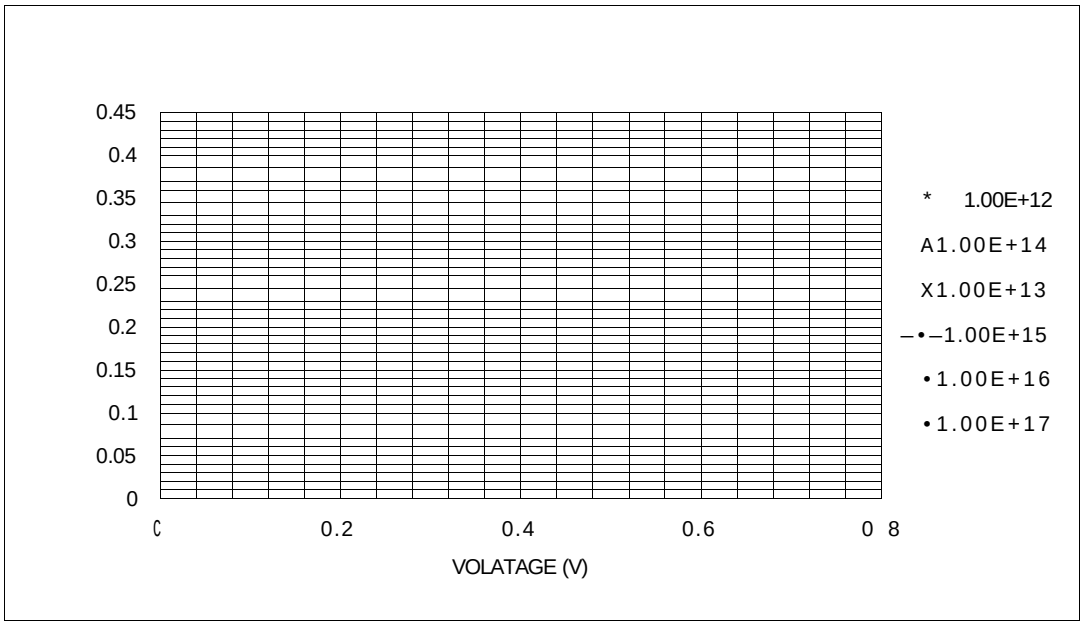

Figure 5.7 Variation of Isc and Voc with doping concentration of p-region.

The impact of various doping concentrations in the p-region on solar panel performance is shown in Table 5.4.

Table 5.4
Result on different doping concentration at p-region AlGaAs/p-Si solar cell.

P-region doping conc. (cm^{-3})	Isc (A)	Voc(V)	Pmax (W)	Fill factor	Efficiency (%)
$1x10^{12}$	0.3882	0.7438	0.2085	0.7221	20.85
$1x10^{13}$	0.3887	0.7438	0.2086	0.7215	20.86
$1x10^{14}$	0.389	0.7439	0.2086	0.7209	20.86
$1x10^{15}$	0.3889	0.7443	0.2074	0.7165	20.74
$1x10^{16}$	0.3889	0.7483	0.1992	0.6845	19.92
$1x10^{17}$	0.3869	0.7747	0.1238	0.4130	12.38

The maximum efficiency of the AlGaAs/p-Si solar cell is 20.86% when the doping concentrations are $1x10^{13}$ cm $^{-3}$ and $1x10^{14}$ cm $^{-3}$. $1x10^{17}$ cm $^{-3}$ is the lowest efficiency determined by Figure 5.8.

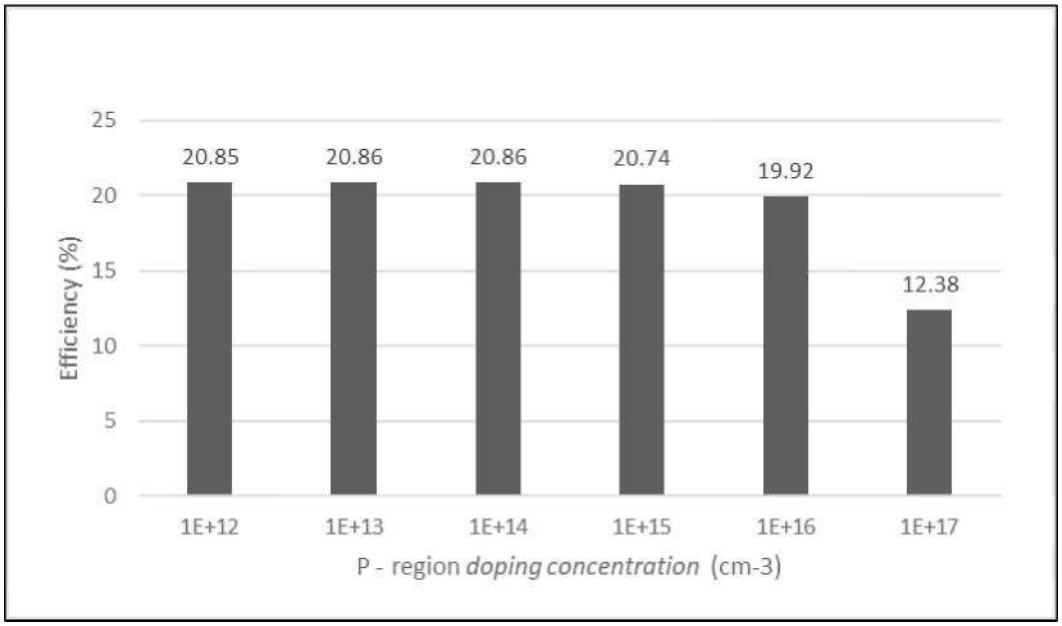

Figure 5.8 Efficiency with p- region doping concentration.

By reducing light transmission, increasing recombination rates, and decreasing absorption, excessive doping concentrations impact the conversion rate of solar power cells (Singh et al., 2022b). Surface recombination effects, in which charge carriers are lost at the semiconductor material's surface, can be exacerbated by high doping concentrations. Increased doping can increase surface recombination rates, which hinders the accumulation of produced carriers and reduces solar cell efficiency (Belghachi et al., 2010). As a result, as Figure 5.8 illustrates, the doping concentration that can provide the highest efficiency is $1x10^{13}$ cm $^{-3}$ and $1x10^{14}$ cm $^{-3}$.

5.2 **ARC**

In this section, the result of the simulation of PC ID is shown. The data output of open circuit voltage (V_{oc}), maximum power output (Pmax), short circuit current (I_{sc}), and efficiency (r|) of different ARC was shown.

Table 5.5
Result data output of no ARC.

	Isc (A)	Voc(V)	Pmax (W)	**Efficiency** (%)
NO **ARC**	0.2503	0.7354	0.1456	14.56

The results of utilizing PC1D software to stimulate a solar cell without an anti-reflective layer are displayed in Table 5.5. Voc, Pmax, and Isc had respective readings of 0.7354V, 0.1456W, and 0.1456A. The efficiency with the lowest efficiency is 14.56%. The efficiency of a solar cell with an anti-reflective coating (ARC) is frequently higher than that of a solar unit without one (Zhang et al., 2021). This is because, in the absence of an ARC, a significant portion of incident light is reflected back, which reduces light absorption and, thus, the efficiency of light-to-energy conversion (Jamaluddin et al., 2024a).

Table 5.6
Result data output of SLARC ZnO[i.]

X, (nm)	**Refractive index**	**Thickness (nm)**	Isc (A)	Voc(V)	**Pmax (W)**	**Efficiency (%)**
250	2.388	26.173	0.2779	0.7375	0.1633	16.33
300	2.404	31.198	0.2899	0.7387	0.1708	17.08
400	2.114	47.304	0.3231	0.7471	0.1919	19.19
500	1.968	63.516	0.3463	0.7435	0.2067	20.67
600	1.913	78.411	0.3554	0.7442	0.2123	21.23
700	1.883	92.937	0.3525	0.7439	0.2105	21.05
800	1.864	107.296	0.3419	0.7431	0.2039	20.39
900	1.851	121.556	0.3281	0.742	0.1951	19.51

The single-layer ARC (SLARC) ZnO outcome data is displayed in Table 5.6. The simulation's outcome indicates that ZnO's SLARC has the maximum efficiency, at 21.23%. Voc and I_{sc} were 0.7442 V and 0.3554 A, respectively, and the wavelength *(X)* with the maximum efficiency is 600 nm. Then, at 700 nm, the second-highest efficiency was 21.05%, with V_{oc} and I_{sc} of 0.7439 V and 0.3525 A, respectively. PCID study on different ARC materials indicated that a ZnO single-layer ARC on a silicon solar cell can achieve efficiency values close to 20.34%, closely following Si3N4 ARC performance (-20.35%) at optimum thickness around 74-75 nm and under similar wavelength conditions, with notable increases over cells without ARC(Jamaluddin et al., 2024a).

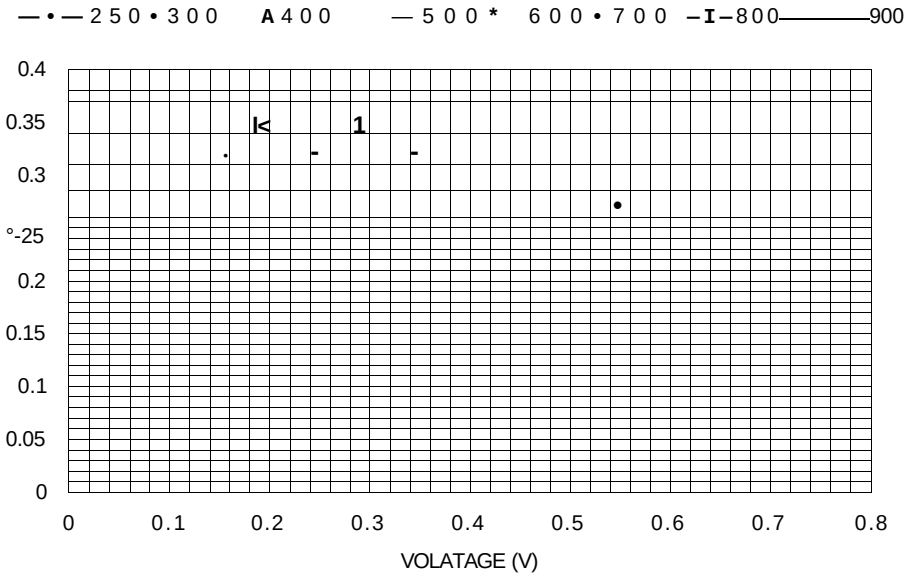

Figure 5.9 I-V characteristic curve for SLARC.

The I-V characteristic curve for the SLARC result using PC 1D simulation at various wavelengths is shown in Figure 5.9. The curve with the weakest correlation to voltage and current is at 250 nm. At 600 nm, the curve is at its maximum (21.23%), followed by a slightly altered curve at 700 nm (21.05%). Regarding how light interacts with the ARC and the solar cell, the incident light's wavelength is also crucial. By appropriately designing the refractive index and thickness of the ARC material, the ARC may control incident light for particular wavelengths, improving the solar cell's efficiency (Jamaluddin et al., 2024a).

In contrast to 1.73 A without the ARC, the Isc increased to 2.39 A when the ARC layer was added, according to the study by Parajuli et al. (2023). More light absorption and electron growth in the solar cell are indicated by an improvement in Isc, which raises efficiency (Hashmi, Akand, et al., 2018; Parajuli et al., 2023). Increasing photon energy absorption, improving short-circuit current (ISC), and optimizing power generation all depend on the anti-reflective coating's enhanced design, which was achieved by multi-objective optimization (Zhang et al., 2021). Consequently, the efficiency of photoelectric conversion is greatly enhanced.

Table 5.7
Result data output of DLARC.

λ (nm)	ZnO Refractive index	ZnO Thickness (nm)	TiO_2 Refractive index	TiO_2 Thickness (nm)	Isc (A)	Voc (V)	Pmax (W)	Efficiency (%)
250	2.388	26.173	2.46	25.407	0.334	0.7426	0.1989	19.89
300	2.404	31.198	3.326	22.55	0.3134	0.7408	0.1853	18.53
400	2.114	47.304	2.68	37.213	0.3513	0.7439	0.2098	20.98
500	1.968	63.516	2.48	50.403	0.3513	0.7439	0.2098	20.98
600	1.913	78.411	2.404	62.396	0.344	0.7433	0.2053	20.53
700	1.883	92.937	2.364	74.027	0.3364	0.7427	0.2005	20.05
800	1.864	107.296	2.341	85.434	0.3308	0.7423	0.1969	19.69
900	1.851	121.556	2.325	96.774	0.3285	0.7421	0.1654	16.54

The double layer ARC (DLARC) ZnO/TiO2 data output that was utilized is displayed in Table 5.7. At 400 and 500 nm wavelengths, the efficiency is at its peak (20.98%), followed by at 600 nm wavelengths (20.53%). At 400 and 500 nm, the results for Voc and =Isc were 0.7439 V and 0.3513 A, respectively.

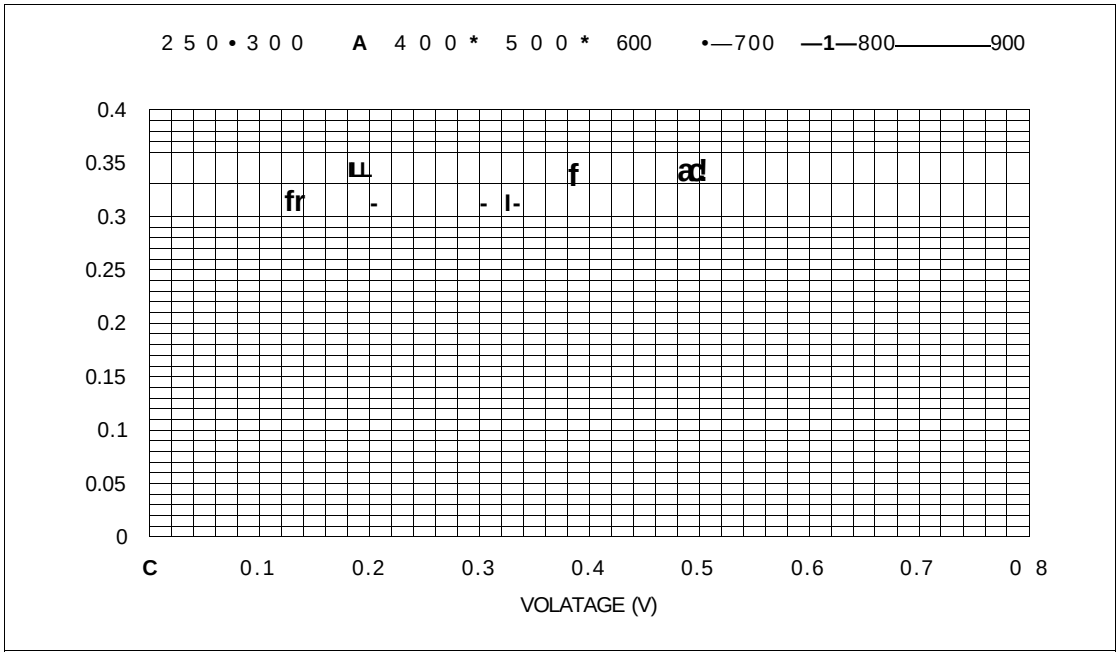

Figure 5.10 I-V characteristic curve for DLARC.

The ZnO/TiO2 DLARC characteristic curve is displayed in Figure 5.10. In the I-V curve, the wavelengths 400 and 500 nm have the highest points, while the wavelength 900 nm has the lowest points. The difference between the highest points of these wavelengths is negligible and only slightly different. The way the light interacts

with the ARC and the solar cell depends on its wavelength. An overall improvement in solar cell efficiency can be achieved by adjusting the thickness and refractive index of the chosen ARC material to optimize light management at particular wavelength regions (Jamaluddin et al., 2024b).

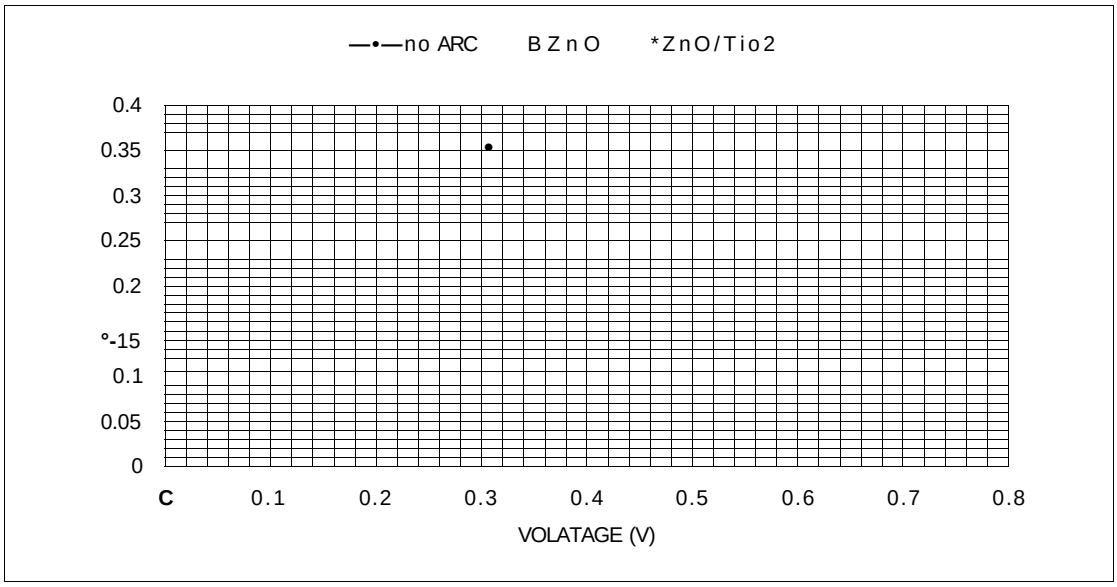

Figure 5.11 I-V characteristic curve for no ARC, SLARC and DLARC**.**

The I-V characteristic curve for PC1D simulations of no ARC, SLARC, and DLARC is displayed in Figure 5.11. ZnO/TiO2's DLARC is the highest point, while ZnO's SLARC comes next. Finally, the no ARC curve is the lowest point. There is hardly any difference between SLARC and DLARC because they reduce reflectance over a wider wavelength range, double-layer anti-reflection coatings (DLARCs) typically give slightly larger efficiency increases than single-layer ARCs (SLARCs) (Al-Turk, 2011). Under normal incidence, DLARCs typically achieve roughly 4% reflectance compared to 10% for SLARCs.(Al-Turk, 2011).

By simply adjusting the coating's refractive index to match silicon's, SLARC significantly reduces light reflection away from the solar cell and increases light penetration into the cell for energy generation. Light interacts with a single interface in a single-layer ARC, which lessens the possibility of destructive force developing in multi-layer structures. Thus, such anti-reflective coatings can decrease reflectance and boost light transmission into the solar cell (Hashmi, Akand, et al., 2018). The major reason for the improvement is the superior reflectance reduction and surface

passivation in particular the blue region wavelength by DLARC. The major reason for the improvement is the superior reflectance reduction and surface passivation in particular the blue region wavelength by DLARC. These factors synergistically contribute to reduce surface recombination and to enhance carrier extraction, leading to an increased EQE and enhanced performance of the full solar cell.These factors synergistically contribute to reduce surface recombination and to enhance carrier extraction, leading to an increased EQE and enhanced performance of the full solar cell.

CHAPTER 6
CONCLUSION

This work demonstrates more general importance of the simulation-based optimization as a robust way for the development of photovoltaic technologies. Through PC ID it has been found that careful tuning of structural and material parameters can be the bridge between theory and practice, which practical experimentalists should seek before beginning device making in earnest. The results also highlight that high performance does not always require exotic materials or complex structures but careful engineering of existing materials and precise optimisation of thickness, doping, and antireflection coatings can yield significant gains. This combination of technical progress and cost makes GaAs/p-Si and AlGaAs/p-Si solar cells even more viable for the future.

This work further offers general findings not limited to the directly studied systems. The optimizations shown here are very relevant for numerous semiconductor technologies, including those based on other III-V materials as well as on perovskite-silicon tandems. Notably, the identified importance of antireflection coatings sets a clear direction for multi-junction solar cells where the broadband absorption of light is of paramount importance. Just as critical is the focus on methods that are sustainable and scalable. Use of materials like ZnO and Ti02 shows that both the pursuit of high efficiency and a high degree of compatibility with abundance, nontoxicity, and manufacturability at large scale are not contradictory but rather are key necessities for global transitioning from fossil fuels to renewable energies.

The conclusions clearly indicate that the performances of the device are strongly dependent on the thickness and doping concentration. For the best efficiency of the GaAs/p-Si solar cell, the thickness of the emitter was slightly reduced to reach 0.1 um, while that of a silicon base was maximized to 150 um. For the best efficiency of the AlGaAs/p-Si solar cell, the thicknesses of the emitter and the silicon base were also optimized to be equal to 0.1 um and 120 um, respectively. Doping studies demonstrated that too high dopant concentration decreased efficiency due to recombination losses, and optimal levels were found to be close to $1><10^{17}$ cirr^{3} (p-region) and $1><10^{16}$ cirr^{3} (GaAs or $lxl0^{12}$-l>$<10^{13}$ cirr^{3} (AlGaAs) (n-region). These results confirm the first aim

through the creation of reliable models that unambiguously identify the optimal un-thinned doping levels. Efficient design of a solar cell is resolved using the models in order to confirm and support the first aim.

The second goal was also met for GaAs/p-Si and AlGaAs/p-Si solar cells, where the maximum efficiency was obtained. For a GaAs/p-Si value, a maximum was attained with a ZnO single-layer ARC (ZnO SLARC) at 600 nm wavelength and 78.411 nm in thickness (23.42%) slightly increasing ZnO/TiCb double-layer ARC (ZnO/TiCb DLARC) of 23.04% value at 500 nm top sub-cell width. For AlGaAs/p-Si, the best power conversion efficiency (PCE) of 20.98%) was realized in ZnO/TiCh DLARC at 400 and 500 nm, respectively (optimized thickness), meanwhile 20.67%) was found in ZnO SLARC at 500 nm. These findings testify to the importance of ARC optimization to reduce reflection loss and increase overall performance. With judicious selection of thickness, doping, and ARC design, the research achieved its objective and demonstrated the optimization of GaAs- and AlGaAs based solar cells with excellent performance.

Finally, the third target has been fulfilled through understanding the IV characteristics, Voc, and fill factor (FF) by the systematic study of the effects of structural parameters. It has been shown on the simulations that the optimization of thickness and doping as well as the use of ARCs allowed to increase Voc and Jsc and further fill factors and effency. As a result, the PC1D modeling process was an effective approach to not only numerically simulate solar cell behaviors but also practically address and to optimize the device. In general, the work successfully demonstrates the significance of parameter engineering in solar cell optimization and offers a task for future efforts toward the extension of such an analysis to the design of multijunction solar cells (MJSCs) and its experimental realization, as part of the universal wide-scale pursuit to implement inexpensive and high efficiency renewable energy devices.

RECOMMENDATION

There are many other parameters beyond those demonstrated here that could be explored in future studies to maximize solar cell performance. Apart from thickness and doping, counterbalancing the production process is obviously the focus attention on to develop and experiment new ARC materials with more advantages optical properties and manufacturing processes that will lead to a great reduction of cost but also without sacrificing the overall efficiency. Furthermore, the long-term stability and durability under various environment conditions (temperature, humidity, UV exposure, etc.) need to be thoroughly investigated, so that the optimized cells will not only be efficient in lab measurements but also be viable for practical applications. The bandgap engineering and electron affinity adjustments, in conjunction with the surface texturing operations, may enhance the light absorbing capability and reduce the reflection losses, thereby enhancing the conversion efficiency of GaAs/p-Si and AlGaAs/p-Si-based solar cells.

Moreover, doping strategies in non-planar parts of the device that could further optimize optical, electronic and transport properties including carrier mobility and bandgap tuning, can also be investigated in future works. This would make possible to develop solar cells with customized properties for various applications such as multi-junction solar cells (MJSCs) or next-generation hybrid devices. A better insight into PC1D software and its constraints will be also crucial, as better modeling can reduce errors and will make simulation more accurate. In addition, coupling PCD1 with other state of the art simulation tools or validating the results with the experimentations on fabrication can improve the trustworthiness of the results obtained. With these improvements, solar cell research will give rise to not only more efficient solar cells but also practical devices promoting the transition to sustainable energy technologies.

One aspect that is also critical for the future researches relates to the solar cell performance testing in the field conditions. Laboratory measurements do not necessarily reflect the potential complexities of outdoor performance, with external factors such as dust accumulation, partial shading and diurnal spectral variation greatly impacting efficiency. Long-term field evaluations in varied climate conditions would, therefore, allow more accurate assessment of durability and consistency of performance. They would also help in developing the coatings and device structure that can endure the localization environmental conditions.

The sustainability of the materials used should also be considered in further studies, since the long-term availability and sustainability of materials used in solar cells is crucial. Examples of the rare, expensive or toxic nature of the elements used, hampering their practical application with a certain limitation in scale, as well as their environmental aspects. Further research could concentrate on replacing scarce materials by abundant, low toxic materials like zink oxide or aluminium oxide, that show similar optical properties. Additionally, investigations on recyclable and biodegradable encapsulation materials may help to cut down the environmental impact of solar cell manufacture in general. Systems analyses that incorporate extraction of raw materials, manufacture, operation, and end-of-life recycling would provide useful additional perspective on the long-term sustainability of solar.

The incorporation of nano-structured and photonic designs represents another interesting direction. The advanced coatings with the graded-index profiles, moth-eye structures or plasmonic nanoparticles could exhibit better performances in broadband AR and light trapping. These principles emulate bioinspired strategies and may potentially result in the efficient collection of solar energy with little reflection loss throughout the entire solar spectrum. In the future, it would be interesting to utilize these nanostructures in combination with antireflective coatings to achieve improved performance.

In simulation, the combination of PC1D with more rigorous modeling would further enhance prediction. For example, finite-difference time-domain (FDTD) modeling or COMSOL multiphysics simulations could be incorporated for combined optical, thermal, and electrical studies. Such a multiphysics model would offer an improved understanding of device performance, particularly under changing environmental conditions. In addition, validation of the simulation results through various experimental methods, including ellipsometry, photoluminescence mapping, and EQE measurements, could increase the trustworthiness of the simulation outcomes.

Also, the integration of optimized solar cells into larger systems should be more prominently addressed. module level studies of encapsulation, wiring and thermal management ared to close the gap between lab-scale devices and industrial deployment. The behavior of high-performance solar cells in building integrated photovoltaics (BIPV) or portable power devices, for instance, can be quite different from that of the or better isolated cells. Meeting these challenges will guarantee that the next GDM cells

not only excel at cell level but that they are also practical, scalable, and economical when deployed in actual applications.

REFERENCES

Akinlami, J. O., & Ashamu, A. O. (2013). Optical properties of GaAs. *Journal of Semiconductors, 34(3).* https://doi.org/10.1088/1674-4926/34/3/032002

Al-Ariki, S., Yahya, N. A. A., Al-A'nsi, S. A., Jumali, M. H. H., Jannah, A. N., & Abd-Shukor, R. (2021). Synthesis and comparative study on the structural and optical properties of ZnO doped with Ni and Ag nanopowders fabricated by sol gel technique. *Scientific Reports,* 77(1), 1-11. https://doi.org/10.1038/S41598-021-91439-l;SUBJMETA=119,639,766,925;KWRD=CONDENSED-MATTER+PHYSICS,NANOSCIENCE+AND+TECHNOLOGY,PHYSICS

Alexander, T. P., Bukowski, T. J., Teowee, G., Uhlmann, D. R., McCarthy, K. C, Dawley, J., & Zelinski, B. J. J. (1996). *Dielectric properties of sol-gel derived ZnO thin films.* Https://Experts.Arizona.Edu/En/Publications/Dielectric-Properties-of-Sol-Gel-Derived-Zno-Thin-Films.

Al-Ezzi, A. S., & Ansari, M. N. M. (2022). Photovoltaic Solar Cells: A Review. In *Applied System Innovation* (Vol. 5, Issue 4). MDPI. https://doi.org/10.3390/asi5040067

Ali, K., Khan, S. A., & Mat Jafri, M. Z. (2014). Effect of Double Layer (Si02/Ti02) Anti-reflective Coating on Silicon Solar Cells. *International Journal of Electrochemical Science,* 9(12), 7865-7874. https://doi.org/10.1016/S1452-3981(23)11011-X

Al-Turk, S. (2011). *ANALYTIC OPTIMIZATION MODELING OF ANTI-REFLECTION CO A TINGS FOR SOLAR CELLS.*

Andras, A., Popescu, F. D., Radu, S. M., Pasculescu, D., Brinas, I., Radu, M. A., & Peagu, D. (2024). Numerical Simulation and Modeling of Mechano-Electro-Thermal Behavior of Electrical Contact Using COMSOL Multiphysics. *Applied Sciences 2024, Vol. 14, Page 4026, 14(10),* 4026. https://doi.org/10.3390/APP14104026

Aswad, A. J., Hassan, N. K., & Ahmed, A. R. (2021). Simulation and Numerical Modelling of CIGSSe-Based Solar Cells by AFORS-HET. *Journal of Physics:*

Conference Series, 2114(1), 012075. https://doi.org/10.1088/1742-6596/2114/1/012075

Bahrami, A., Mohammadnejad, S., Abkenar, N. J., & Soleimaninezhad, S. (2013a). *Optimized Single and Double Layer Antireflection Coatings for GaAs Solar Cells* (Vol. 3, Issue 1).

Bahrami, A., Mohammadnejad, S., Abkenar, N. J., & Soleimaninezhad, S. (2013b). *Optimized Single and Double Layer Antireflection Coatings for GaAs Solar Cells* (Vol. 3, Issue 1).

Balent, J., Smole, F., Topic, M., & Krc, J. (2022). Analysis of effects of dangling-bond defects in doped a-Si:H layers in heterojunction silicon solar cells with different electron affinities of ITO contacts. *Informacije MIDEM, 52(2).* https://doi.org/10.33180/InfMIDEM2022.206

Battaglia, C, Cuevas, A., & De Wolf, S. (2016). High-efficiency crystalline silicon solar cells: Status and perspectives. *In Energy and Environmental Science* (Vol. 9, pp. 1552-1576). Royal Society of Chemistry, https://doi.org/10.1039/c5ee03380b

Belarbi, M., Benyoucef, A., & Benyoucef, B. (2014). SFMULATION OF THE SOLAR CELLS WITH PC ID, APPLICATION TO CELLS BASED ON SILICON. In *Advanced Energy: An International Journal (AEIJ)* (Vol. 1, Issue 3).

Belghachi, A., Abderrachi, H., & Cheknane, A. (2010). High efficiency all-GaAs solar cell. *Progress in Photovoltaics: Research and Applications, 18(2),* 79-82. https://doi.org/10.1002/pip.928

Benkhira, L., Ferhat, M. F., Khaled, M. T. O., Messai, R., Bounedjar, N., Tedjani, M. L., Zoukel, A., Humayun, M., & Bououdina, M. (2024). Multifunctional assessment of copper-doped ZnO nanoparticles synthesized via gliding arc discharge plasma technique: antioxidant, antibacterial, and photocatalytic performance. *Environmental Science and Pollution Research,* 37(31), 43743-43756. https://doi.org/10.1007/S11356-024-34054-7/METRICS

Beye, M., Faye, M. E., Ndiaye, A., Ndiaye, F., & Seidou Maiga, A. (2013). Optimization of SiNx Single and Double Layer ARC for Silicon Thin Film Solar Cells on Glass. *Research Journal of Applied Sciences, Engineering and Technology, 6(3),* 412-416. https://doi.Org/10.19026/RJASET.6.4094

Bhusal, P. (2024). *SIMULATION AND MODELLING OF AlGaAs/GaAs BASED SOLAR CELL USINGPC1D.* https://doi.Org/10.13140/RG.2.2.25909.65767

Channa, I. A., Ashfaq, J., Gilani, S. J., Shah, A. A., Chandio, A. D., & Jumah, M. N. Bin. (2022). UV Blocking and Oxygen Barrier Coatings Based on Polyvinyl Alcohol and Zinc Oxide Nanoparticles for Packaging Applications. *Coatings 2022, Vol. 12, Page 897, 12(1),* 897. https://doi.org/10.3390/COATINGS12070897

Chenni, R., Makhlouf, M., Kerbache, T., & Bouzid, A. (2007). A detailed modeling method for photovoltaic cells. *Energy, 32(9),* 1724-1730. https://doi.Org/10.1016/j.energy.2006.12.006

Chuah, L. S., Hassan, A. M., & Rais, A. R. M. (2026). Numerical Optimization and Performance Analysis of Monocrystalline Silicon Solar Cells via PC ID Simulation. *Silicon.* https://doi.org/10.1007/S12633-025-03607-X

Clugston, D. A., & Basore, P. A. (1997). *PC1D VERSION 5: 32-BIT SOLAR CELL MODELING ON PERSONAL COMPUTERS.* https://doi.Org/https://doi.org/10.1109/PVSC. 1997.654065

Devendra, K. C, Shah, D. K., Wagle, R., Shrivastava, A., & Parajuli, D. (2020). Ingap window layer for gallium arsenide (Gaas) based solar cell using pcld simulation. *Journal of Advanced Research in Dynamical and Control Systems, 12(1* Special Issue), 2878-2885. https://doi.org/10.5373/JARDCS/V12SP7/20202430

Dhungel, S. K., Yoo, J., Kim, K., Jung, S., Ghosh, S., & Yi, J. (2006). Double-Layer Antireflection Coating of MgF 2 /SiN x for Crystalline Silicon Solar Cells. In *Journal of the Korean Physical Society* (Vol. 49, Issue 3).

Dolecek, R. L., Morin, P. J., & Maita, J. P. (1954). *Electrical Properties of Silicon Containing Arsenic and Boron.* https://doi.Org/https://doi.org/10.1103/PhysRev.96.28

Ebanezar John, A., Mishra, D., Thankaraj Salammal, S., & Akram Khan, M. (2024). Factors that enhance the efficiency of Ti02 based heterogeneous photocatalyst for its application in waste water treatment containing organic dye. *Sustainable Water Resources Management, 10(3),* 1-15. https://doi.org/10.1007/S40899-024-01074-7/METRICS

Fedawy, M., Mostafa Ali, S., & Abdolkader, T. (2018). Efficiency Enhancement of GaAs Solar Cell using Si3N4 Anti-reflection Coating. *Journal of Advanced Research in Materials Science, 42,* 1-7. www.akademiabaru.com/arms.html

Garfield, E. (2007). The evolution of the science citation index. *International Microbiology,* 70(1), 65-69. https://doi.org/10.2436/20.1501.01.10

Giebink, N. C, Wiederrecht, G P., Wasielewski, M. R., & Forrest, S. R. (2011). Thermodynamic efficiency limit of excitonic solar cells. *Physical Review B - Condensed Matter and Materials Physics,* 53(19), 195326. https://doi.Org/10.1103/PHYSREVB.83.195326/FIGURES/4/THUMBNAIL

Goryashin, N. N., & Sidorov, A. S. (2013). Comparison of dynamic performance of single-and multijunction solar cells. *IEEE Electron Device Letters, 34(2),* 280-282. https://doi.org/10.1109/LED.2012.2229959

Gullu, H. H., Yildiz, D. E., Yildmm, M., Demir, I., & Altuntas, I. (2024). Electrical characteristics of Al/AlGaAs/GaAs diode with high-Al concentration at the interface. *Journal of Materials Science: Materials in Electronics, 35(2).* https://doi.org/10.1007/sl0854-023-11907-4

Gulyaev, D. V., Zhuravlev, K. S., Bakarov, A. K., Toropov, A. I., Yu Protasov, D., Gutakovskii, A. K., Ya Ber, B., & Yu Kazantsev, D. (2016). Influence of the additional p+ doped layers on the properties of AlGaAs/InGaAs/AlGaAs heterostructures for high power SHF transistors. *Journal of Physics D: Applied Physics, 49(9).* https://doi.Org/10.1088/0022-3727/49/9/095108

Hashmi, G., Akand, A. R., Hoq, M., & Rahman, H. (2018). Study of the Enhancement of the Efficiency of the Monocrystalline Silicon Solar Cell by Optimizing Effective Parameters Using PC ID Simulation. *Silicon, 10(4),* 1653-1660. https://doi.org/10.1007/sl2633-017-9649-3

Hashmi, G., Rashid, M. J., Mahmood, Z. H., Hoq, M., & Rahman, M. H. (2018a). Investigation of the impact of different ARC layers using PC ID simulation: application to crystalline silicon solar cells. *Journal of Theoretical and Applied Physics, 12(A),* 327-334. https://doi.org/10.1007/s40094-018-0313-0

Hashmi, G., Rashid, M. J., Mahmood, Z. H., Hoq, M., & Rahman, M. H. (2018b). Investigation of the impact of different ARC layers using PC ID simulation:

application to crystalline silicon solar cells. *Journal of Theoretical and Applied Physics, 12(4),* 327-334. https://doi.org/10.1007/s40094-018-0313-0

Hirst, L. C, & Ekins-Daukes, N. J. (2011). Fundamental losses in solar cells. *Progress in Photovoltaics: Research and Applications, P9(3),* 286-293. https://doi.org/10.1002/PIP.1024

Hou, X., Aitola, K., & Lund, P. D. (2021). Ti02 nanotubes for dye-sensitized solar cells—A review. *Energy Science & Engineering, 9(7),* 921-937. https://doi.org/10.1002/ESE3.831

Hu, D., Liu, D., Zhang, J., Wu, L., & Li, W. (2018). Preparation and stability study of broadband anti-reflection coatings and application research for CdTe solar cell. *Optical Materials, 77,* 132-139. https://doi.Org/10.1016/J.OPTMAT.2018.01.029

Humaidan, Raed. M., Dahham, A. T., & Majeed, Z. N. (2022). Designed and Simulation of AlGaAs: GaAs Thin Film Solar Cell Using PC ID Program. *NeuroQuantology, 20(3),* 265-270. https://doi.Org/10.14704/nq.2022.20.3.nq22254

Irede, E. L., Awoyemi, R. F., Owolabi, B., Aworinde, O. R., Kajola, R. O., Hazeez, A., Raji, A. A., Ganiyu, L. O., Onukwuli, C. O., Onivefu, A. P., & Ifijen, I. H. (2024). Cutting-edge developments in zinc oxide nanoparticles: synthesis and applications for enhanced antimicrobial and UV protection in healthcare solutions. *RSC Advances, 14(29),* 20992-21034. https://doi.org/10.1039/D4RA02452D

Jamaluddin, N. I. I. M., Yusoff, M. Z. M., & Malek, M. F. (2024a). Modelling and analysis of high efficiency silicon solar cell using double layers anti-reflection coatings (ARC). *Https://Doi.Org/10.1142/S0217984924502014*, 35(23). https://doi.org/10.1142/S0217984924502014

Jamaluddin, N. I. I. M., Yusoff, M. Z. M., & Malek, M. F. (2024b). Numerical Modelling of High Efficiency Silicon Solar Cell Using Various Anti Reflective Coatings (ARC). *Trends in Sciences, 21(3).* https://doi.org/10.48048/tis.2024.7337

Javadi, M. (2020). Theoretical efficiency limit of graphene-semiconductor solar cells. *Applied Physics Letters, 117(5).* https://doi.org/10.1063/5.0020080/39356

Ji, C, Liu, W., Bao, Y., Chen, X., Yang, G., Wei, B., Yang, F., & Wang, X. (2022). Recent Applications of Antireflection Coatings in Solar Cells. *Photonics 2022, Vol. 9, Page 906*, 9(12), 906. https://doi.org/10.3390/PHOTONICS9120906

Jordehi, A. R. (2016). Parameter estimation of solar photovoltaic (PV) cells: A review. In *Renewable and Sustainable Energy Reviews* (Vol. 61, pp. 354-371). Elsevier Ltd. https://doi.Org/10.1016/j.rser.2016.03.049

Kamdem, C. F., Ngoupo, A. T., Kouadio Konan, F., Joel, H., Nkuissi, T., Hartiti, B., & Ndjaka, J.-M. (2019). *Study of the Role of Window Layer Al 0.8 Ga 0.2 As on GaAs-based Solar Cells Performance.* https://doi.org/10.17485/ijst/2019/vl2i37/147207

Kaygusuz, K. (2001). Renewable energy: Power for a sustainable future. In *Energy Exploration and Exploitation* (Vol. 19, Issue 6). https://doi.org/10.1260/0144598011492723

Kc, D., Wagle, R., Gaib, R., Shrivastava, A., & Nath Mishra, L. (2020). *Modelling and simulation of AlGaAs/GaAs solar cell. 9,* 218-223. www.ajer.org

Khairuddin, N. S., Mohd Yusoff, M. Z., & Hussin, H. (2023). The effects of thickness and doping concentration on the solar efficiency of GaN/p-Si based solar cells. *Chalcogenide Letters, 20(9),* 629-637. https://doi.org/10.15251/CL.2023.209.629

Khlyustova, A., Sirotkin, N., Kraev, A., Kusova, T., Titov, V., & Agafonov, A. (2021). Mo-doped Ti02 using plasma in contact with liquids: advantages and limitations. *Journal of Chemical Technology and Biotechnology, 96(4),* 1125-1131. https://doi.org/10.1002/JCTB.6628;JOURNAL: JOURNAL: 10974660; WGROUP : STRING:PUBLIC ATION

Khorsand Zak, A., Esmaeilzadeh, J., & Hashim, A. M. (2024). Exploring the gelatin-based sol-gel approach: A convenient route for fabricating high-quality pure and doped ZnO nanostructures. *Ceramics International,* 50(8), 12649-12663. https://doi.Org/10.1016/J.CERAMINT.2024.01.254

Klimm, D. (2014). Electronic materials with a wide band gap: Recent developments. *IUCrJ, J,* 281-290. https://doi.org/10.1107/S2052252514017229

Laurent, A. (2016). *Modelling and analysis of multi-junction photovoltaic cells using MATLAB/Simulinkfor the improvement of conversion efficiency.*

Lee, Y. J., Ruby, D. S., Peters, D. W., McKenzie, B. B., & Hsu, J. W. P. (2008). ZnO nanostructures as efficient antireflection layers in solar cells. *Nano Letters, 8,* 1501-1505. https://doi.org/10.1021/nl080659j

Lei, Y., Li, Y., & Jin, Z. (2022). Photon energy loss and management in perovskite solar cells. *Energy Reviews,* 7(1), 100003. https://doi.Org/10.1016/J.ENREV.2022.100003

Liu, F., Sneck, A., Eskelinen, P., Halonen, O., Gillan, L., & Leppaniemi, J. (2025). ALD-Grown ZnO TFTs Patterned by High-Resolution Reverse-Offset Printing. *ACS Applied Materials and Interfaces,* 77(23), 34150-34160. https://doi.org/10.1021/ACSAMI.5C03321/ASSET/JMAGES/LARGE/AM5C03 3210008.JPEG

Liu, Y., Xin, B., Newton, M. A. A., Li, L., & Huang, D. (2024). Advanced photocatalytic self-cleaning membrane for highly efficient oil-water separation using C/Ti02/Si02 composite. *Journal of Water Process Engineering, 59,* 104969. https://doi.org/10.1016/JJWPE.2024.104969

Lukong, V. T., Ukoba, K., & Jen, T. C. (2022). Review of self-cleaning Ti02 thin films deposited with spin coating. *The International Journal of Advanced Manufacturing Technology 2022 122:9, 122(9),* 3525-3546. https://doi.org/10.1007/S00170-022-10043-3

Luque, A. (Antonio), & Hegedus, Steven. (2011). *Handbook of photovoltaic science and engineering.* Wiley.

Luque, A., & Hegedus, S. (2011). Handbook of photovoltaic science and engineering: Second edition. *Handbook of Photovoltaic Science and Engineering: Second Edition,* 1-1132. https://doi.org/10.1002/9780470974704

Luque, A., & Marti, A. (2011). *Theoretical Limits of Photovoltaic Conversion andNew-Generation Solar Cells,* https://doi.org/10.1002/9780470974704.ch4

Mackenzie, R. C. I., Balderrama, V. S., Schmeisser, S., Stoof, R., Greedy, S., Pallares, J., Marsal, L. F., Chanaewa, A., & Von Hauff, E. (2016). Loss Mechanisms in

High Efficiency Polymer Solar Cells. *Advanced Energy Materials, 6(4),* 1501742. https://doi.org/10.1002/AENM.201501742

Makableh, Y. F., Vasan, R., Sarker, J. C, Nusir, A. I., Seal, S., & Manasreh, M. O. (2014). Enhancement of GaAs solar cell performance by using a ZnO sol-gel anti-reflection coating. *Solar Energy Materials and Solar Cells, 123,* 178-182. https://doi.Org/10.1016/j.solmat.2014.01.007

Martin, G., Strite, S., Thornton, J., & Morkoc, H. (1991). Electrical properties of GaAs/GaN/GaAs semiconductor-insulator- semiconductor structures. *Applied Physics Letters,* 55(21), 2375-2377. https://doi.org/10.1063/L104875

Mercy, P. A. M., & Wilson, K. S. J. (2024). Comparative Study of Polarization-Dependent Conversion Efficiency of GaAs and Si Solar Cells at Oblique Incident Angles Using Surface DLAR Coating of MgF2/ZnSe. *Crystal Research and Technology, 59(5),* 2300035. https://doi.org/10.1002/CRAT.202300035

Mohamed, E. T., Maka, A. O. M., Mehmood, M., Direedar, Al. M., & Amin, N. (2021). Performance simulation of single and dual-junction GalnP/GaAs tandem solar cells using AMPS-ID. *Sustainable Energy Technologies and Assessments, 44.* https://doi.Org/10.1016/j.seta.2021.101067

Moradi, M., & Rajabi, Z. (2013). Efficiency Enhancement of Si Solar Cells by Using Nanostructured Single and Double Layer Anti-Reflective Coatings. In *JNS* (Vol. 3).

Nair, G. B., & Dhoble, S. J. (2021). Semiconductor LEDs. In *The Fundamentals and Applications of Light-Emitting Diodes* (pp. 61-86). Elsevier. https://doi.org/10.1016/b978-0-12-819605-2.00003-3

Ozmente§, R., & Hassanien, A. S. (2025). Characterizations and optical discussions of thermally evaporated titanium dioxide thin films. *Journal of Optics (India), 54(3),* 1322-1340. https://doi.org/10.1007/S12596-024-02207-Z/METRICS

Parajuli, D., Gaudel, G S., Kc, D., Khattri, K. B., & Rho, W. Y. (2023). Simulation study of Ti02 single layer anti-reflection coating for GaAs solar cell. *AIP Advances,* 73(8). https://doi.Org/10.1063/5.0153197

Patra. (2023). *Titanium dioxide \ Description & Uses \ Britannica.* Https://Www.Britannica.Com/Science/Titanium-Dioxide.

Plante, M. C, & LaPierre, R. R. (2008). Control of GaAs nanowire morphology and crystal structure. *Nanotechnology,* 79(49). https://doi.org/10.1088/0957-4484/19/49/495603

Priyalakshmi Devi, K., Goswami, P., & Chaturvedi, H. (2022). Fabrication of nanocrystalline Ti02 thin films using Sol-Gel spin coating technology and investigation of its structural, morphology and optical characteristics. *Applied Surface Science, 591,* 153226. https://doi.Org/10.1016/J.APSUSC.2022.153226

Qiao, Y., Feng, S., Xiong, C, Ma, X., Zhu, H., Guo, C, & Wei, G. (2013). The thermal properties of AlGaAs/GaAs laser diode bars analyzed by the transient thermal technique. *Solid-State Electronics, 79,* 192-195. https://doi.Org/10.1016/j.sse.2012.07.007

Ranabhat, K., Patrikeev, L., Revina, A. A. evna, Andrianov, K., Lapshinsky, V., & Sofronova, E. (2016). An introduction to solar cell technology. *Journal of Applied Engineering Science, 14(4),* 481-491. https://doi.org/10.5937/jaesl4-10879

Ray, M. K., Sasmal, S., & Maity, S. (n.d.). Improvement of Quantum Efficiency and Reflectance of GaAs Solar Cell. *International Journal of Engineering Research and General Science, 3(2).* www.ijergs.org

Rengifo-Herrera, J. A., Osorio-Vargas, P., & Pulgarin, C. (2022). A critical review on N-modified Ti02 limits to treat chemical and biological contaminants in water. Evidence that enhanced visible light absorption does not lead to higher degradation rates under whole solar light. *Journal of Hazardous Materials, 425,* 127979. https://doi.Org/10.1016/J.JHAZMAT.2021.127979

Righini, G. C, & Enrichi, F. (2019). Solar cells' evolution and perspectives: A short review. In *Solar Cells and Light Management: Materials, Strategies and Sustainability* (pp. 1-32). Elsevier. https://doi.org/10.1016/B978-0-08-102762-2.00001-X

Roshi, Singh, B., & Gupta, V. (2022). Modelling and simulation of silicon solar cells using PC ID. *Materials Today: Proceedings, 54.* https://doi.Org/10.1016/j.matpr.2021.ll.092

Saari, J., Ali-Loytty, H., Lahtonen, K., Hannula, M., Palmolahti, L., Tukiainen, A., & Valden, M. (2022). Low-Temperature Route to Direct Amorphous to Rutile Crystallization of Ti02Thin Films Grown by Atomic Layer Deposition. *Journal of Physical Chemistry C, 126(36),* 15357-15366. https://doi.org/10.1021/ACS.JPCC.2C04905/ASSET/IMAGES/MEDnJM/JP2C04905_0007.GIF

Saidarsan, A., Guruprasad, S., Malik, A., Basumatary, P., & Ghosh, D. S. (2025). A critical review of unrealistic results in SCAPS-1D simulations: Causes, practical solutions and roadmap ahead. *Solar Energy Materials and Solar Cells, 279,* 113230. https://doi.Org/10.1016/J.SOLMAT.2024.113230

Salman, K. A. (2017). Effect of surface texturing processes on the performance of crystalline silicon solar cell. *Solar Energy, 147,* 228-231. https://doi.Org/10.1016/j.solener.2016.12.010

Sandhu, M., & Thakur, T. (2017). Design and modeling of hybrid MPPT MJSC photovoltaic and wind based microgrid using multilevel inverter. *2016 5th International Conference on Wireless Networks and Embedded Systems, WECON 2016.* https://doi.org/10.1109/WECON.2016.7993493

Sathya, P., & Supriya, P. (2017). Design and analysis of AlGaAs/GaAs/Si multi junction solar cell using PC1D. *2017 International Conference on Microelectronic Devices, Circuits and Systems, ICMDCS 2017, 2017-January,* 1-6. https://doi.org/10.1109/ICMDCS.2017.8211589

Schygulla, P., Lang, R., & Lackner, D. (2023). Effective radiative recombination coefficient of p-AlGaAs for varying aluminium concentrations. *Journal of Crystal Growth, 605,* 127054. https://doi.org/10.1016/JJCRYSGRO.2022.127054

Shah, D. K., KC, D., Muddassir, M., Akhtar, M. S., Kim, C. Y., & Yang, O. B. (2021). A simulation approach for investigating the performances of cadmium telluride solar cells using doping concentrations, carrier lifetimes, thickness of layers, and band gaps. *Solar Energy, 216,* 259-265. https://doi.Org/10.1016/J.SOLENER.2020.12.070

Shah, D. K., KC, D., Parajuli, D., Akhtar, M. S., Kim, C. Y., & Yang, O. B. (2022). A computational study of carrier lifetime, doping concentration, and thickness of

window layer for GaAs solar cell based on A1203 antireflection layer. *Solar Energy, 234,* 330-337. https://doi.Org/10.1016/J.SOLENER.2022.02.006

Shanmugam, N., Pugazhendhi, R., Elavarasan, R. M., Kasiviswanathan, P., & Das, N. (2020). Anti-reflective coating materials: A holistic review from PV perspective. *Energies,* 73(10). https://doi.org/10.3390/enl3102631

Sharma, R., Gupta, A., & Virdi, A. (2017). Effect of single and double layer antireflection coating to enhance photovoltaic efficiency of silicon solar. *Journal ofNano- and Electronic Physics, 9(2).* https://doi.org/10.21272/JNEP.9(2).02001

Singh, B., Roshi, & Gupta, V. (2022a). Impact of different parameters on the performance of GaAs solar cell using PC ID simulation. *Materials Today: Proceedings,* <52(P12), 6407-6411. https://doi.Org/10.1016/j.matpr.2022.03.675

Singh, B., Roshi, & Gupta, V. (2022b). Impact of different parameters on the performance of GaAs solar cell using PC ID simulation. *Materials Today: Proceedings,* <52(P12), 6407-6411. https://doi.Org/10.1016/j.matpr.2022.03.675

Sozzi, G., Troni, F., & Menozzi, R. (2014). On the combined effects of window/buffer and buffer/absorber conduction-band offsets, buffer thickness and doping on thin-film solar cell performance. *Solar Energy Materials and Solar Cells, 121,* 126-136. https://doi.Org/10.1016/J.SOLMAT.2013.10.037

Sulciute, A., Nishimura, K., Gilshtein, E., Cesano, F., Viscardi, G., Nasibulin, A. G., Ohno, Y., & Rackauskas, S. (2021). ZnO Nanostructures Application in Electrochemistry: Influence of Morphology. *Journal of Physical Chemistry C, 125(2),* 1472-1482. https://doi.org/10.1021/ACS.JPCC.0C08459/SUPPL_FILE/JP0C08459_LIVESLIDES.MP4

Sun, C, Zhang, J., Zhang, Y., Zhao, F., Xie, J., Liu, Z., Zhuang, J., Zhang, N., Ren, W., & Ye, Z. G. (2021). Design and fabrication of flexible strain sensor based on ZnO-decorated PVDF via atomic layer deposition. *Applied Surface Science, 562,* 150126. https://doi.Org/10.1016/J.APSUSC.2021.150126

Tayyib, M., Odden, J. O., Ramchander, N., Prakash, M. B., Surendra, T. S., Muneeshwar, R., Sarma, A. V., Ramanjaneyulu, M., & Saetre, T. O. (2013). Performance assessment of a grid-connected mc-Si PV system made up of silicon

material from different manufacturing routes. *Conference Record of the IEEE Photovoltaic Specialists Conference.* https://doi.org/10.1109/PVSC.2013.6744110

Vetrivel, M., Jagadeeshwaran, A., & Sangeetha, B. (2024). Performance evaluation of nanostructured ZnO on silicon based solar cells. *Journal of Ovonic Research, 20(6),* 841-849. https://doi.org/10.15251/JOR.2024.206.841

Wang, S., Peng, Y., Li, L., Zhou, Z., Liu, Z., Zhou, S., & Yao, M. (2022). Impact of loss mechanisms on performances of perovskite solar cells. *PhysicaB: Condensed Matter, 647,* 414363. https://doi.Org/10.1016/J.PHYSB.2022.414363

Wang, W.-J., Liao, M.-L., Yuan, J., Luo, S.-Y., & Huang, F. (2022). Enhancing performance of GaN-based LDs by using GaN/InGaN asymmetric lower waveguide layers. *Chinese Physics B, 31(7),* 074206. https://doi.org/10.1088/1674-1056/ac597c

Wang, X., Sun, X., Guan, X., Wang, Y., Chen, X., & Liu, X. (2021). Tannic interfacial linkage within ZnO-loaded fabrics for durable UV-blocking applications. *Applied Surface Science, 568,* 150960. https://doi.Org/10.1016/J.APSUSC.2021.150960

Wang, Z., Zhang, H., Dou, B., Zhang, G, & Wu, W. (2022). Theoretical and experimental evaluation on the electrical properties of multi-junction solar cells in a reflective concentration photovoltaic system. *Energy Reports, 8,* 820-831. https://doi.Org/10.1016/J.EGYR.2021.12.018

Winkler, M. T., Wang, W., Gunawan, O., Hovel, H. J., Todorov, T. K., & Mitzi, D. B. (2014). Optical designs that improve the efficiency of Cu2ZnSn(S,Se) 4 solar cells. *Energy and Environmental Science,* 7(3), 1029-1036. https://doi.org/10.1039/c3ee42541j

Yan, Y., Zhang, Y., Zhao, Y., Ding, F., Lei, Y., Wang, Y., Zhou, J., & Kang, W. (2025). Review on Ti02 nanostructured photoanode and novel dyes for dye-sensitized solar cells application. *Journal of Materials Science 2025 60:11, 60(11),* 4975-5005. https://doi.org/10.1007/S10853-025-10734-8

Yang, F., Hou, Y., Xia, Y., Hou, W., & Sun, B. (2021). Enhanced photochemical properties of S-doped ZnO half-arc mesoporous superstructured nanowires.

Journal of Photochemistry and Photobiology A: Chemistry, 409, 113135. https://doi.Org/10.1016/J.JPHOTOCHEM.2021.113135

Yeo, C. II, Choi, H. J., Song, Y. M., Kang, S. J., & Lee, Y. T. (2015). A single-material graded refractive index layer for improving the efficiency of III-V triple-junction solar cells. *Journal of Materials Chemistry A, 3,* 7235-7240. https://doi.org/10.1039/c4ta0611 lj

Zhang, W. W., Qi, H., Ji, Y. K., He, M. J., Ren, Y. T., & Li, Y. (2021). Boosting photoelectric performance of thin film GaAs solar cell based on multi-objective optimization for solar energy utilization. *Solar Energy, 230,* 1122-1132. https://doi.Org/10.1016/j.solener.2021.ll.031

AUTHOR'S PROFILE

Fazlin Binti Mohamad Rahimi obtained Bachelor of Science in Physics (Hons.) in 2023 from University Teknologi Mara (UiTM), Arau, Pedis. Then, she further her studies in Master of Science (Applied Physics) at University Teknologi Mara (UiTM), Shah Alam, Selangor. Her Master (Msc) thesis involves Numerical Simulation and Optimization of High-Efficiency Gaas/P-Si and Algaas/P-Si Based Solar Cells.

LIST OF PUBLICATIONS:

Rahimi, F. M., Yusoff, M. Z. M., Yahya, M. S., Sapeli, M. M. I., & Zulkepli, N. (2025). Modelling and analysis of solar cells based on GaAs/p-Si: impact on arc dependency. Journal of Optoelectronic and Biomedical Materials, 17(2), 77-85. https://doi.org/10.15251/JOBM.2025.172.77

Rahimi, F. M., & Yusoff, M. Z. M. (2025). Numerical simulation and characterization of solar cells based on GaAs/p-Si: influence on thickness and doping concentration dependence. International Journal of Nanoelectronics and Materials (IJNeaM), 18(3), 451-456. https://doi.org/10.58915/IJNEAM.V18I3.774